

**POLITECNICO DI TORINO**

**Corso di Laurea Magistrale  
in Ingegneria Meccanica**

**Tesi di Laurea Magistrale**

**Adaptation of low cost hybrid architecture  
to a general purpose platform**



**Relatori**

Prof. Ing. Giovanni Belingardi  
Prof.ssa Ing. Francesca Maria Curà  
Ing. Michele Spina  
Ing. Paolo Barengo

*firma dei relatori*

.....

**Candidato**

Gabriele Ferlito  
*firma del candidato*

.....

**A.A.2017-2018**



# Index

1. Introduction .....	4
2. Emission standard scenario in Europe .....	6
2.1 History and future trends .....	6
2.2 CO <sub>2</sub> target definition .....	7
2.3 NEDC (New European Drive Cycle) .....	10
2.4 WLTC (Worldwide Harmonized Light Vehicles Test Cycle).....	11
2.5 Comparison between NEDC and WLTC .....	12
3. Impact of mass change on CO <sub>2</sub> target and emissions.....	16
3.1 Evaluation of possible future scenarios .....	17
3.1.1 +5% Fleet Mass 2020 scenario .....	17
3.1.2 -5% Fleet Mass 2020 scenario .....	18
3.2 Considerations .....	19
4. Fundamentals on Hybrid Electric Vehicles (HEVs) .....	21
4.1 Hybrid functions .....	21
4.1.1 Start&Stop technology .....	21
4.1.2 E-assist .....	22
4.1.3 Regenerative braking .....	22
4.1.4 Coasting .....	23
4.2 Classification of HEVs based on powertrain layout.....	24
4.2.1 Series hybrid .....	24
4.2.2 Parallel hybrid .....	24
4.2.3 Series-Parallel hybrid.....	25
4.3 Classification of HEVs based on degree of hybridization.....	25
4.3.1 Micro Hybrid .....	25
4.3.2 Mild Hybrid .....	26
4.3.3 Full Hybrid.....	26
4.4 Classification of parallel hybrid vehicles based on electric machine position .....	27
4.4.1 P1f layout .....	27
4.4.2 P1r layout .....	28
4.4.3 P2 layout .....	29

4.4.4 P3 layout .....	29
4.4.5 P4 layout .....	30
5. Overview on components of hybrid systems .....	31
5.1 Electric machine .....	31
5.2 Power electronics.....	33
5.2.1 Inverter or AC/DC Converter .....	33
5.2.2 DC/DC converter .....	34
5.2.3 Power switches.....	34
5.2.4 Lithium-Ion Battery .....	35
6. Description of Micro-Hybrid architectures .....	36
6.1 Conventional starter and alternator.....	36
6.2 Reinforced starter .....	37
6.2.1 Reinforced starter by Bosch.....	37
6.2.2 Reinforced starter by Valeo .....	38
6.2.3 Reinforced starter by Denso.....	38
6.3 Introduction of BSG 12V system by Valeo.....	39
6.4 P1f 12V system.....	40
6.4.1 Components of P1f 12V system .....	40
6.4.2 Impact of a P1f 12V system on vehicle architecture .....	43
6.4.3. Focus on the modifications required on the FEAD .....	45
6.4.4. Benchmarking on P1f 12V systems.....	47
7. Description of Mild-Hybrid architectures .....	49
7.1 P1f 48 V system.....	50
7.1.1 P1f 48V components.....	50
7.1.2 Impact of a P1f 48V system on vehicle architecture .....	53
7.2 P2 48 V system.....	55
7.2.1 P2 48V components .....	55
8. Application of P1f 12 V system on vehicle architecture.....	59
8.1 Installation of the belt driven electric machine .....	59
8.2 Positioning of lithium-ion battery.....	60
8.2.1 Scenario 1.....	61

8.2.2 Scenario 2.....	62
9. Application of P2 48 V system on vehicle architecture .....	64
9.1 Installation of electric machine.....	64
9.2 Positioning of lithium-ion battery.....	65
9.3 Positioning of DC/DC converter .....	66
9.3.1 Scenario 1.....	67
9.3.2 Scenario 2.....	68
9.3.3. Scenario 3.....	69
10. Creation of a model to estimate Performance Index, Fuel Consumption and CO <sub>2</sub> emissions .....	70
9.1 Vehicle Demand Energy (VDE).....	70
10.2 PI (Performance Index) calculation .....	71
10.3 Fuel consumption and CO <sub>2</sub> emission calculation .....	74
10.4 Validation of the numerical model .....	76
11. Analysis of results .....	77
11.1 PI simulations .....	78
11.1.1 PI simulation on vehicles equipped with P1f 12V system.....	78
11.1.2 PI simulation on vehicles equipped with P1f 48V system.....	79
11.1.3 PI simulation on vehicles equipped with P2 48 V system.....	81
11.1.4 Summary on PI improvement .....	82
11.2 Fuel consumption and CO <sub>2</sub> emissions simulations.....	84
11.2.1 FC and CO <sub>2</sub> emission simulations on vehicles equipped with P1f 12V .....	85
11.2.2 FC and CO <sub>2</sub> emission simulations on vehicles equipped with P1f 48 V .....	88
11.2.3 FC and CO <sub>2</sub> emission simulations on vehicles equipped with P2 48 V.....	91
11.2.4 Summary on FC and CO <sub>2</sub> emission reduction .....	94
12. Cost analysis.....	96
13. Comparative analysis .....	98
14. Conclusions .....	100
Bibliography.....	101
List of Figures .....	103
List of tables .....	106

# 1. Introduction

In these years the entire automotive industry is committed to developing technical solutions which can guarantee the compliance with future emissions targets. Beside the conventional vehicles, the Hybrid Electric Vehicles (HEVs), which combine one or more electric machines to the internal combustion engine, are gradually earning larger market shares.

This thesis work has been realized during the internship in FCA Vehicle Architecture, which is currently working on hybrid applications projects. Architecture team deals with the concept phase of new car models through a system approach. A modular and flexible architecture development strategy has been investigated in order to maximize synergies between different vehicles and to enhance industrial efficiency. Within architectural perimeter, shown in Figure 1, there are parts “transparent” to customer and which can be shared across different cars without losing the vehicle differentiation demanded by the market.

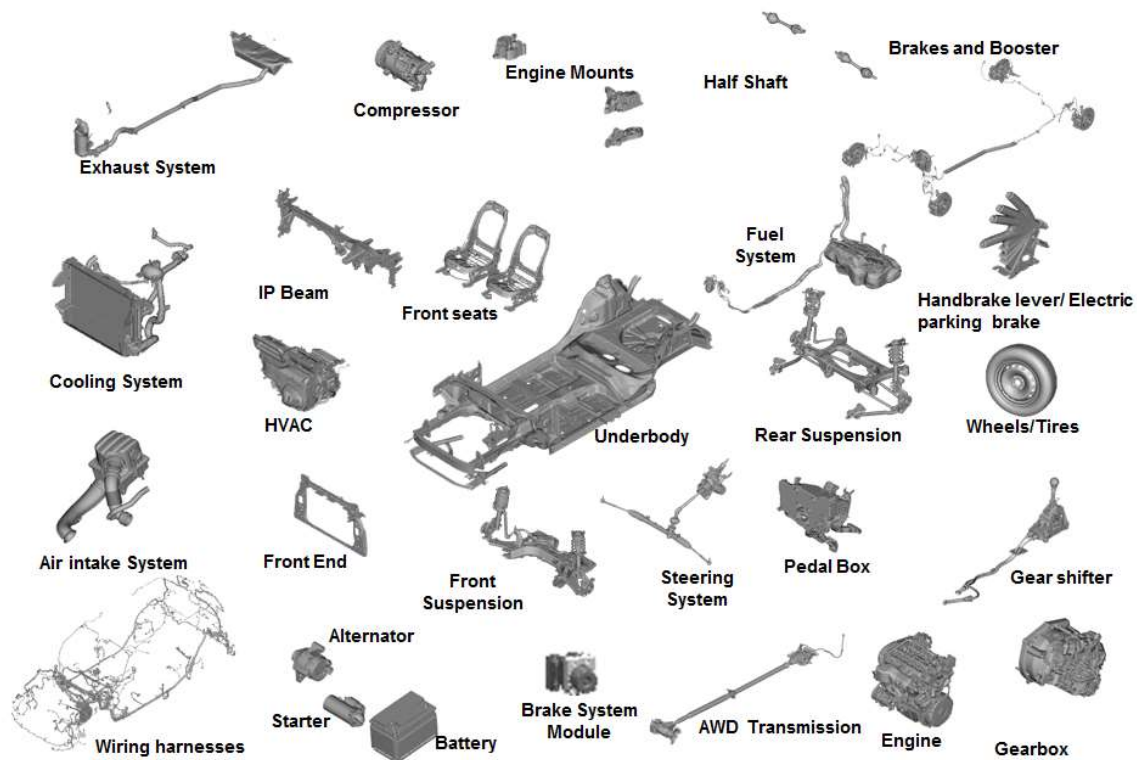


Figure 1. Architectural perimeter

The main purpose of this work is to examine different low cost hybrid architectures, that is essentially low voltage systems, in terms of installation, performance, CO<sub>2</sub> emissions and cost. First of all, each system is analyzed mentioning technical literature and company know-how. This allows to comprehend installation constraints due to the various components and represents the reference theoretical basis.

The architectural implications are investigated by means of CAD software, called Vismockup, whereas for the performance and emissions is adopted a numerical approach implementing a calculation code on Scilab.

In the final part the analysis considers also the cost-benefit ratio related to the introduction of these technologies.

## 2.Emission standard scenario in Europe

### 2.1 History and future trends

Over the last decades, in Europe various emission standards have been introduced in the automotive field to limit carbon dioxide (CO<sub>2</sub>), the main greenhouse gas, and pollutants dangerous for human health, such as carbon monoxide (CO), unburned hydrocarbons (HC), oxides of nitrogen (NO<sub>x</sub>) and particulate matter (PM).

The first European CO<sub>2</sub> emission standard was approved in 2009 and became effective from 1<sup>st</sup> January 2012. Whereas the first European regulation regarding other pollutants was introduced for passenger cars in 1993 with Euro 1 standard that required the switch to unleaded gasoline and the universal adoption of catalytic converters for gasoline vehicles. The Euro 2 standard (1996) decreased further the limit for CO and reduced the combined limit for HC and NO<sub>x</sub> for both gasoline and diesel vehicles. In 2000 the Euro 3 standard modified the test procedure eliminating the engine warm-up period and continued to reduce CO and diesel PM limits. It also added a separate NO<sub>x</sub> limit for diesel engines. The Euro 4 (2005) and Euro 5 (2010) standards concentrated on cleaning up emissions from diesel cars, especially reducing NO<sub>x</sub> and PM. The Euro 5 standard imposed the necessity of particulate filters for all diesel cars, more tightening NO<sub>x</sub> limits and, for the first time, a particulates limit specific for gasoline engines applicable only to direct injection engines. The Euro 6 standard (2015) imposed a significant reduction in NO<sub>x</sub> emissions from diesel engines. A summary on the targets prescribed by each regulation is reported on Table 1.

	Useful Life (km)	Gasoline			Diesel		
		HC+NO <sub>x</sub> (g/km)	CO (g/km)	PM (g/km)	HC+NO <sub>x</sub> (g/km)	CO (g/km)	PM (g/km)
EURO-1 1993	80k	0.95	2.72	0.14	0.95	2.72	0.14
EURO-2 1996	80k	0.5	2.2	N/A	0.7	1	0.08
EURO-3 2000	80k	0.35	2.3	N/A	0.56	0.64	0.05
EURO-4 2005	100k	0.18	1	N/A	0.3	0.5	0.025
EURO-5 2010	160k	0.16	1	0.005	0.23	0.5	0.005
EURO-6 2015	160k	0.16	1	0.0045	0.17	0.5	0.0045

Table 1. EU emission standards

Concerning the pollutant emissions reduction, the principal strategy has been to improve combustion process in internal combustion engine and adopt after treatment systems of exhaust gases.

Regarding to CO<sub>2</sub>, considering that it is the result of an ideal combustion process, the only way to decrease its quantity is to lower the amount of burned fuel. In this perspective, in addition to increased engines efficiency other possible solutions has been the reduction in rolling resistance, aerodynamics improvements and vehicle body lightening.



CO<sub>2</sub> limits imposed by EU regulation and the resulting efforts of car makers, especially in terms of Research and Development investments, have conducted to a sensible CO<sub>2</sub> fall during the last years, as shown in Figure 2.

Nevertheless, CO<sub>2</sub> values from vehicles have to continue on their downward trend and the automotive industry is committed to delivering on this. By 2021, CO<sub>2</sub> emissions of new cars in the EU will be 42% lower than in 2005. A such ambitious target is imposing the necessity of hybridization of the powertrain, combining the internal combustion engine with one or more electrical machines.

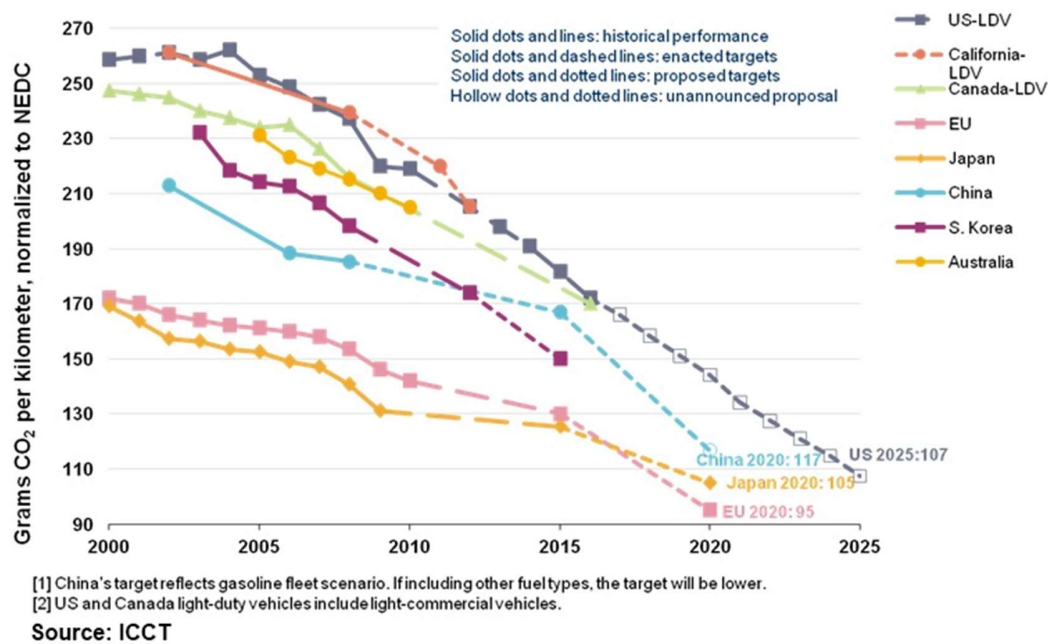


Figure 2. CO<sub>2</sub> trend in the last years

## 2.2 CO<sub>2</sub> target definition

Fuel consumption, CO<sub>2</sub> and pollutant emissions for approval test are obtained by means of standard drive cycles, which are conceived to represent the most frequent situations in road transports.

NEDC (*New European Drive Cycle*) was the drive cycle adopted until 1<sup>st</sup> September 2017. After this date, it was introduced WLTC (*Worldwide Harmonized Light Vehicles Cycle*), also called WLTP (*Worldwide Harmonized Light Vehicles Procedure*) for new type vehicles homologation. From 1<sup>st</sup> September 2018 WLTC will be extended to all new vehicles registration. Until 2020, CO<sub>2</sub> values have to be assessed under NEDC conditions, whereas starting from 2021 under WLTC conditions. In the period of coexistence of NEDC and WLTC, CO<sub>2</sub> value obtained performing WLTP must be converted on NEDC basis, by a back correlation using CO2MPASS software or by measurement (double test). Major details on drive cycles will be reported on the following paragraphs.

European Commission Regulation No. 443/2009 and No. 333/2014 prescribes CO<sub>2</sub> target for new passenger cars of each manufacturer, calculated by using the formula ( 1 ).

$$NEDC\ CO_2\ Target = (NEDC\ CO_2\ Target\ at\ M_0) + a \times (M - M_0) \quad (1)$$

Where:

- $NEDC\ CO_2\ Target$  is the manufacturer's NEDC CO<sub>2</sub> target based on its fleet average mass;
- $NEDC\ CO_2\ Target\ at\ M_0$  is the nominal NEDC CO<sub>2</sub> target for Europe, corresponding to a fleet with average weight equal to  $M_0$ . Its value is reported on Table 2, the 95 g/km limit in 2020 is extended to 95% fleet (phase-in), while from 2021 it is extended to 100% fleet;
- $a$  is the slope of the EU target function, its value is reported on Table 2;
- $M$  is manufacturer's fleet averaged mass in running order;
- $M_0$  is the European fleet averaged mass, its value is reported on Table 2.

	2017	2018	2019	2020
<b><math>NEDC\ CO_2\ Target\ at\ M_0</math> [g/km]</b>	130	130	130	95
<b><math>a</math>[(g/km)/kg]</b>	0,0457	0,0457	0,0457	0,0333
<b>EU Mass <math>M_0</math> [kg]</b>	1392,4	1380	1380	1380

Table 2. Input parameters formula ( 1 ).

2020 represents a strong discontinuity compared to the past, because CO<sub>2</sub> target is set to 95 g/km versus 130 g/km and the slope function of target respect to the mass is 0,0333 [(g/km)/kg] versus 0,0457 [(g/km)/kg]. These modifications responds to EU demand to make limits more stringent.

Figure 3 shows the CO<sub>2</sub> target dependence on mass and 2015 situation of CO<sub>2</sub> emission for all manufacturers, that in 2020 must reduce CO<sub>2</sub> emissions by 27% compared to their 2015 targets.

When the manufacturer's average emissions of CO<sub>2</sub> exceed the target, it will be applied a penalty of 95 € for every g/km excess the target multiplied by the number of vehicles sold, so this forces car makers to greater efforts to be compliant.

For 2021 CO<sub>2</sub> target, it needs to calculate  $WLTP\ CO_2\ Target_{2020}$  through formula ( 2 ).

$$WLTP\ CO_2\ Target_{2020} = NEDC\ CO_2\ Target_{2020} \times \frac{WLTP_{2020\ CO_2}}{NEDC_{2020\ CO_2}} \quad (2)$$

Where:

- $WLTP\ CO_2\ Target_{2020}$  is the manufacturer's CO<sub>2</sub> target WLTP based on its fleet average mass;
- $NEDC\ CO_2\ Target_{2020}$  is the manufacturer's CO<sub>2</sub> target NEDC based on its fleet average mass;

- $\frac{WLTP_{2020\ CO_2}}{NEDC_{2020\ CO_2}}$  is the ratio between WLTP 2020 CO<sub>2</sub> and NEDC 2020 CO<sub>2</sub> emissions, for a given manufacturer.

In 2021 and following years, CO<sub>2</sub> target WLTP based depends on 2020 scenario in terms of target  $WLTP\ CO_{2\ Target2020}$  and mass difference ( $M_{2020} - M_{0,2020}$ ). It is calculated by using formula ( 3 ).

$$WLTP\ CO_{2\ Target2020} = NEDC\ CO_{2\ Target2020} \times \frac{WLTP_{2020\ CO_2}}{NEDC_{2020\ CO_2}} \quad (3)$$

Where:

- $M_i$  is manufacturer's fleet averaged mass in running order;
- $M_{0,i}$  is the European fleet averaged mass;
- $i$  is the year of reference;

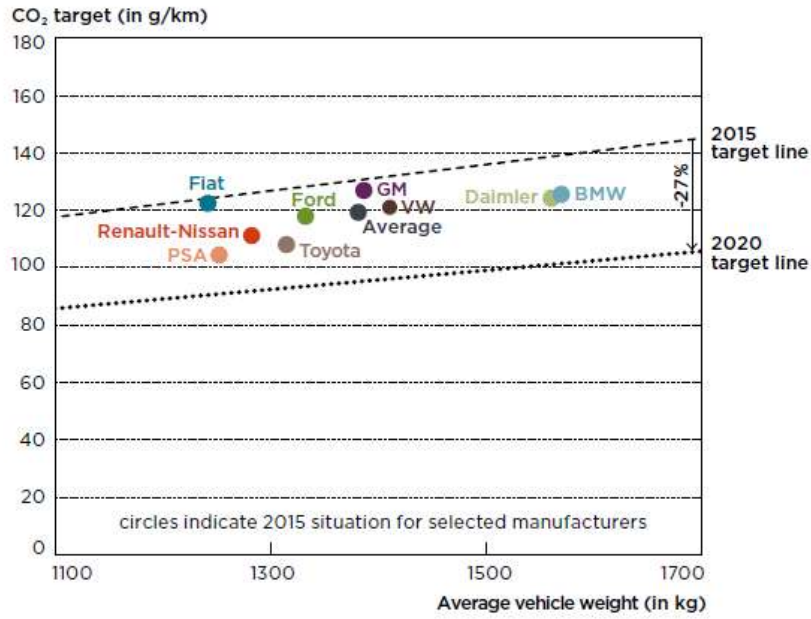


Figure 3. CO<sub>2</sub> target and weight relationship in 2015 and 2020

## 2.3 NEDC (New European Drive Cycle)

In 2000 it was approved the *New European Driving Cycle* derived from MVEG-A cycle used originally for EU type approval testing of emissions of light duty vehicles. It prescribes a first part with four repetitions of the ECE 15 cycle, representative of urban driving with vehicle speeds up to 50 km/h, and a second part with EUDC cycle, representative of highway driving made up of more aggressive acceleration and higher vehicle speed up to 120 km/h. The test is performed on a chassis dynamometer. Differently from MVEG-A cycle in which there was an idling period before the test, engine start at 0 s and the emission sampling begins at the same time. The speed profile of drive cycle is shown in Figure 4. NEDC speed profile and relative data are reported on Table 3.

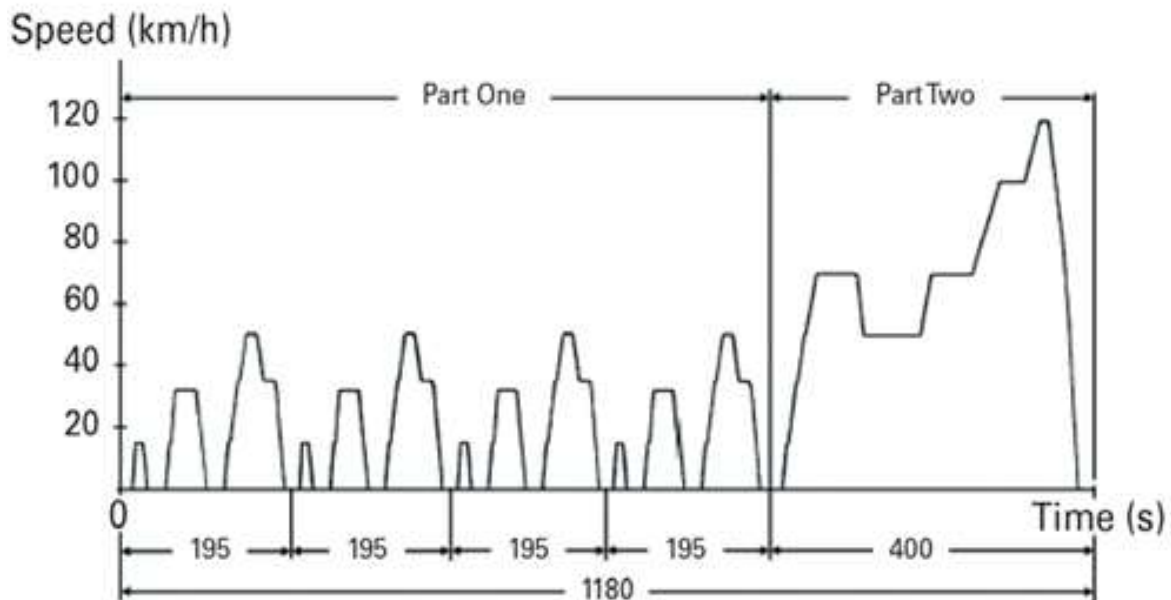


Figure 4. NEDC speed profile

Characteristics	Unit	ECE 15	EUDC	NEDC†
Distance	km	0.9941	6.9549	10.9314
Total time	s	195	400	1180
Idle (standing) time	s	57	39	267
Average speed (incl. stops)	km/h	18.35	62.59	33.35
Average driving speed (excl. stops)	km/h	25.93	69.36	43.10
Maximum speed	km/h	50	120	120
Average acceleration <sup>‡</sup>	m/s <sup>2</sup>	0.599	0.354	0.506
Maximum acceleration <sup>‡</sup>	m/s <sup>2</sup>	1.042	0.833	1.042

† Four repetitions of ECE 15 followed by one EUDC  
<sup>‡</sup> Calculated using central difference method

Table 3. NEDC statistics

Analyses performed by several research institutes demonstrate the discrepancy between NEDC and the real world driving, essentially due to:

- more “dynamic” driving than the NEDC (higher vehicle accelerations/decelerations caused by more aggressive drivers’ behaviours and different traffic conditions);
- vehicle mass which is generally higher than type approval;
- environmental conditions;

A research conducted by ICCT (International Council on Clean Transportation) underlines that the difference between official laboratory and real-world CO<sub>2</sub> emissions was around 7% in 2001 and this value has been increased continuously since then coming up to around 30% in 2013.

## 2.4 WLTC (Worldwide Harmonized Light Vehicles Test Cycle)

The increasing gap between official laboratory and real-world on-road emission values has created a common agreement that a revision of the vehicle test procedures was needed and it conducted to WLTC (*Worldwide Harmonized Light Vehicles Cycle*). This is the main reason why it derives from real-drive data, in EU as statistical base was used eight vehicles and a distance covered of about 400.000 km. The WLTC provides three different categories classified on the basis of the power/weight ratio. Essentially, most modern cars belong to the class 3b, for which Power Weight ratio > 34kW/t and  $v_{max} > 120$  km/h.

The speed profile used for the class 3b Figure 5 is a composition of Low, Medium, High and Extra-High cycles whose data are reported on Table 4.

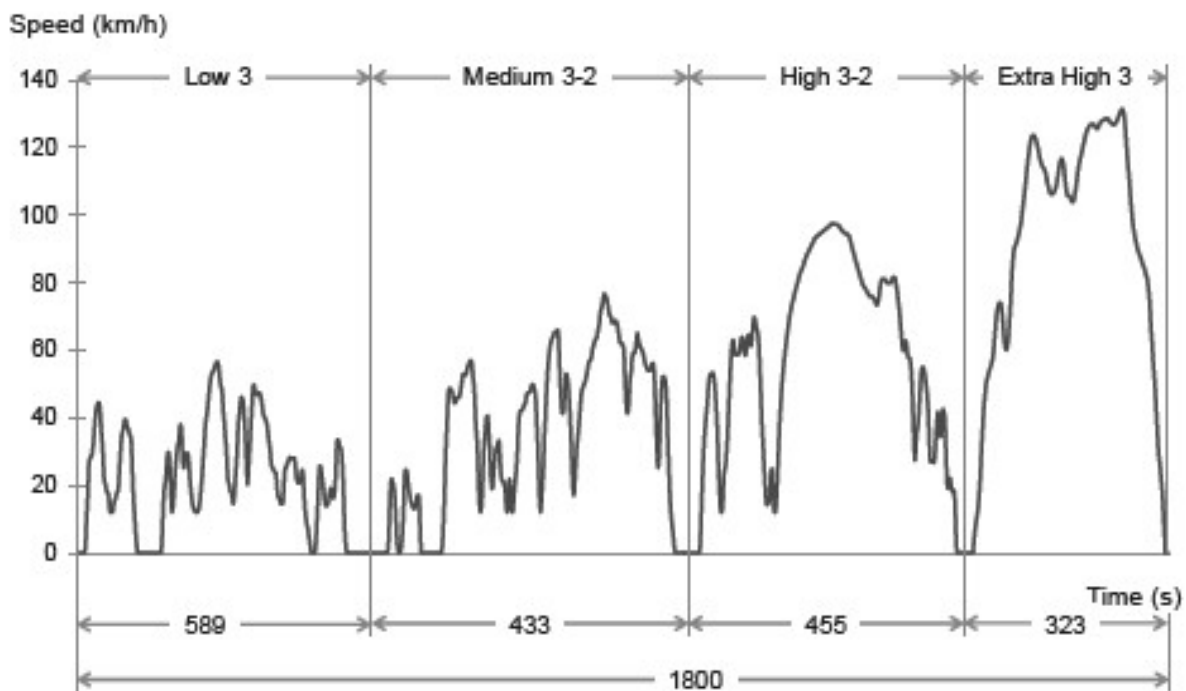


Figure 5. WLTC speed profile

Phase	Duration	Stop Duration	Distance	p_stop	v_max	v_ave w/o stops	v_ave w/ stops	a_min	a_max
	s	s	m		km/h	km/h	km/h	m/s <sup>2</sup>	m/s <sup>2</sup>
<b>Class 3b (v_max ≥ 120 km/h)</b>									
Low 3	589	156	3095	26.5%	56.5	25.7	18.9	-1.47	1.47
Medium 3-2	433	48	4756	11.1%	76.6	44.5	39.5	-1.49	1.57
High 3-2	455	31	7162	6.8%	97.4	60.8	56.7	-1.49	1.58
Extra-High 3	323	7	8254	2.2%	131.3	94.0	92.0	-1.21	1.03
Total	1800	242	23266						

Table 4. WLTC statistics

## 2.5 Comparison between NEDC and WLTC

WLTC is based on real-driving data, whereas NEDC is based on theoretical driving, and so it matches better on-road car performance.

Definitely, the differences of WLTP respect to NEDC regard several aspects:

- More driving phases (Low, Medium, High and Extra High) are representative of a greater range of driving situations, like urban, suburban, main road and motorway. Practically, there are a 52% urban phase and a 48% non-urban phase. The shorter stops reduce sensibly the positive effect of Start&Stop, but the increased decelerations are an opportunity to improve regenerative braking effectiveness.
- Test distance is longer, totally 23.26 km versus 10.93 km. This implies a major cumulated fuel consumption and, consequently, CO<sub>2</sub> emission. Thanks to its distance, the cold start influence decreases in WLTC..
- Average and maximum speed are higher, respectively 46.5 km/h versus 33.6 km/h and 131 km/h versus 120 km/h, so it is more relevant aerodynamic drag contribution.
- For vehicles with manual transmission, WLTC utilizes an algorithm (Steven's tool) in order to compute the optimal shift points, respect to NEDC where gear shifts are fixed. Both in NEDC and WLTC, for hybrid vehicles the optimal shift points is advised to driver through gear shift indicator.
- Each model of vehicle must have its CO<sub>2</sub> value with a range that depends on specific equipment. WLTP takes in account additional features, different for every car.
- WLTP ambient temperatures of 23°C /14°C are more realistic than NEDC ones of 20°/30°C because closer to European average temperature. In more detail, measurements are executed at 23°C, but CO<sub>2</sub> values obtained are corrected to 14°C. The procedure prescribes to performing WLTP and, after engine shut-off, the vehicle is stored in a conditioned room at 14°C for 9 hours. At this point, only High cycle of WLTP is performed. This allows to compute ATCT (Ambient Test Correction Test) that is used to correct the CO<sub>2</sub> values from WLTP.
- CO<sub>2</sub> emission values with WLTP are higher because it is a more dynamic and longer test. This does not mean increased fuel consumption per km, but rather a more realistic CO<sub>2</sub> value due to the changed way to test the vehicles.

A summary concerning the main differences between NEDC and WLTC is reported on Figure 6 and on Table 5.

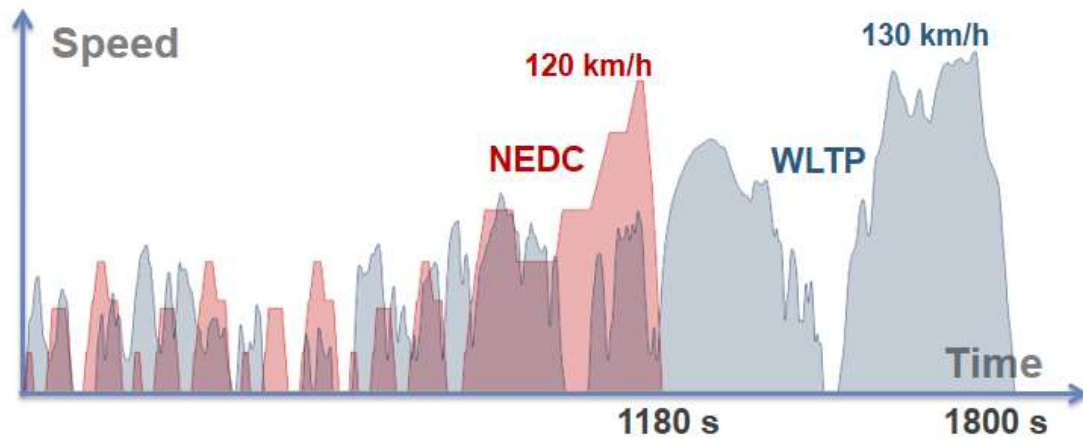


Figure 6. Speed profile NEDC vs WLTC

	Units	NEDC	WLTC
Start condition		cold	cold
Duration	s	1180	1800
Distance	km	11.03	23.27
Mean velocity	km/h	33.6	46.5
Max. velocity	km/h	120.0	131.3
Stop phases		14	9
<b>Durations:</b>			
• Stop	s	280	226
• Constant driving	s	475	66
• Acceleration	s	247	789
• Deceleration	s	178	719
<b>Shares:</b>			
• Stop		23.7%	12.6%
• Constant driving		40.3%	3.7%
• Acceleration		20.9%	43.8%
• Deceleration		15.1%	39.9%

Table 5. NEDC vs WLTC statistics

The NEDC test procedure allows to use mass of the lightest vehicle model version, usually that one with no optional equipment on board, for CO<sub>2</sub> compliance testing. The test mass is calculated adding to the Standard-A mass (defined as mass of unloaded vehicle, complete with spare wheel, accessories and 100% refueling) 75 kg for the weight of the driver and 25 kg for the weight of luggage. Then the test mass is used to perform an interpolation from a series of discrete equivalent masses, called inertia classes.



Resulting value is finally used to determine the CO<sub>2</sub> emissions of the vehicle and of all vehicles of the same family.

Differently, the WLTC procedure takes into account optional equipment in the vehicle actual mass calculation, but to facilitate homologation the physical test regards only two vehicle versions: one vehicle (Low) that requires the least amount of energy to drive the test (with no optional equipment, lowest rolling resistance and lowest aerodynamic drag), and one (High) which has the highest energy demand, that has all optional equipment available on board, highest rolling resistance and greatest aerodynamic drag. For all other vehicle model versions in between, individual CO<sub>2</sub> emissions are based on a regression line that connects the two tested model versions. Figure 7 shows a line representative of interpolation family defined by Low and High version. Furthermore the WLTP prescribes for mass calculation to add to empty vehicle 100 kg plus 15% of the maximum vehicle load within a vehicle family.

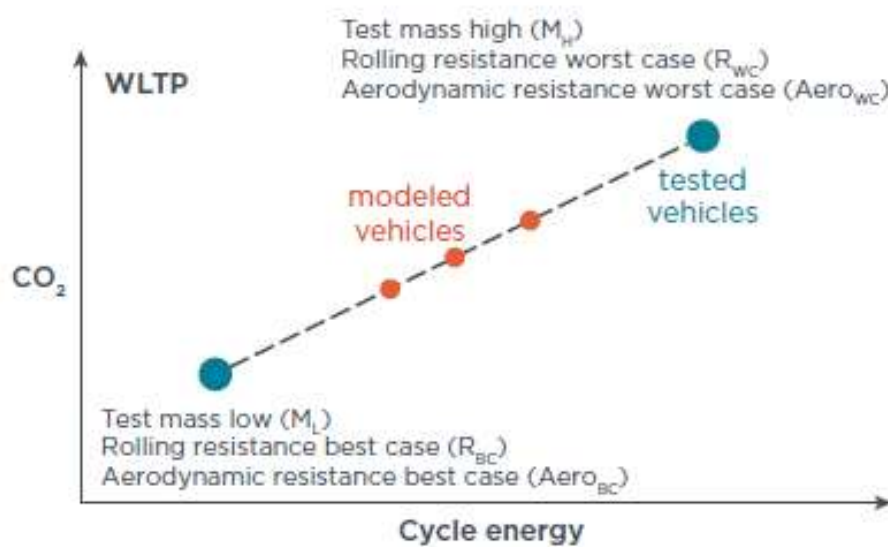


Figure 7. Interpolation family

Vehicles belonging to an interpolation family, defined by two vehicle versions (Low and High), have in common vehicle/powertrain/transmission characteristics:

- Type of internal combustion engine: fuel type, combustion type, engine displacement, full-load characteristics, engine technology, and charging system, and also other engine subsystems or characteristics that have a non-negligible influence on CO<sub>2</sub> mass emission under WLTP conditions;
- Operation strategy of all CO<sub>2</sub> mass emission influencing components within the powertrain;
- Transmission type (e.g. manual, automatic, CVT) and transmission model (e.g. torque rating, number of gears, number of clutches, etc.);
- n/v ratios (engine rotational speed divided by vehicle speed). This requirement is considered fulfilled if, for all transmission ratios concerned, the difference with respect to the transmission ratios of the most commonly installed transmission type is within 8 per cent;
- Number of powered axles.



Besides, the use of interpolation family is possible only if the difference in CO<sub>2</sub> between test vehicles L and H is larger than 5 g/km and lower than 30 g/km or 20 per cent of the CO<sub>2</sub> emissions from vehicle H. At the request of the manufacturer and with approval of the responsible authority, the interpolation line may be extrapolated to a maximum of 3 g/km above the CO<sub>2</sub> emission of vehicle H and/or below the CO<sub>2</sub> emission of vehicle L. Nevertheless this extension is valid only within the absolute boundaries of the interpolation range specified above. The CO<sub>2</sub> emissions for each vehicle in an interpolation family can be calculated by the interpolation method, which consists of deriving individual road load from Low and High ones and, consequently, vehicle demand energy (VDE), explained in the paragraph 10.1.

### 3. Impact of mass change on CO<sub>2</sub> target and emissions

The CO<sub>2</sub> EU regulation is conceived to adapt targets to the vehicle mass, according to formula ( 1 ). The targets are more stringent for lighter vehicles than for heavier ones, because it is implicit that CO<sub>2</sub> values are strictly associated with vehicle weight.

In fact, mass influences the resistance to movement, technically called road load, in terms of inertia forces and rolling resistance and consequently the amount of energy required to complete a drive cycle, so this impacts on fuel consumption and on CO<sub>2</sub> emissions.

While the relationship between CO<sub>2</sub> target and mass is clear by using the equation ( 1 ) , it is harder to find an univocal equation to link mass to CO<sub>2</sub> emissions because each vehicle has its specific mass change sensitivity. ICCT (*International Council on Clean Transport*) in its study *CO<sub>2</sub> Reduction technologies for the European car and van fleet(2017)* demonstrated the relationship between emissions and mass is nonlinear but with a reasonable approximation can be assumed linear for a wide range of vehicle masses.

The future scenarios depends on manufacturer's fleet mass because European fleet mass is fixed to 1380 kg for three years, by 2019 to 2021. Figure 8 shows the mass dependence of CO<sub>2</sub> emissions and CO<sub>2</sub> target on NEDC basis. CO<sub>2</sub> target is plotted by adopting formula ( 1 ) and setting 2020 CO<sub>2</sub> limit (95 g/km) and 1380 kg as European fleet averaged mass. CO<sub>2</sub> target has a slope greater than of the CO<sub>2</sub> emission, exactly 0,0333 [(g/km)/kg] versus 0,0431 [(g/km)/kg] so the effect of 100 kg mass change on target is around 3,3 g/km, while on emission is around 4,3 g/km. This means that part of benefits occurring with mass reduction is discounted by the lower target as well as part of penalization occurring with mass increase is discounted by the higher target.

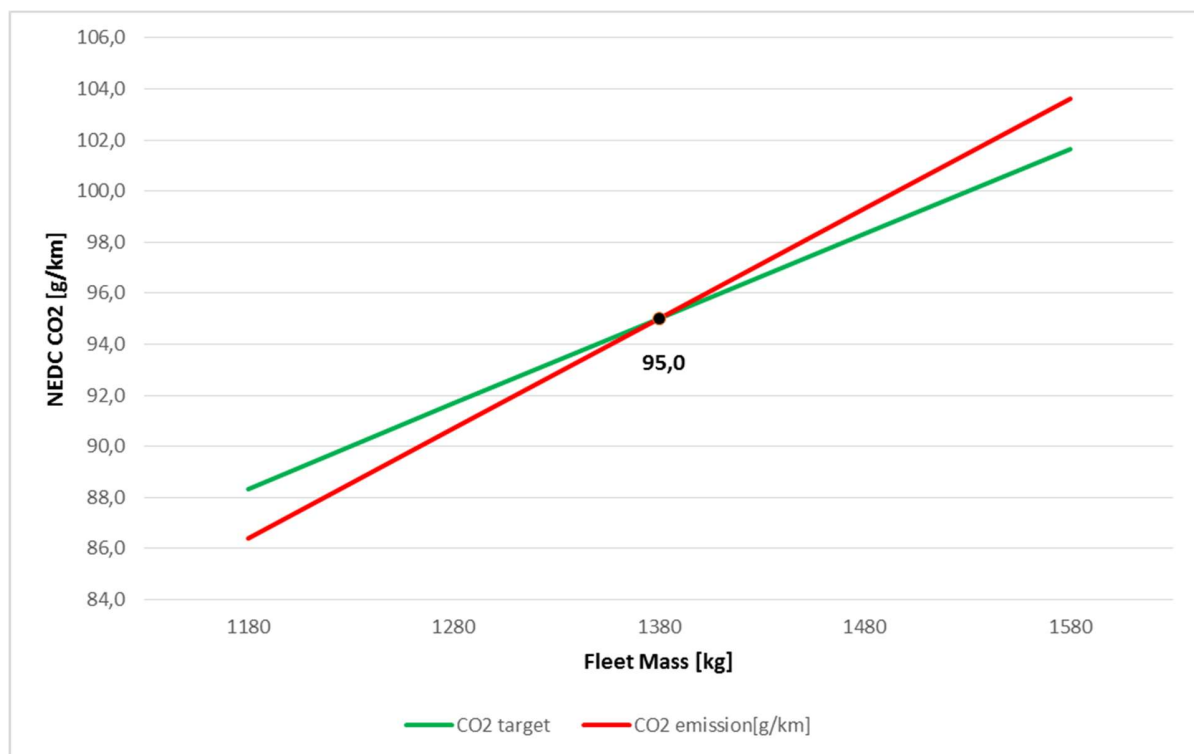


Figure 8. Effect of mass on CO<sub>2</sub> target and emission

### 3.1 Evaluation of possible future scenarios

Here it is studied an example to investigate what are the effects of mass change in 2020 on undercompliance or gap, defined as the deviation between CO<sub>2</sub> emissions and target, starting from a sample initial situation reported on Table 6.

European Fleet Mass [kg]	1380
Generic car maker Fleet Mass [kg]	1380
sCO <sub>2</sub> emission [g/km]	105
CO <sub>2</sub> target [g/km]	95
Gap [g/km]	10

Table 6. Initial situation data

A mass change plausible for  $M$  was estimated around 5% of 1380 kg, equal about to 70 kg and possible scenarios analyzed are: fleet mass increase (+5%), fleet mass decrease (-5%), constant fleet mass.

#### 3.1.1 +5% Fleet Mass 2020 scenario

Heavier fleet causes increased CO<sub>2</sub> emission but also higher CO<sub>2</sub> target, as shown in Figure 9.

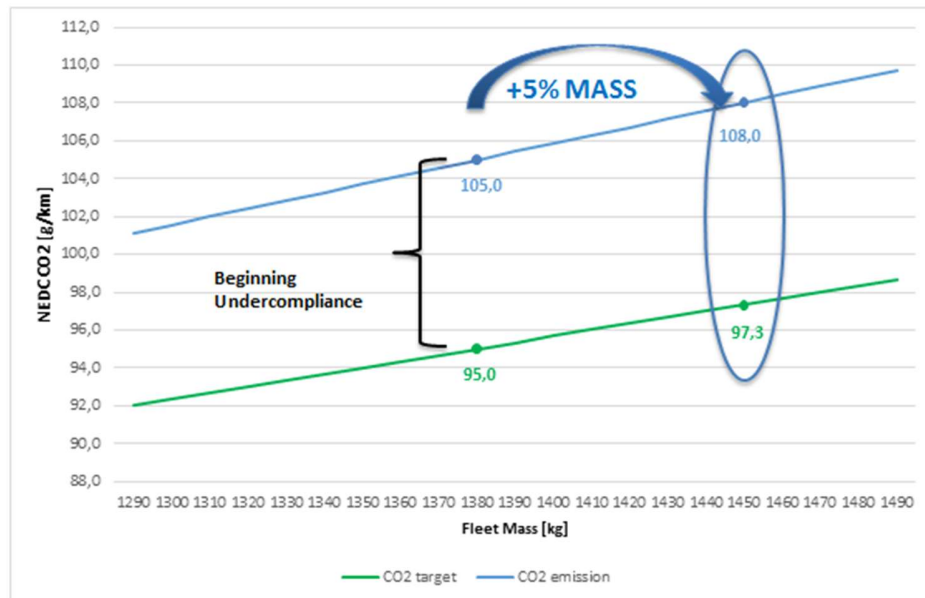


Figure 9. +5% Fleet Mass 2020 scenario

When a car maker implements a 5% mass increase, its gap rises because the two straight lines diverge towards higher masses because of different slopes of target and emissions, as shown in the histogram in Figure 10.

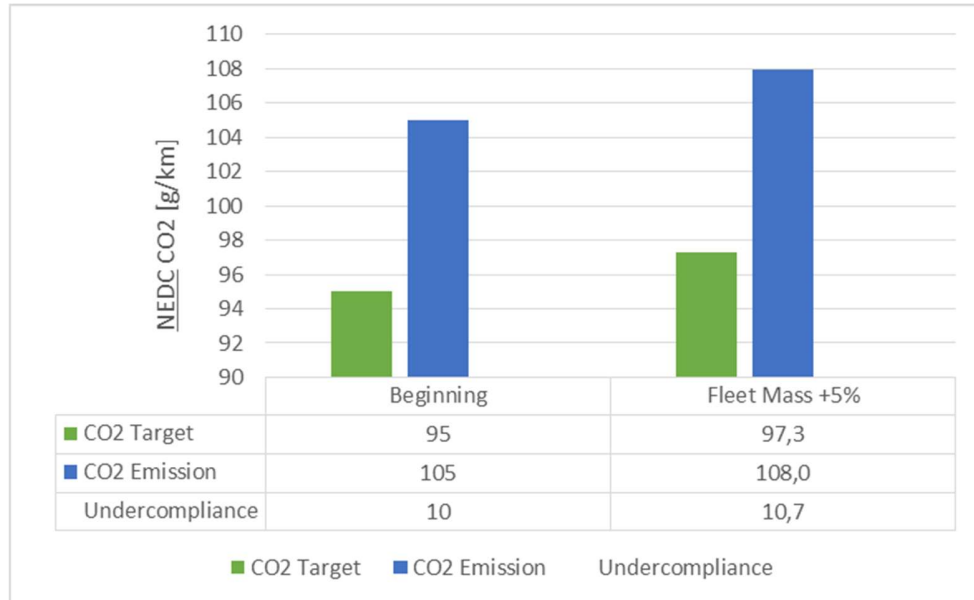


Figure 10. Target and emission trend +5% Fleet Mass 2020 scenario

The delta gap for this scenario is equal to +0,7 g/km.

### 3.1.2 -5% Fleet Mass 2020 scenario

Lighter fleet causes decreased CO<sub>2</sub> emission but also lower CO<sub>2</sub> target, as shown in Figure 11.

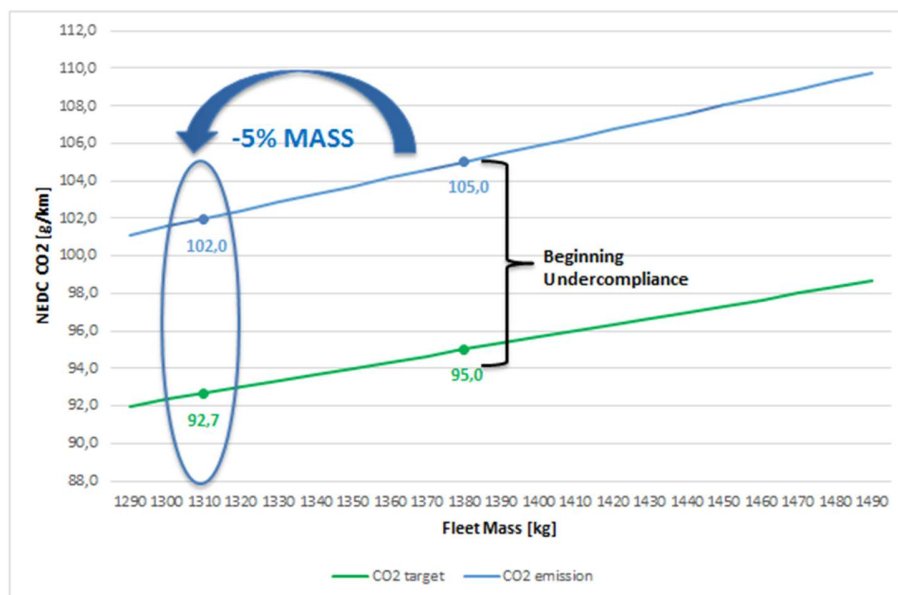


Figure 11. -5% Fleet Mass 2020 scenario

When a car maker implements a 5% mass reduction, its gap falls because the two straight lines converge versus lower masses, because of different slopes of target and emissions, as shown in histogram in Figure 12.

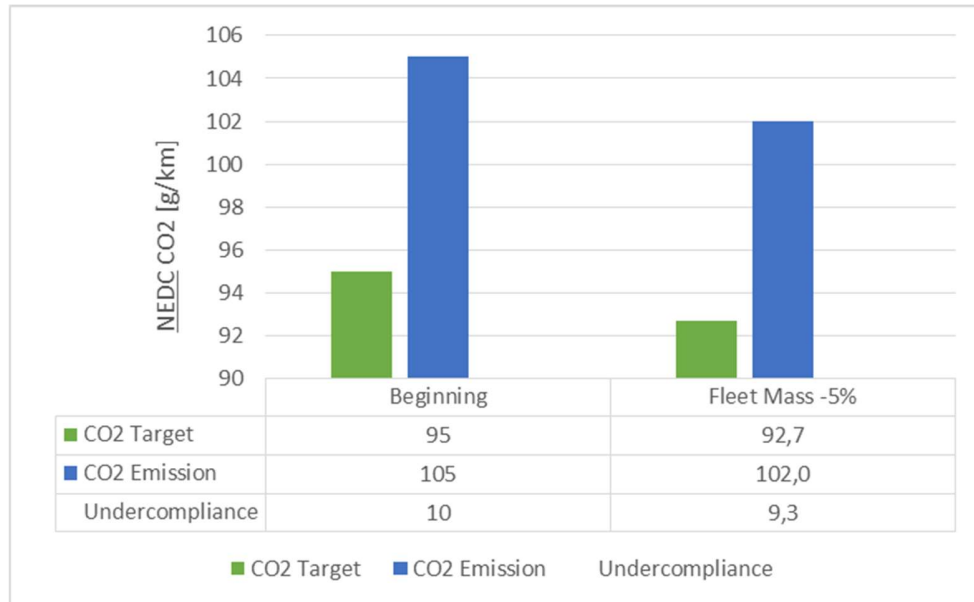


Figure 12. Target and emission trend -5% Fleet Mass 2020 scenario

The delta gap for this scenario is equal to -0,7 g/km.

### 3.2 Considerations

As underlined by Table 7, a mass increase accentuates the gap because CO<sub>2</sub> emissions grows with the mass more rapidly than target. Vice versa, a mass reduction leads the manufacturer to move closer to the compliance, although part of deriving CO<sub>2</sub> reduction is discounted by a tighter target. The strategy to let the fleet mass constant implicates same CO<sub>2</sub> levels and with EU fleet mass constant the gap is not subject to any variation.

Scenario	Delta gap [g/km]
Fleet Mass increase +5%	+0,7
Fleet Mass increase -5%	-0,7
Fleet Mass constant	0

Table 7. Summary on mass change scenarios

Given these considerations, it is evident the importance for each car maker to take under control its fleet mass change. As a general rule a fleet aligned to EU mass conducts to better scenarios in terms of gap. Therefore a technical solution CO<sub>2</sub> effective but that tends to raise all fleet mass reduces partially the advantage of its own introduction. For this reason, every solution in the future of automotive included hybridization has to be evaluated not only in terms of its power to reduce CO<sub>2</sub> emissions but also of its weight implications, being the target influenced by mass.

## 4. Fundamentals on Hybrid Electric Vehicles (HEVs)

The worldwide demand to reduce emissions and to economize on fuel contributed to the development and entry in the automotive market of hybrid electric vehicles (HEVs). In fact, internal combustion engines improvements (e.g. variable valve actuating in gasoline engines, high pressure injection systems in diesel engines, etc.) and other interventions on the vehicle (reduction in rolling resistance and aerodynamic drag) are not sufficient to guarantee car maker's compliance with future CO<sub>2</sub> targets.

HEVs adopts a powertrain including an internal combustion engine and one or more electric machines and they allows to decrease fuel consumption and emissions using different functionalities such as:

- Start&Stop technology;
- E-assist;
- Regenerative braking;
- Coasting.

In the paragraph 4.1 each of this operations mode will be analyzed. In the successive paragraphs hybrid architectures will be classified on the basis of powertrain layout (4.2) and degree of hybridization (4.3).

Finally the paragraph 4.4 contains a focus on classification regarding parallel hybrid topology.

### 4.1 Hybrid functions

#### 4.1.1 Start&Stop technology

The Start&Stop technology consists essentially in shutting down the engine when it is operating at idle speed. It can be executed when the vehicle is stationary (conventional Start&Stop) or also when the vehicle is still moving during deceleration (advanced or enhanced Start&Stop).

Conventional Start&Stop can be fulfilled with a reinforced starter or with belt driven starter generator. The second offers faster start time thanks to the higher output power of the electric machine, in addition to less noise and vibrations.

The impact on emissions and fuel consumption of conventional Start&Stop depends on the stop time of drive cycle. It is more relevant on NEDC cycle than on WLTP cycle, because the first one has longer stop time than the second one (25% compared with 13% of the entire drive cycle).

Enhanced Start&Stop (ESS) consists in stopping the engine when the driver brakes and the vehicle is moving with a speed below a certain threshold (around 15 km/h), but before it requires the transmission disconnected. This function allows to manage Change of Mind situations (CoM), which occurs when the driver brakes and the vehicle speed drops below the threshold but suddenly the driver releases the brake pedal and an engine restart is requested. In this type of situations to maintain an acceptable level of vehicle drivability it is necessary a very short engine restart and fast transmission reconnection.

### 4.1.2 E-assist

Electric assist (E-assist), also called torque boost or torque assist, provides additional torque to assist engine during transients, such as starting and fast accelerations. The electric motor provides torque necessary to meet the driver's requirement without need to gear down and this optimized gear shift schedule enables the engine to operate more efficiently with an evident advantage on fuel economy. The power and duration of electric assist is limited by the battery capacity, motor mechanical characteristics and thermal constraints of system.

### 4.1.3 Regenerative braking

Regenerative braking captures kinetic energy from the wheels during decelerations, transforming mechanical power, usually dissipated by braking system on conventional vehicles, into electrical power.

During the braking a reverse torque is applied on the crankshaft by the generator in order to recover energy, addressed to charge the battery. A typical braking power curve during deceleration, shown in Figure 13, underlines that regenerative brake contribution is significant in a limited speed range because it depends on the speed range where electric machine performs major reverse torques.

Furthermore the energy effectively stored in the battery is limited by the battery capacity and by maximum power generator characteristics.

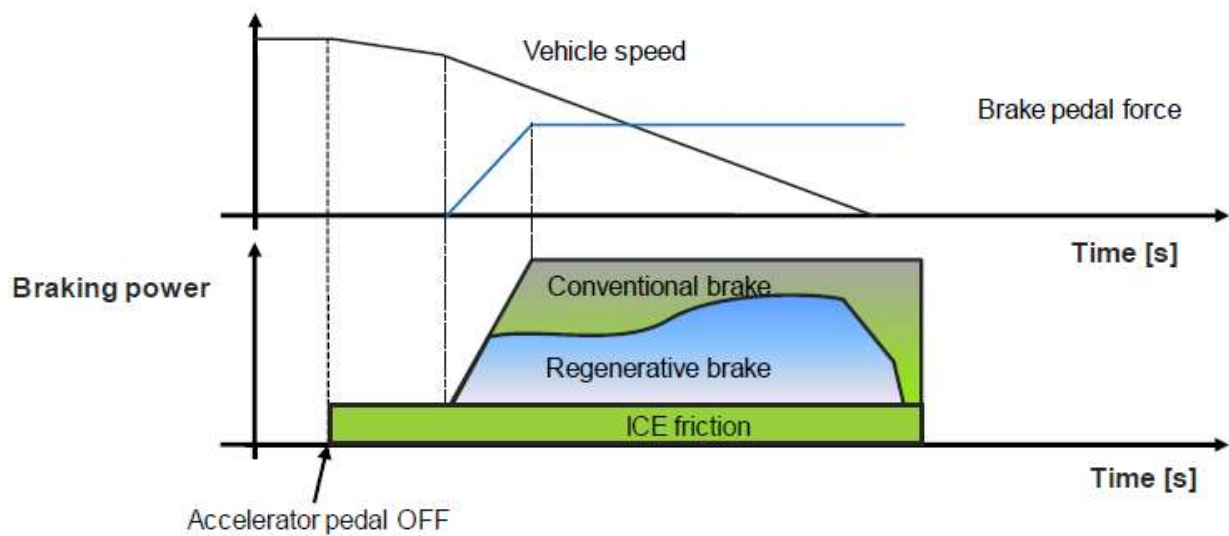


Figure 13. Influence of regenerative braking on braking power



#### 4.1.4 Coasting

Coasting, also called Sailing, means disconnecting the engine from the transmission and stopping or idling the engine, while the vehicle is travelling at low speeds. The transmission disconnection usually is performed by e-clutch, which is essentially a clutch driven by wire.

The Coasting function is activated when the driver releases slowly the accelerator and consequently the vehicle decelerates without any action on brake pedal. When it is performed with the engine at idle speed is called Idle Coasting, whereas when it is performed with the engine off is called Off Coasting. The concept behind this function is that less fuel is required to cover the same distance disconnecting the engine compared to overrun situations. Overrun occurs when the driver takes the foot off the gas pedal and the wheels try to drive the engine at a higher rotational speed.

Looking at graph in Figure 14, it is evident that the distance covered with Off Coasting function is clearly longer compared with the case of engine connected to the transmission.

In fact, there are no more engine losses that decelerates the vehicle and it is essentially propelled by its own inertia.

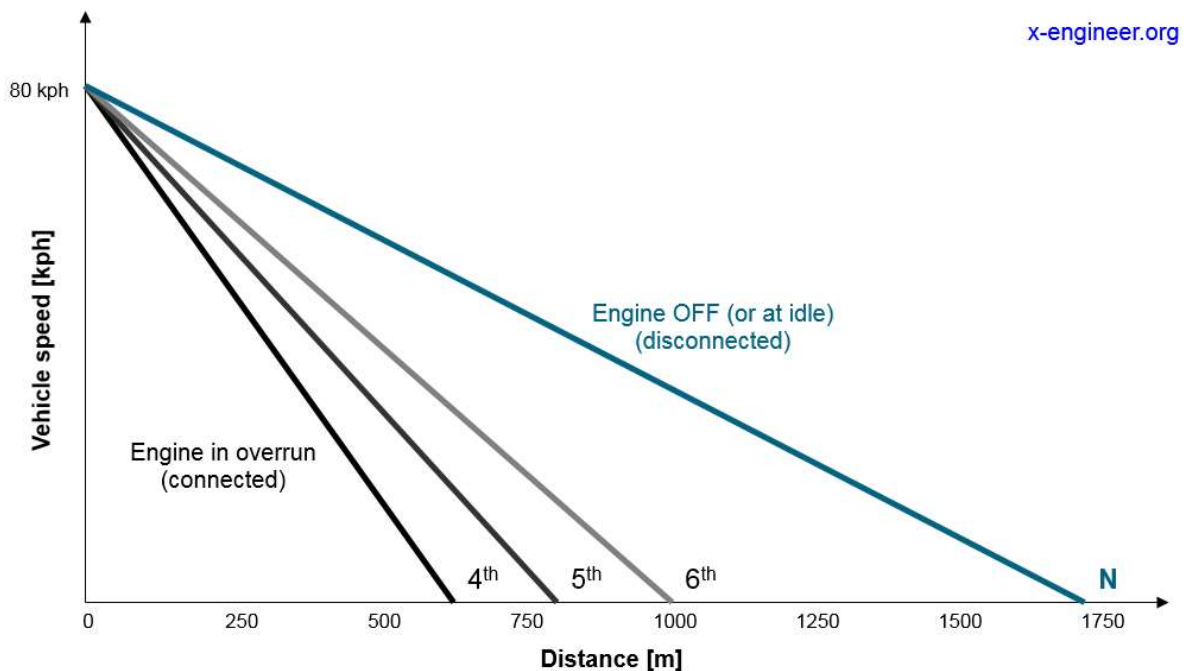


Figure 14. Coasting effect on distance covered

## 4.2 Classification of HEVs based on powertrain layout

A classification of hybrid electric vehicles based on powertrain layout includes three categories:

- Series
- Parallel
- Series-Parallel

### 4.2.1 Series hybrid

Series hybrid consists of a serial connection of an internal combustion engine and two electric machines, as shown in Figure 15. An electric machine operates as generator whereas the other one as motor. The internal combustion engine is not connected to the wheels, it supplies mechanical power to the generator which charges the battery.

The series hybrid is not much used in passenger cars, the most common application is in the buses that frequently travel in stop-and-go traffic.

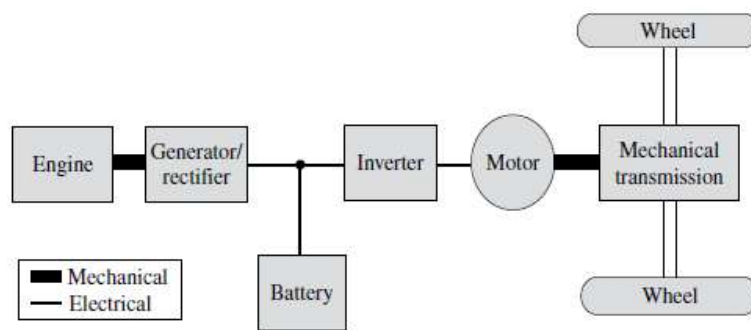


Figure 15. Series hybrid layout

### 4.2.2 Parallel hybrid

Parallel hybrid requires only an electric motor that can work both as generator and as motor in addition to the internal combustion engine, as shown in Figure 16. This can be coupled to the internal combustion engine by a belt drive, on the front end accessory drive or on the gearbox side, alternatively it can be mounted coaxially to the crankshaft on the gearbox side.

A focus on this layout is reported on paragraph 4.3.

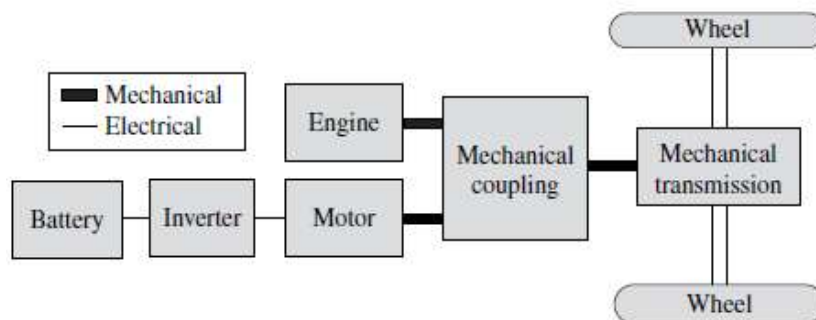


Figure 16. Parallel hybrid layout

### 4.2.3 Series-Parallel hybrid

Series-Parallel hybrid shown in Figure 17 is a combination of series and parallel hybrid. It is composed by an internal combustion engine and two electrical machines, besides it uses a planetary gear system that allows flexibly to delivery part of internal combustion engine power to the wheels while other part to the electric generator.

Electrical energy can be stored in high-voltage battery or directly delivered to the electric engine. It was introduced for the first time in Toyota Prius and represent an example of full hybridization.

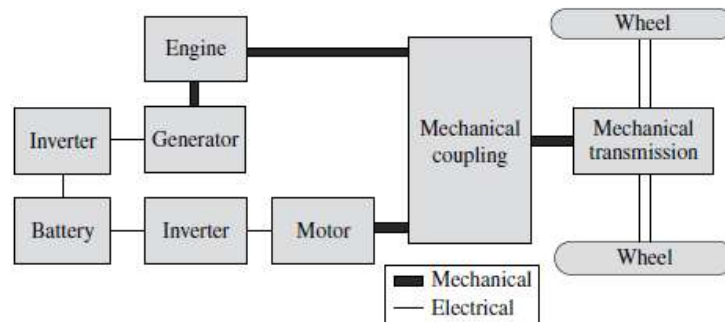


Figure 17. Split power hybrid layout

## 4.3 Classification of HEVs based on degree of hybridization

A classification of hybrid powertrains regards the degree of hybridization, intended as the contribution of electric machine to the overall traction power. HEVs can be categorized into three groups:

- Micro hybrid;
- Mild hybrid;
- Full hybrid.

### 4.3.1 Micro Hybrid

Micro Hybrid is the lightest form of hybridization which permits essentially to implement Start&Stop function. The internal combustion engine is switched off when the vehicle stops, whereas it is cranked by the electrical machine, when the vehicle starts again. In the simplest systems, the conventional starter mounted on flywheel is replaced with a reinforced starter optimized for S&S. In the most advanced systems the starter and the alternator is substituted with a belt driven electric machine mounted on Front End Accessory Drive, which can perform also Enhanced Start&Stop.

Regenerative braking is limited because the kinetic energy recovered from the wheels has to be discounted of engine drag and the torque assist contribution is modest because of electric machine power.

BSG ( *Belt driven Starter & Generator*) 12V systems , which have an electric motor with power between 2 and 3 kW, belong to this category. It guarantees a fuel consumption saving on NEDC up to 5%, compared with baseline vehicles adopting conventional Start&Stop.

#### **4.3.2 Mild Hybrid**

Mild hybrid is characterized by more powerful powertrains because the electric motor power can reach up to 20 kW and the voltage adopted by many suppliers is 48V. In addition to the enhanced Start & Stop, the torque boost and regenerative braking performed becomes relevant in terms of performance and fuel consumption.

Besides, some system is able to support also pure electric driving although with a limited range (about 2 km).

BSG (*Belt driven Starter & Generator*) 48V system and ISG (*Integrator Starter Generator*) 48 V are applications of mild hybrid concept. They achieve a CO<sub>2</sub> reduction on NEDC, respectively, up to 9% and 20%, compared with baseline vehicle adopting conventional Start&Stop.

#### **4.3.3 Full Hybrid**

Full hybrid architectures presents electric motor power higher than 25 kW and voltages up to 400V. In addition to hybrid functions already seen, they can cover in pure electric mode a distance higher than 50 km.

Plug-in hybrid is a variant of full hybrid in which the traction battery can be charged also externally from the power socket in order to extend the autonomy in pure electric driving.

Their need of larger batteries represents the main disadvantage in terms of weight and cost.

## 4.4 Classification of parallel hybrid vehicles based on electric machine position

The parallel hybrid combines two traction systems, one based on internal combustion engine and one based on electric machine that works both as motor and as generator. They are coupled on the same axis at crankshaft level or on different axis through the road. The torques of the two drives are added while the rotational speeds have a constant ratio, so it is not possible selecting independently operating points of two motors.

The main classification of parallel hybrid depending on the electric machine position is clarified on Figure 18.

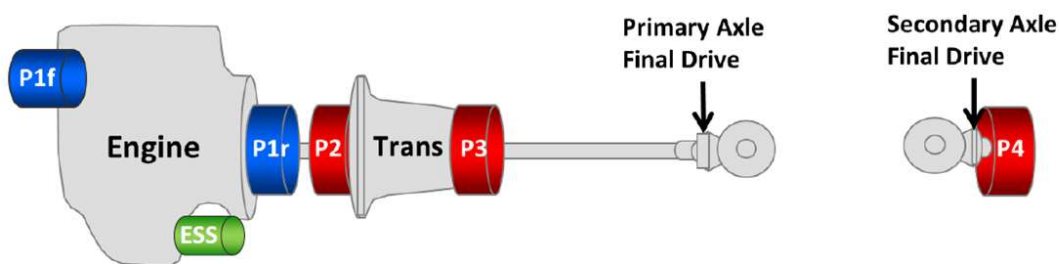


Figure 18. Classification of parallel hybrids

### 4.4.1 P1f layout

The P1f layout, also called P0, requires the internal combustion engine connected with electric machine by means of a pulley belt system on front end accessory drive, as schematized in Figure 19. This topology is often designated as BSG (*Belt driven Starter & Generator*), independently from the voltage. Pure electric mode is theoretically possible but e-machine should to drag ICE with resulting losses, noise and vibrations therefore generally it is not performed.

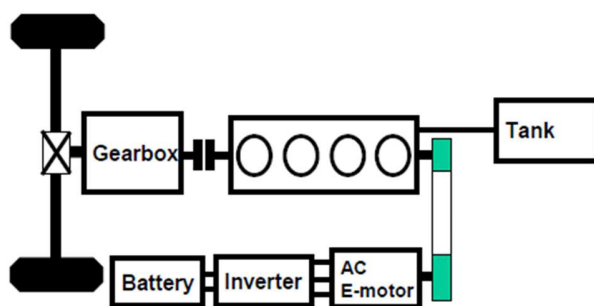


Figure 19. P1f layout



Figure 20. Installation of Valeo BSG 12V

#### 4.4.2 P1r layout

The P1r layout, also called P1, requires the electric machine mounted coaxially to the engine without any clutch, as schematized in Figure 21. It allows an optimal integration with ICE because its rotor replaces flywheel reducing axial clearances. Nevertheless during regenerative braking phase, the fact that electric motor is constantly attached to the engine reduces the recovered energy because of friction and pumping losses.

Two examples of this topology is IMA (*Integrated Motor Assist*) system developed by Honda (Figure 22), that adopts VVA (*Valve Variable Actuation*) by which the intake and exhaust valves of the engine can be easily closed to reduce engine drag losses, and Blue Hybrid on Daimler S400 (Figure 23).

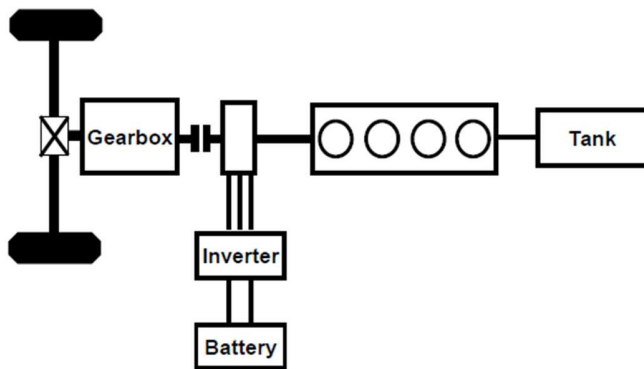


Figure 21. P1r layout



Figure 22. Integrated Motor Assist (IMA) by Honda

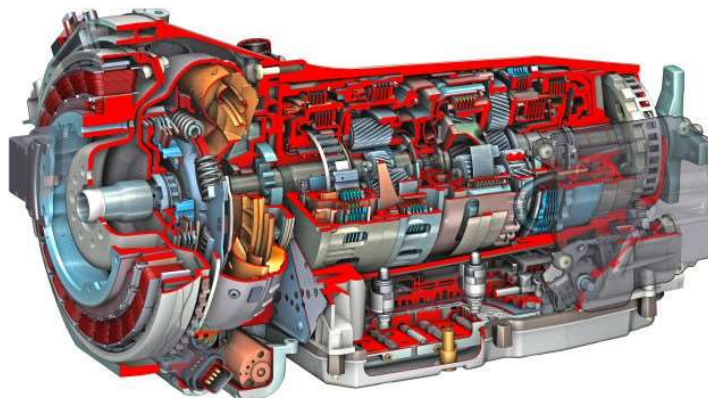


Figure 23. P1r application on Daimler S400

#### 4.4.3 P2 layout

In P2 layout an additional clutch, usually called K0, is positioned between the internal combustion engine and the electric machine. During regenerative braking, the engine drag losses is eliminated by opening the clutch, which disconnects combustion engine from the drivetrain. During pure electric mode, the clutch open allow to keep ICE switched off and disconnected from the drivetrain.

The applications of P2 are the BSG systems on the driveline side (P2 Non-coaxial, shown in Figure 24 ) and ISG systems (P2 Coaxial, shown in Figure 26), independently from the voltage.

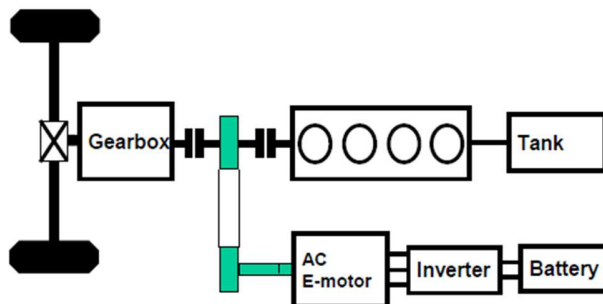


Figure 24. P2 non-coaxial layout



Figure 25. P2 non-coaxial by Continental

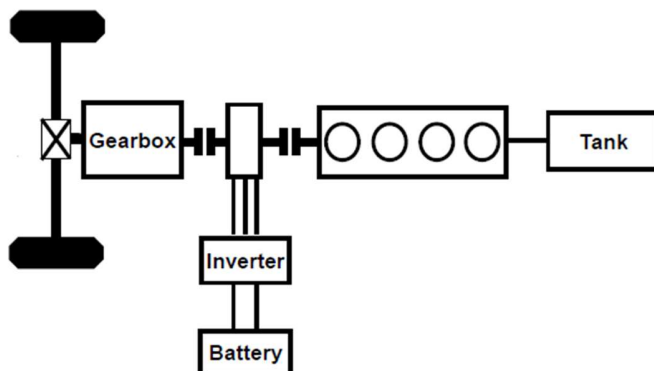


Figure 26. P2 coaxial layout



Figure 27. P2 coaxial application by Mercedes-Benz

#### 4.4.4 P3 layout

In P3 layout the Internal combustion engine and electric machine are coupled on the same axis at transmission level, for instance, by means of chain system (Borg Warner, Figure 28). Besides the torque addition, it gives the opportunity to choose separately the speed both of the ICE and the e-machine. The potential of regenerative braking is higher because the motor is upstream the gearbox and it is not affected by transmission losses.





Figure 28. P3 e-machine by Borg Warner

#### 4.4.5 P4 layout

In the P4 layout the thermal and the electrical drivetrains are placed separately on the two axles. The addition of the torque, necessary to propel the vehicle, is obtained through the road (TTR, *Through The Road*, hybrid) and the rotational speeds depend on the wheel diameters and slip.

The functions of regenerative braking and pure electric mode is realized via the electric rear axle, in the case of front-wheel-drive vehicles. P4 makes it possible to obtain high levels of efficiency in regenerative braking and pure electric mode. Furthermore, when both motors are active it enables an electric four-wheel-drive. Because when the vehicle is stationary the e-machine cannot produce electrical power, it is introduced an electric generator coupled with the combustion engine and this constitutes P1f-P4 system.



Figure 29. P4 e-machine by Borg Warner



## 5. Overview on components of hybrid systems

The majority of hybrid systems, independently from the specific application, shares a number of additional components compared to conventional vehicles, here listed:

- Electric machine
- Power electronics
- Lithium-Ion Battery

In this chapter each of these components will be analyzed more in detail.

### 5.1 Electric machine

The electric machine converts the electrical energy delivered by battery into mechanical energy (motor mode), which contributes to vehicle motion, or vice versa (generator mode), in order to perform regenerative braking and charge on-board energy storage.

As highlighted in Figure 30, a generic electric machine in motor mode has a large constant torque speed range suitable especially for engine cranking. The higher torque values compared to the conventional starter allows to achieve short cranking time which make the engine restart more comfortable. While the constant power speed range is used to perform torque boost function.

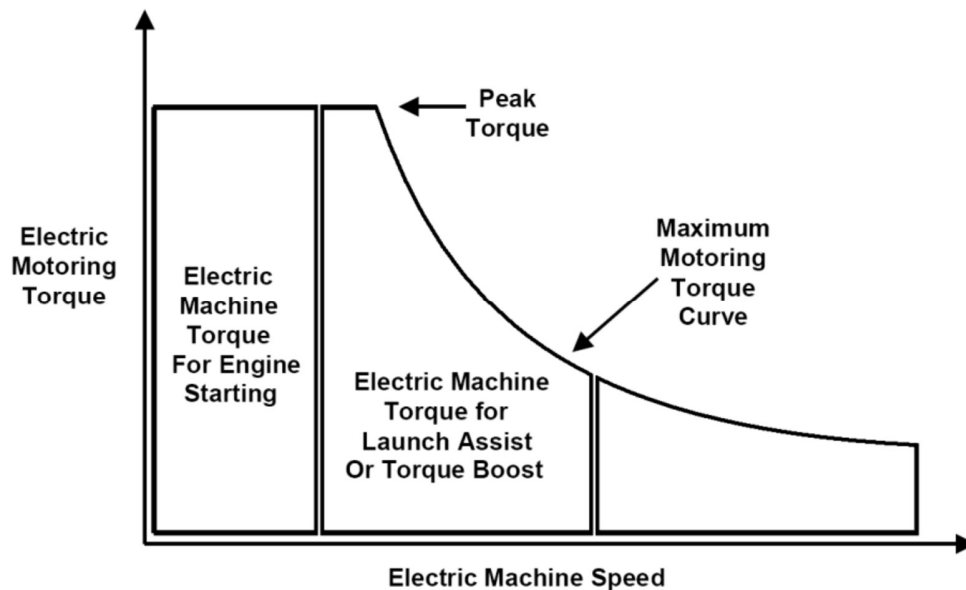


Figure 30. Motoring torque curve

Considering a generic electric machine generating power curve in Figure 31, it is evident the regenerative braking capability is limited at very low speeds. Therefore the fraction of braking power delivered by hydraulic system has to be increase for low vehicle speeds.

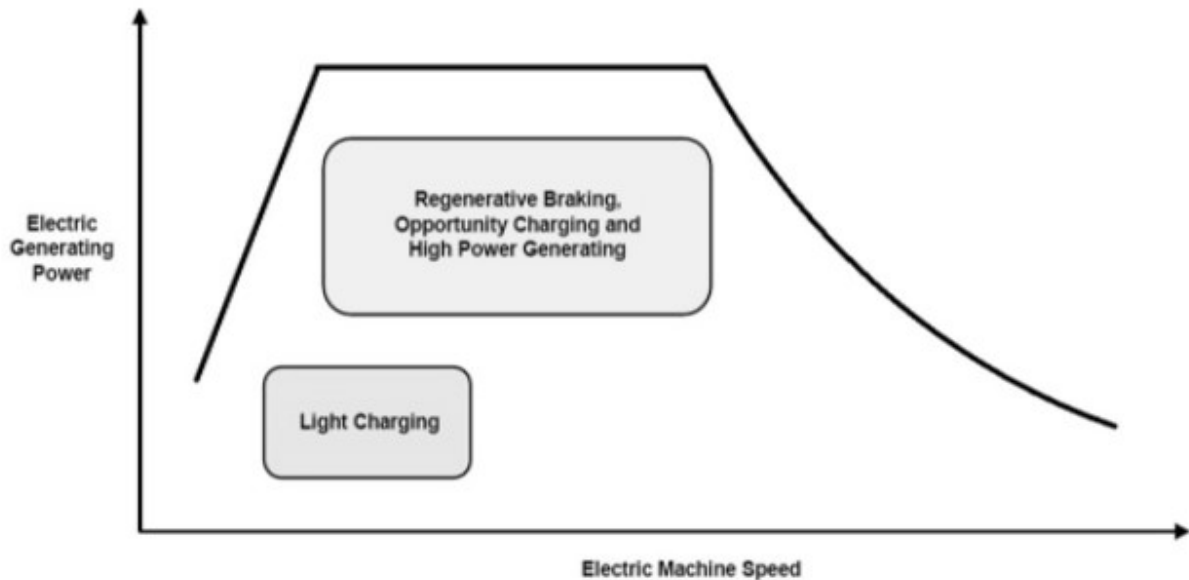


Figure 31. Generating power curve

For hybrid applications here studied, the electric machines proposed by various suppliers are permanent magnet synchronous machines (PMSM). They are so called because the rotor must follow the magnetic rotating field produced by the stator windings at synchronous speed. When the stator windings are supplied with a three-phase sinusoidal current, it generates a magnetic rotating field which attracts the rotor magnets (motor mode). When the rotor is driven by an external source, the consequent magnetic field induces a three-phase sinusoidal voltage in the stator winding (generator mode). Permanent magnets in the rotor are appropriately shaped and their magnetization directions controlled to have on the rotor induced waveforms sinusoidal. PMSMs are classified according the position of magnets in the rotor. If the magnets are glued on the surface of the rotor, it is called surfaced-mounted PM motor (SPM). If the magnets are inserted inside the rotor, it is called interior permanent magnet rotor (IPM). SPMs are simpler structurally but could have problems at very high speed, due to the high centrifugal forces. IPMs are more complex structurally but they can operate at higher speed and provide a constant power over a wider speed range.

Both for BSG and ISG systems the electric machine belongs to IPM category, and for BSG it is named often claw pole machine.

## 5.2 Power electronics

The power electronics are used to supply the electric machine with correct voltage and current and as interface between motor and on board electrical network. Here it will be analyzed inverter, usually integrated in the electric machine, and DC/DC converter, required when there are different voltages on the vehicle systems. Furthermore a paragraph will be dedicated also to elementary explanation of power switches.

### 5.2.1 Inverter or AC/DC Converter

The inverter converts the direct current (DC) supplied by the battery in alternating current (AC) to feed the electric machine, during motor mode. Vice versa it converts AC generated by the electric machine to DC which is stored in the battery, during generator mode. Usually the inverter is integrated in the electric machine housing, therefore there are no external cable between inverter and e-machine.

The circuit of a typical inverter used to control a three-phase motor is shown in Figure 32. It has three legs feeding the three phases of the electric motor and every leg is constituted by two series of a diode in parallel with a switch, usually a MOSFET.

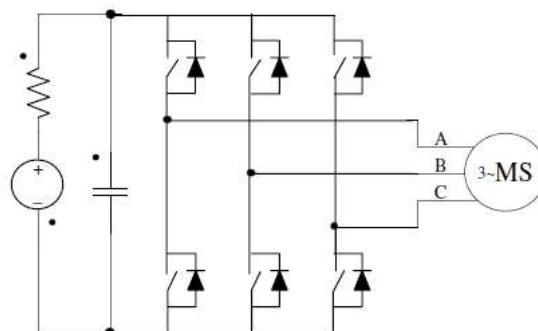


Figure 32. Circuit of an inverter

The output of a voltage insource inverter is controlled by means of pulse width modulation (PWM) to produce sinusoidal waveforms. Actually the resulting voltage consists of a series of voltage steps whose width varies depending on the modulation strategy, as shown in Figure 33. The voltage steps which supply each phase of electric machine, thanks to the inductive effect in the windings, create a roughly sinusoidal current of the required amplitude and frequency.

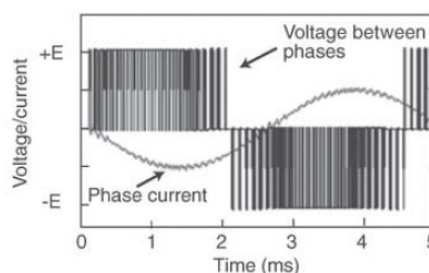


Figure 33. Pulse Width Modulation

### 5.2.2 DC/DC converter

A DC/DC converter allows to link two sources at different direct voltages. In general, it consists of a single leg with two power switches, generally MOSFET for 12/48V systems, in parallel to two switches, as clearly showed in Figure 34.

Usually DC/DC converter adopted is buck-boost type which offers an output voltage lower than input (buck mode), but also an output voltage higher than input (boost). Besides it is a bidirectional device, which means the current direction can be changed also during converter operations.

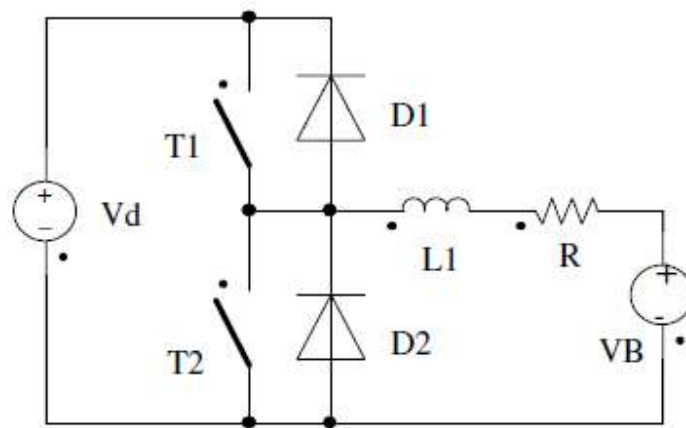


Figure 34. Circuit of a DC/DC converter

### 5.2.3 Power switches

The diode schematized in Figure 35 is an electric dipole with two electrodes, anode and cathode, and current can flow through the diode only if the anode potential is greater than the cathode potential. When the diode is conducting (direct polarization), the diode behaves like a closed switch, when the diode is not conducting (reverse polarization), the diode behaves like an open switch. The diode conducts current only in one direction and blocks voltage in the negative direction. Therefore the main application of diodes regards the rectification of alternating current (diode rectifiers), for example to link electric machine to 12 V onboard network.

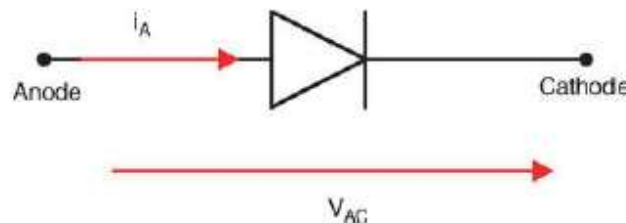


Figure 35. Diode scheme

The MOSFET (Metal Oxide Semiconductor Field Effect Transistor), shown in Figure 36, is a component often used in low voltage applications, such as starter-alternator or adaptation between network at different voltages. It is a switch formed by three terminals: gate, drain and

source. The MOSFET allows forward flow of current and blocks forward voltage between drain and source. Essentially it is a switch controlled by the voltage between gate and drain.

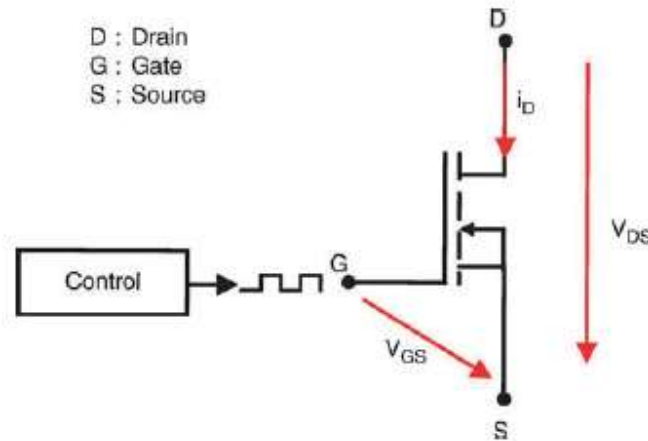


Figure 36. MOSFET scheme

## 5.2.4 Lithium-Ion Battery

Lithium-Ion battery is particularly suitable for hybrid applications, due to its elevated energy and power density. In fact, compared to other technologies such as lead acid (PbA) and nickel cadmium (NiCd), it results much lighter and less voluminous. Furthermore this type of batteries supports high peak power levels, necessary especially with regenerative braking and torque boost functions.

The performance map of various batteries reported on the Ragone plot in Figure 37 underlines that Li-Ion technology is practically the best solution. Li-Ion technology offers acceptable power output at low state of charge, especially if compared to PbA, but meanwhile it requires more control monitoring to avoid undesirable overcharge and over temperature. From the cost point of view, lithium and NiMh batteries are comparable, instead they are more expensive than lead acid. Nevertheless it seems that this type of battery thanks to higher energy, higher power and the potential for decreasing cost is the optimal candidate for hybrid vehicles also in the future.

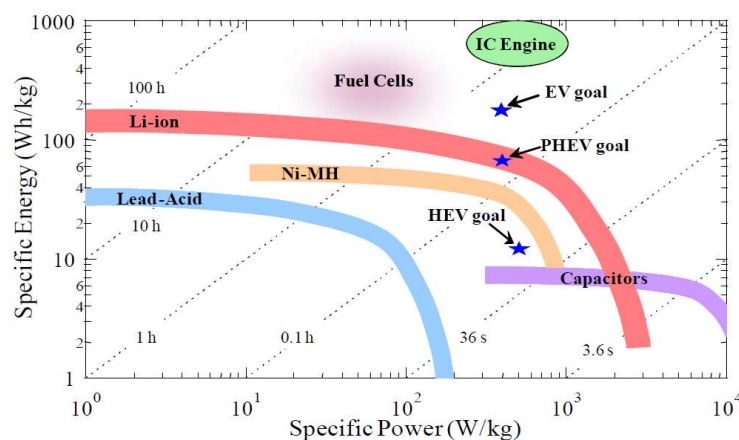


Figure 37. Ragone Plot

## 6. Description of Micro-Hybrid architectures

In the actual state of the art the main application of Micro-Hybrid is P1f layout with a BSG 12V (P1f 12V), which allows to enhance Start&Stop function, compared to reinforced starter, and in addition to implement torque boost and regenerative braking.

Basically it can be considered the result of a gradual development realized by automotive suppliers over the last years. In the next paragraphs will be discussed this development from conventional starter and alternator, whereas in the paragraph 6.4 it will be described entirely P1f 12V system and its architectural implications.

### 6.1 Conventional starter and alternator

On the conventional vehicles electric power is generated by an alternator driven by a belt on front end accessory drive (FEAD). It supplies the DC 12 V on board electrical network by mean a diode bridge which converts one-sidedly alternating current (AC) into direct current (DC). The unidirectional performance of diode bridge implies the alternator cannot operate as motor and a starter motor is required for engine cranking.

An example of conventional on-board electrical network is shown in Figure 38.

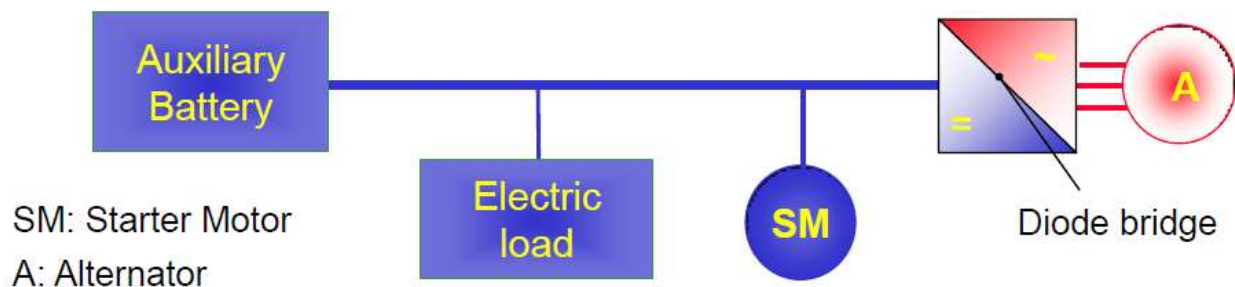


Figure 38. Conventional on-board electrical network

The increased power of vehicle network and the research towards minor fuel consumption have conducted many suppliers to improve the electrical machine, its power electronics and its control strategy, enhancing the global efficiency of the system.

Regarding to the control, a strategy introduced has been the battery charging preferably during decelerations, when the engine is driven by the wheels, in order to recover a small portion of kinetic energy. Inversely, the alternator is switched to run at zero torque during accelerations phases, while 12 V battery supplies the accessories with electricity. A system with this functionality is, for example, *Volt Control* by Valeo.

The next step has been the introduction of Start&Stop (S&S), which permits to switch off the engine, when it is not producing a driving force to propel the vehicle, for example in the urban traffic condition, to insure a fuel consumption saving and consequently emissions reduction.

A continuum of technical solutions has been adopted to enhance S&S performance, as explained in the following paragraphs 5.2 and 5.3

## 6.2 Reinforced starter

The first solution adopted has been the reinforced starter, also called enhanced starter. The conventional starter is boosted and its meshing mechanism is reinforced. A specific battery, based on Absorbent Glass Mat (AGM) or Enhanced Flooded Battery (EFB) technology, replaces the conventional 12 V battery to cope with the greater number of charge/discharge cycles. Therefore this system can withstand large number of engine starts (up to 600.000) guaranteeing low noise emissions and vibrations. Its integration does not require adaptation of the powertrain components and its industrialization cost is limited.

Nevertheless keeping the starter mounted on the flywheel makes it difficult to restart engine when it is still rotating. The engine can be shut off only with vehicle at standstill and this means that a reinforced starter is able to perform only conventional Start&Stop.

In the next sections it is presented the reinforced starters proposed by the various suppliers.

### 6.2.1 Reinforced starter by Bosch

Bosch has developed a series of reinforced starter motors called *Efficiency Line*, which is specifically used on vehicles with Start&Stop. The starter motor named Nose-type is suitable for passenger cars and that one named Nose-less is suitable for heavy duty vehicles. The reinforced starter allows to deal with higher number of starting operations because the bearings and pinion-engaging mechanics is strengthened, the planetary gear mechanism is improved and commutator is optimized for longer life.

The series production of these starter motors has begun since 2007 and initially found application in cars such as Porsche Panamera, VW Passat, Fiat 500 and Audi A8.

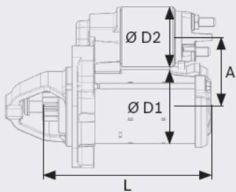
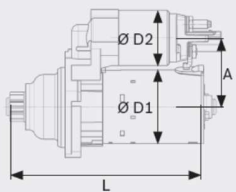
			Nose-type starter motor		Noseless starter motor	
						
			SC70-S	SC70-M	SC70-L	S78-M
			Gasoline		Diesel	
Weight	Nose-type	[kg]	2.8	2.9	3.1	4.3
	Noseless	[kg]	3.1	3.2	3.4	4.7
Length	(L)	[mm]	166	170	180	190
	Noseless		197	201	213	220
Stator housing	Ø (D1)	[mm]	70	70	70	78
Relay	Type		305	305	305	305
	Ø (D2)	[mm]	52.5	52.5	52.5	52.5
Axle distance						
Relay/stator housing	(A)	[mm]	65.5	65.5	65.5	71
Max. battery	(DIN)	[Ah/A]	66/300	66/300	88/395	143/570

Figure 39. *Efficiency Line* specifics

### 6.2.2 Reinforced starter by Valeo

Valeo proposes *ReStart reinforced starter*, which allows to switch off the engine only when the vehicle is stationary. It is controlled by the ECU (Electronic Control Unit) in dependence of the signals from brake and clutch pedal sensor, battery sensor, neutral gear sensor and engine coolant sensor.

An exploded view is reported on Figure 40.

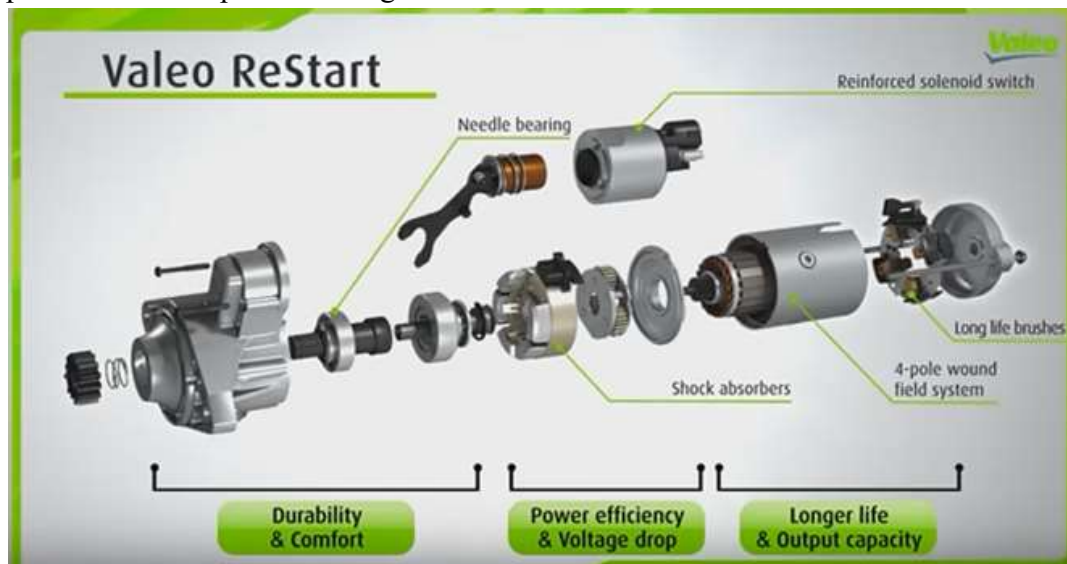


Figure 40. *ReStart reinforced starter*

### 6.2.3 Reinforced starter by Denso

Denso has commercialized reinforced starter allowing fly starting, so it does not need to wait for the engine speed to reach zero speed before restarting. This optimization is achieved by precisely synchronizing the speeds before engaging the pinion (*Tandem Solenoid Starter*) or by permanent engagement of the starter pinion on the flywheel, disconnecting the pinion at high speed through use of a free wheel (*Permanent engaged Starter*).

#### Tandem Solenoid Starter

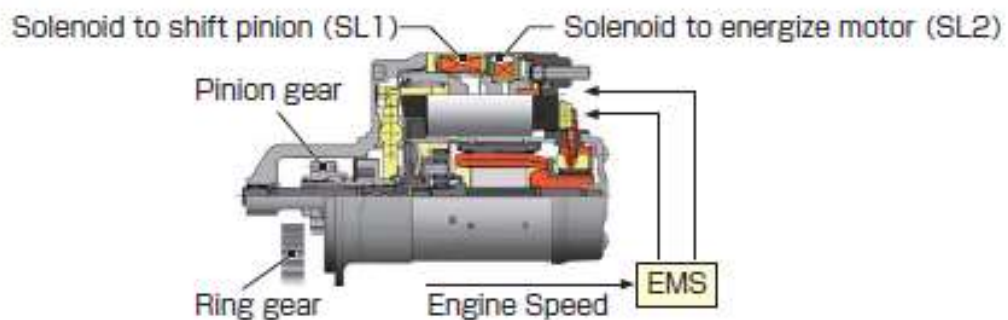


Figure 41. *Tandem Solenoid Starter*



### 6.3 Introduction of BSG 12V system by Valeo

The first BSG 12V system commercialized was Valeo *StARS* (*Starter Alternator Reversible System*) in 2004, fitted on Citroën C1 and C2 Stop-start and on the Daimler Benz Smart Fortwo MHD. Its principle is to operate Start&Stop through the use of a generator, which is used also as motor to restart engine. The components of this system are, essentially, a reversible belt driven 12V e-machine and a separated 2.5 kW voltage source inverter to allow both starter and alternator operations, shown in Figure 42.



Figure 42. Valeo *StARS*

Successively Valeo developed a second generation of BSG system, called *i-StARS* (*integrated Starter Alternator Reversible System*), with the aim to integrate all the power electronics at the rear of the electrical machine, as illustrated in Figure 43, differently from the *StARS* generation in which it is positioned in an external box.



Figure 43. Exploded view of *i-StARS*

*StARS* and the first generation of *i-StARS* could not implement regenerative braking because the energy which has to be stored during deceleration phases is excessive and potentially damaging for a lead acid battery because of the peaks of current. For this reason, the successive generations of *i-StARS* was developed by Valeo to store the energy during the regenerative breaking inside a lithium-ion battery or alternatively into supercapacitors. Currently the first solution is the most diffused between OEMs, the second solution is adopted only by PSA and Mazda.

## 6.4 P1f 12V system

P1f layout with a Belt Starter Generator 12V (P1f 12V) can be considered a second development of Start&Stop concept because the engine can be shut off also when the vehicle is still moving at low speeds (Enhanced S&S) and because the cranking results more comfortable compared to previous systems. Nevertheless, it is usual to install also conventional starter to perform cold engine cranking in order to guarantee a redundant solution.

Besides the system can performs torque boost and regenerative braking functions even if with modest performances, because of it limited power.

The alternator is replaced by a reversible machine which acts both as starter and alternator because its power electronics adopts a bidirectional device, a MOSFETs inverter bridge, which makes it possible to operate on the all four quarters of plan torque-speed. It is connected to engine by pulley-belt system, analogously to a conventional alternator, but to make it possible transmission of torque in both directions a tensioning system on the two strands is required. In addition to lead acid battery, a lithium-ion is required on the one hand in order to absorb current peaks and store energy, during regenerative braking, and on the other one in order to supply energy to electric motor, during E-assist. A typical layout of P1f 12V is reported on Figure 44.

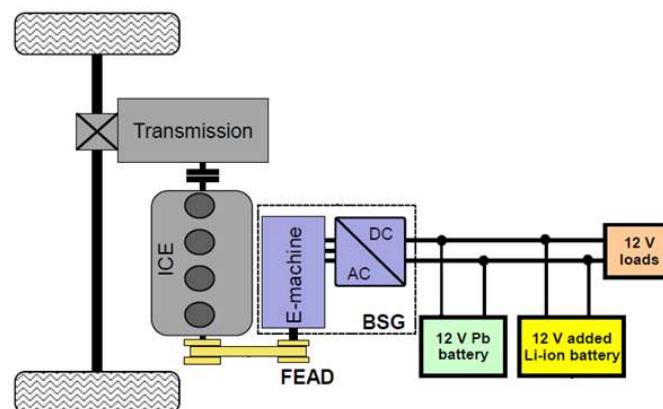


**Figure 44. P1f 12V layout**

### 6.4.1 Components of P1f 12V system

The components of P1f 12V system available on the market are numerous but they have all comparable characteristics. The electric machine chosen for this study is a Valeo *i-StARS* BSG 12V, whose technical specifications are reported on Table 8.

The power curve in motor mode, reported on Figure 45, and in generator mode, reported on Figure 46, highlights that the e-machine has different performance as motor and generator both in terms of power and of maximum speeds.

12 V BSG (Valeo i-StARS Gen. 3)	
Technology	Synchronous claw poles inner magnets
Torque boost power [kW]	2,5
Maximum speed motor mode [rpm]	6000
Regenerative braking power[kW]	6
Maximum speed generator mode [rpm]	20000
Max Torque cranking [Nm]	50
Geometry (Diameter x Length) [mm]	152 x 157
Weight [kg]	8
Cooling [kg]	Air cooled

Table 8. BSG 12V Valeo *i-StARS* specifications

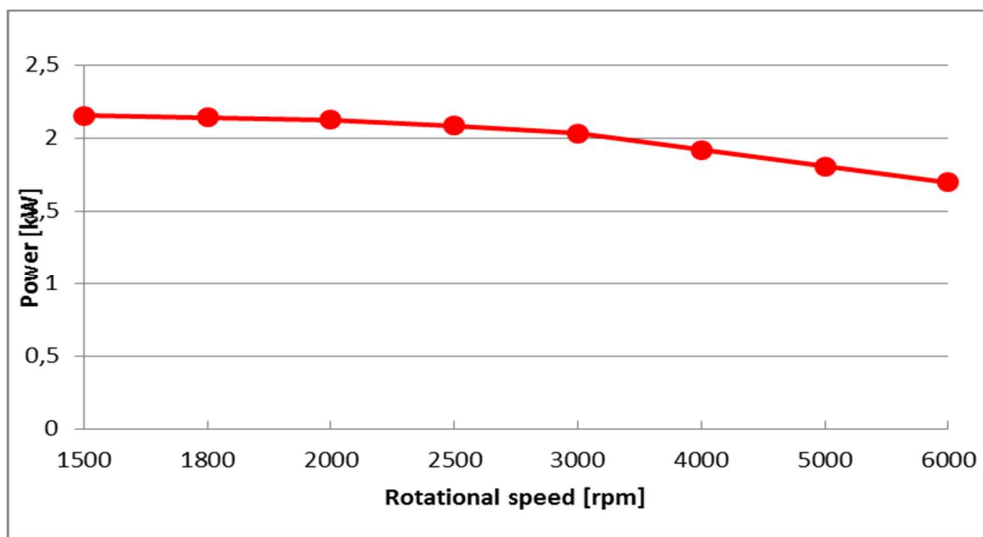


Figure 45. Power curve BSG 12V Valeo *i-StARS* in motor mode

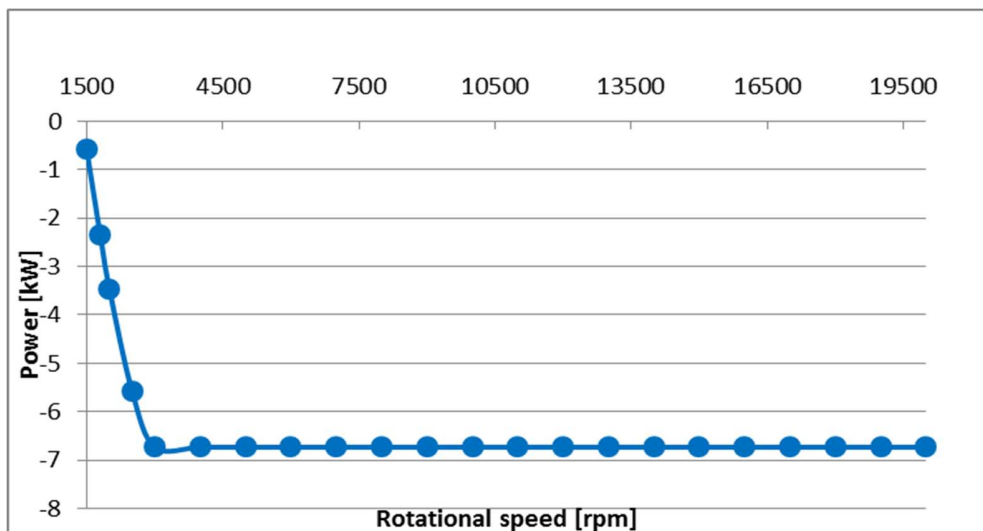


Figure 46. Power curve BSG 12V Valeo *i-StARS* in generator mode

As energy storage, it is described a Lithium-Ion battery by Samsung (Figure 47), whose technical description is reported on Table 9.

12 V Lithium-Ion Battery by Samsung	
Capacity [Ah]	12,6 Ah
Available energy [Wh] (SOC 70%-30%)	60
Voltage range [V]	11-15,5
Geometry (L x W x H) [mm]	175 x 110 x 188
Weight [kg]	4,5
Cooling	Passive air

Table 9. Samsung 12V Lithium-Ion Battery data

The main constraints regarding its installation are on the one side the risk of fire, in the case of crash or at temperatures higher than 70 °C, and on the other side the necessity to limit the distance from electric machine in order to contain Joule effect losses and drop voltage in the wires.



Figure 47. Samsung 12V Lithium-Ion Battery

### 6.4.2 Impact of a P1f 12V system on vehicle architecture

On the whole this system modifies the conventional vehicle architecture essentially because it requires:

- Installation of a belt driven electric machine on FEAD ( Front End Accessory Drive);
- Positioning of a lithium-ion battery;
- Modification of on-board electric network.

Therefore the integration of this system involves a series of operations here listed:

- The conventional alternator is usually removed because it is substituted by the belt driven starter generator. In order to transfer the mechanical power between combustion engine and electric machine in both two directions, the front end accessory drive has to be adapted modifying pulleys, tensioners, idlers and belts. It is required a bidirectional drive-tensioning system, as discussed in paragraph 6.4.3;
- It is necessary to find the optimal location of the lithium-ion battery complying with following constraints:
  - It has not to be too far from the electric machine to avoid relevant losses, due to the Joule effect and to the voltage drop;
  - It must fulfill the safety compliance respect to crash test;
  - It cannot be positioned in the engine compartment due to the high risk of fire, at temperatures over 70 °C and in case of damage by crash;
  - Its position has not to impact excessively on the vehicle roominess;
- New wires are installed in order to link electric machine to the lithium-ion battery;
- The electrical network is modified because the starter generator is linked to the lithium-ion battery but also to the lead acid battery and this requires a power switch which has to be opportunely located;
- It could be necessary to review the engine mounts for NVH (Noise, Vibration and Harmonics) requirements.

The interventions required to integration of P1 12 V system are summarized on Table 10.

Furthermore, this system adds weight to the base car due to introduction of the mentioned components.

An indicative estimation of P1f 12V impact on vehicle weight is reported on the Table 11. It needs to underline the “Starter” delta is relative to the installation of a lighter reinforced starter without S&S.

<b>Electric machine</b>	<ul style="list-style-type: none"> <li>• Eventual packaging modifications in the engine compartment</li> <li>• Modification of Front End Accessory Drive (FEAD) in terms of tensioning system and belt</li> <li>• Possible variations of engine mounts</li> </ul>
<b>Lithium-Ion battery</b>	<ul style="list-style-type: none"> <li>• Position decided in order to: <ul style="list-style-type: none"> <li>○ reduce the distance from the electric machine;</li> <li>○ fulfil safety requirement;</li> <li>○ to not impact negatively on vehicle roominess.</li> </ul> </li> </ul>
<b>Electrical onboard network</b>	<ul style="list-style-type: none"> <li>• Introduction of power switch and its mounting bracket</li> <li>• New cables and their integration</li> </ul>

**Table 10. Summary on interventions required for P1f 12V integration**

<b>Component</b>	<b>Delta weight [kg]</b>
<b>Belt starter generator</b>	+8
<b>Alternator</b>	-6
<b>Li-Ion battery</b>	+4,5
<b>Power switch</b>	+0,5
<b>Mounting brackets</b>	+1
<b>Wires</b>	+2,5
<b>Starter</b>	-0,5
<b>Total</b>	<b>+10</b>

**Table 11. Additional weight due to P1f 12V system**

### 6.4.3. Focus on the modifications required on the FEAD

In the combustion engines all the accessories are driven by V-ribbed belt, on the front end accessory drive (FEAD), Figure 48. A belt system has to guarantee constant belt force during its lifetime and, as far as possible, reduced slip and noise. Usually mechanical or hydraulic belt tensioners are the solutions used to achieve this mission.



Figure 48. Front End Accessory Drive

On conventional vehicle, belt drive is characterized by accessories which operates as load, so the power is always transferred from the engine to the accessory.

On the applications of BSG, the power is transferred also from the electrical machine to the engine. Therefore, in order to permit the transfer of torque in both directions, often the solution is based on two mechanical belt tensioners, as shown in Figure 49 and Figure 50.

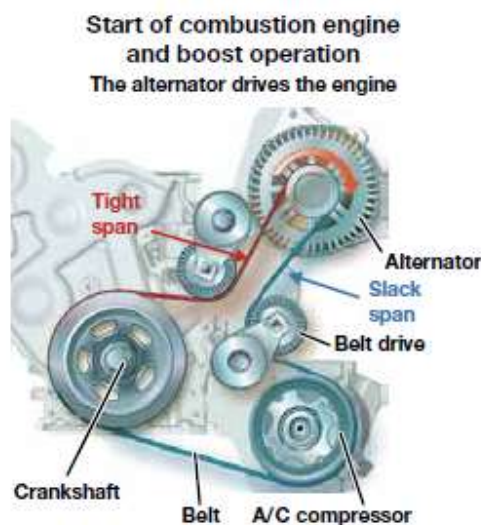
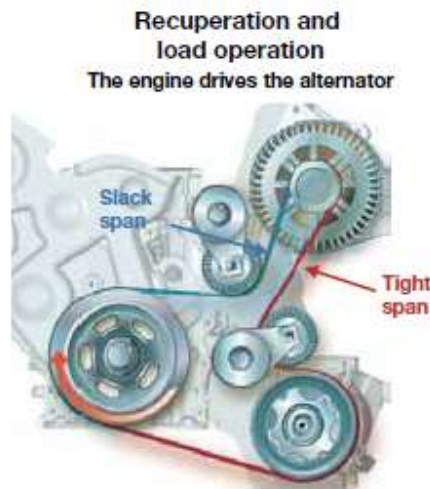


Figure 49. Motor mode

When the engine is driven by the e-machine, as represented in Figure 49, the power is transferred via tight span on the left tensioner.



**Figure 50. Generator mode**

When the e-machine works as load, as represented in Figure 50, the torque is transferred by tight span on right tensioner. The limit of this is mainly linked to resonance situations at very low speed.

Another type of design requires only a tensioner, which can rotate around the alternator's axis and offers several advantages, compared to the two tensioners assembly. It improves retention of pre-tensioned load in the slack run and, furthermore, is subject to lower dynamic loads in the belt drive due to engine excitation.

The tensioner is composed of a housing which is connected to the starter alternator by a plain bearing and it can be completely rotated around electrical machine's axis. A tensioner pulley is permanently fixed to this housing, while other tensioner pulley is located on a moving lever and is spring-mounted against the housing by means of an arc spring assembly. This allows the tensioner pulley to create the necessary belt pre-tensioning load and to compensate tolerances in the belt drive.

An example of this system is reported on Figure 51.

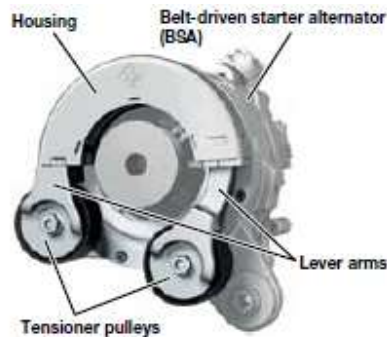


**Figure 51. Decoupling tensioner**



#### 6.4.4. Benchmarking on P1f 12V systems

The most relevant P1f 12V systems available on the market are SVHS by Suzuki and e-HDi by PSA group.

SVHS (Smart Hybrid Vehicle System) has been introduced by Suzuki on Baleno and Swift models and allows a minimal capability of recovery of energy during braking and reduced boost capability (up to 50Nm of and 2,2 kW of power). In the sum the impact on vehicle performance and CO<sub>2</sub> emissions is negligible but the car equipped with this assembly can be homologated as hybrid in Italy.

In addition to belt starter generator, it includes a 12 V 55Ah PbA battery and a 12 V 3 Ah Lithium-Ion battery supplied by Denso and positioned under front passenger seat (Figure 53).

The is usually combined with two gasoline engine: a 3 cylinders Turbo 1.0 l and a 4 cylinders 1.2 l.

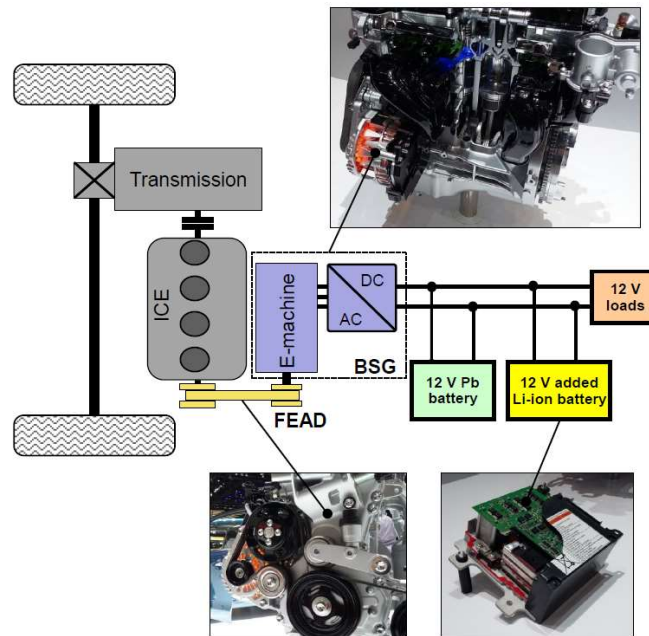


Figure 52. SVHS by Suzuki



Figure 53. Installation of Lithium-Ion Battery

e-HDi has been introduced by PSA initially on all Citroën and Peugeot cars equipped with PSA Diesel 1.6 l engines and after also on those equipped with PSA Diesel 1.4 engines. The starter generator is a Valeo i-StARS 2<sup>nd</sup> generation which offers a boost of 2,2 kW power and about 50 Nm at crankshaft level. The typical element of e-HDi system is that the energy storage necessary for electrical boost and regenerative braking is represented by supercapacitors supplied by Maxwell, instead of Lithium-Ion battery.

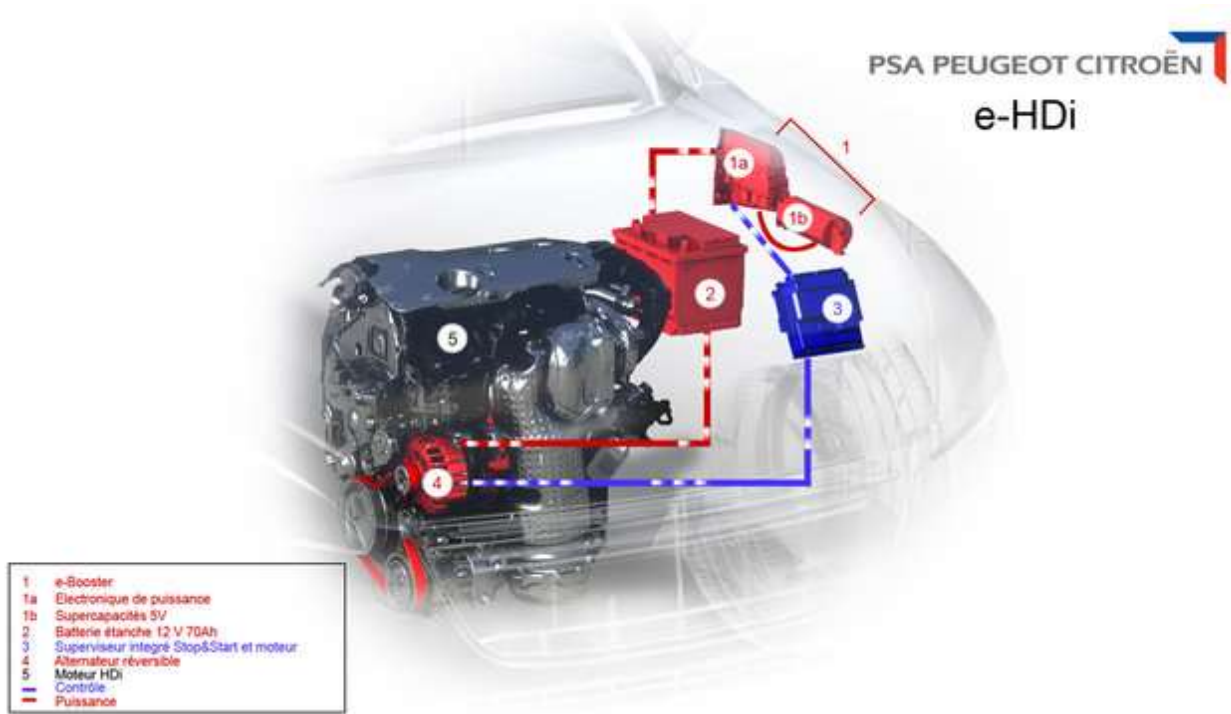


Figure 54. e-HDi by PSA

## 7. Description of Mild-Hybrid architectures

The majority of automakers around the world are implementing Mild-Hybrid concept by introducing 48 V systems. In fact they allows to achieve more reduced CO<sub>2</sub> emission compared with Micro-Hybrid systems and to improve driving experience making the equipped vehicles more attractive for end-consumers.

Their cost is relatively low because they are not subject to safety requirement of high voltage systems (>60 V), such as the galvanic isolation required between high voltage and low voltage electrical subsystems and vehicle chassis. They offer a significant advantage in terms of fuel economy without adding excessive complexity and costs peculiar of high voltage systems. Definitely nowadays 48 V systems seems an optimal compromise between CO<sub>2</sub> emissions reduction and cost.

The main advantage introduced by voltage increase from 12 V to 48 V is that it is possible support larger power demands without an excessive increase of electric current and consequently of power losses.

The 48 V Mild-Hybrid systems can be divided essentially into two categories depending on the positioning the electric machine: P1f 48 V (non-coaxial mounted on FEAD) and P2 48 V (coaxial mounted on the transmission side).

The first ones minimizes the integration cost because they requires the fewest changes on the existing vehicle architecture, while the second ones offers the highest flexibility in terms of functions, for instance pure electric driving.

A generic 48 V mild hybrid system is made up basically of following additional components:

- Electric machine (with integrated inverter)
- DC/DC converter
- 48 V Lithium-Ion battery

## 7.1 P1f 48 V system

The P1f 48V system shown in Figure 55 can be considered an evolution of P1f 12 V. It offers with a similar layout essentially the same hybrid functions with better performances thanks to more powerful components.

The introduction of a higher voltage circuit requires a DC/DC converter, which works as interface with already existent 12V network. Whereas the electric machine specifications and the battery capacity are opportunely adapted, as it will be described in following paragraph.

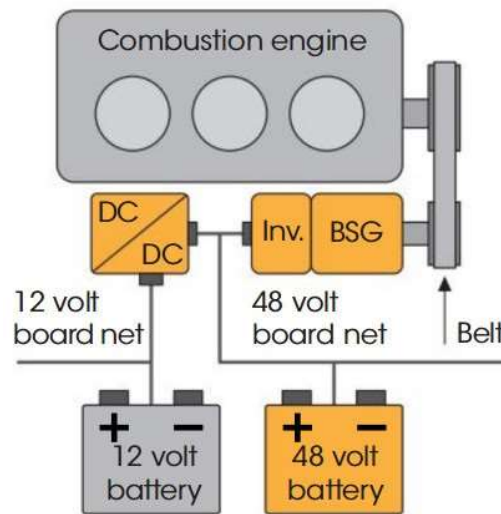


Figure 55. P1f 48V layout

### 7.1.1 P1f 48V components

The components of P1f 48V system available on the market are numerous but they have comparable characteristics. The electric machine described in this study is a Bosch 48V BRM (Boost Recuperation Machine) shown in Figure 57, whose technical specifications are reported on Table 12.

Bosch 48V BRM	
Technology	Synchronous claw poles inner magnets
Torque boost power [kW]	10
Maximum speed motor mode [rpm]	10000
Regenerative braking power[kW]	12
Maximum speed generator mode [rpm]	18000
Max Torque cranking [Nm]	56
Geometry (Diameter x Length) [mm]	148 x 168
Weight [kg]	9
Cooling [kg]	Air cooled with internal fan or liquid cooled

Table 12. Bosch 48V BRM specifications

The power curves both in motor and generator mode reported on Figure 56 highlights that the e-machine has different performance as motor and generator both in terms of power and of maximum speeds.

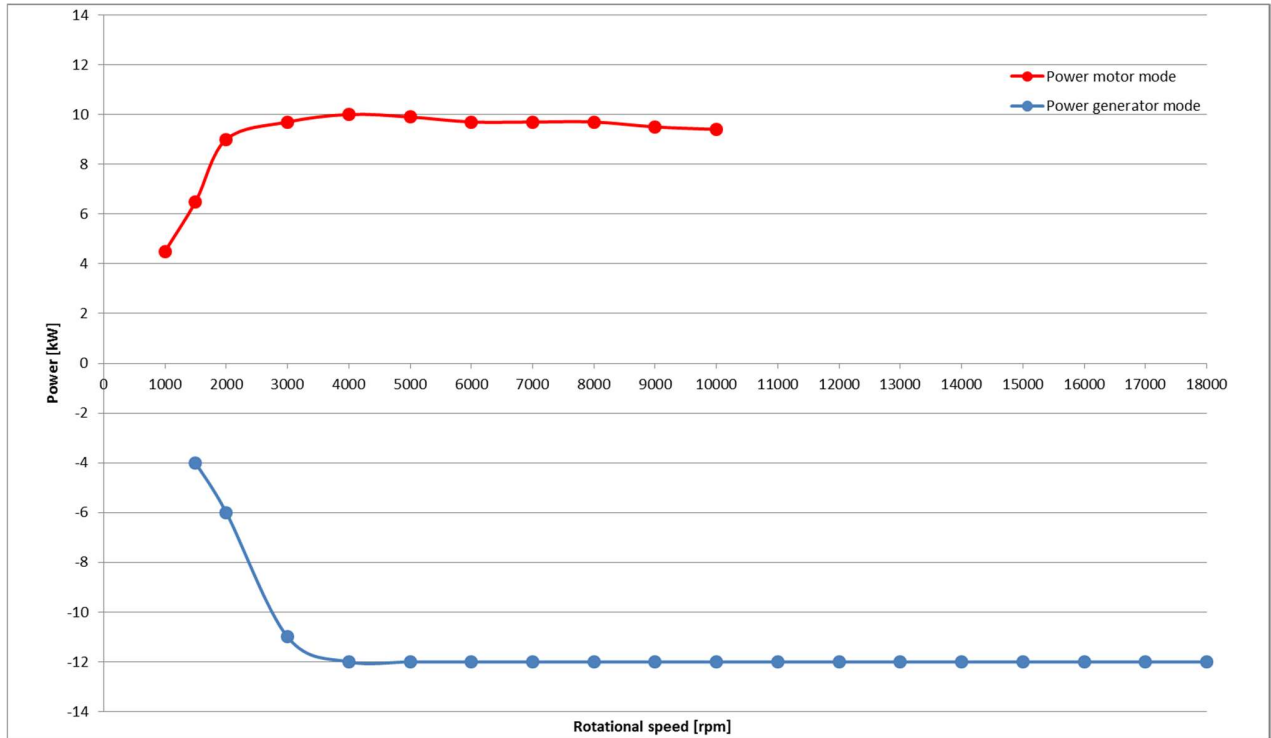


Figure 56. Bosch 48V BRM power curves



Figure 57. Bosch 48V BRM

The energy storage described is a Lithium-Ion battery by Bosch (Figure 58), whose technical description is reported on Table 13.

48 V Lithium-Ion Battery by Bosch	
Capacity [Ah]	8 Ah
Available energy [Wh] (SOC 70%-30%)	143
Voltage range [V]	24-54
Geometry (L x W x H) [mm]	300 x 175 x 90
Weight [kg]	7 kg
Cooling	Passive air

Table 13. Bosch 48V Lithium-Ion Battery data



Figure 58. Bosch 48V Lithium-Ion

The main constraints regarding its installation are practically equal to the case of P1f 12V case with respect to risk of fire, whereas the effect of cable length on losses is less relevant because to higher voltage.

In a 48V system electrical energy has to be transferred also to 12V network, therefore it is necessary a DC/DC converter to interface two circuits, shown in Figure 59. A DC/DC converter can be operated in buck-mode, when converts from 48 to 12 V, or in boost-mode, when converts from 12 V to 48 V.

The devices proposed by the various supplier are similar for characteristics. Here it is described a DC/DC converter manufactured by Bosch (Figure 60), whose technical description is reported on Table 14.

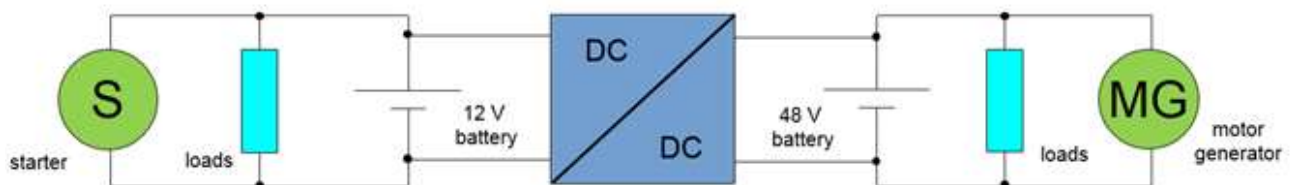


Figure 59. Electrical layout of 48V systems



Figure 60. Bosch DC/DC converter

DC/DC converter by Bosch	
Output power [kW]	1,5-2,5
Geometry (L x W x H) [mm]	197 x 180 x 95
Weight [kg]	3
Cooling	Passive or active air

Table 14. Bosch DC/DC converter

### 7.1.2 Impact of a P1f 48V system on vehicle architecture

The impact of a P1f 48 V system on vehicle architecture share many aspects with P1f 12V already described, but here it will be done a complete description, even if some considerations could appear redundant.

In general this system modifies the conventional vehicle architecture essentially because it requires:

- Installation of a belt driven electric machine on FEAD ( Front End Accessory Drive);
- Positioning of a lithium-ion battery, dimensionally larger than P1f 12V case;
- Positioning of a DC/DC converter;
- Modification of on-board electric network.

Therefore the integration of this system involves a series of operations here listed:

- The conventional alternator is usually removed because it is substituted by the belt driven starter generator. In order to transfer the mechanical power between combustion engine and electric machine in both two directions, the front end accessory drive has to be adapted modifying pulleys, tensioners, idlers and belts. It is required a bidirectional drive-tensioning system, , as discussed in paragraph 6.4.3;
- It is necessary to find the optimal location of the lithium-ion battery complying with following constraints:
  - It must fulfill the safety compliance respect to crash test;
  - It cannot be positioned in the engine compartment due to the high risk of fire, at temperatures over 70 °C and in case of damage by crash;
  - Its position has not to impact excessively on the vehicle roominess;
  - Its correct refrigeration has to be insured;

- The DC/DC converter position has to be chosen according to the following constraints:
  - It must fulfill the safety compliance, for instance respect to crash test;
  - Its position has not to impact excessively on the vehicle roominess;
  - Its correct refrigeration has to be insured;
  - It has not to be too far from the lead acid battery to avoid relevant losses, due to the Joule effect and to the voltage drop through the wires;
- New wires are installed in order to link electric machine to the lithium-ion battery;
- It could be necessary to review the engine mounts for NVH (Noise, Vibration and Harmonics) requirements.

The interventions required to integration of P1f 48 V system is summarized on Table 15.

Furthermore, this system adds weight to the base car due to introduction of the mentioned components. An indicative estimation of P1f 48V impact on vehicle weight is reported on the Table 16. It needs to underline the “Starter” delta is relative to the replacement of a reinforced starter with S&S function with a conventional starter without S&S.

<b>Electric machine</b>	<ul style="list-style-type: none"> <li>• Eventual packaging modifications in the engine compartment</li> <li>• Modification of Front End Accessory Drive (FEAD) in terms of tensioning system and belt</li> <li>• Possible variations of engine mounts</li> </ul>
<b>Lithium-Ion battery</b>	<ul style="list-style-type: none"> <li>• Position decided in order to:               <ul style="list-style-type: none"> <li>○ reduce the distance from the electric machine;</li> <li>○ fulfil safety requirement</li> <li>○ not impact negatively on vehicle roominess;</li> </ul> </li> </ul>
<b>Electrical onboard network</b>	<ul style="list-style-type: none"> <li>• New cables and their integration</li> </ul>

Table 15. Summary on interventions required for P1f 48V integration

<b>Component</b>	<b>Delta weight [kg]</b>
<b>Belt starter generator</b>	+9
<b>Alternator</b>	-6
<b>Li-Ion battery</b>	+7
<b>DC/DC converter</b>	+3
<b>Mounting brackets</b>	+4
<b>Wires</b>	+6
<b>Electric and electronics other components</b>	+9
<b>Starter</b>	-0,5
<b>Total</b>	<b>31,5</b>

Table 16. Additional weight due to P1f 48V system



## 7.2 P2 48 V system

The P2 48V system shown in Figure 61 is made up fundamentally of an electric machine coaxially mounted to the crankshaft between engine and gearbox, of a DC/DC converter and a Lithium-Ion battery. A clutch named K0 between engine and e-machine makes this architecture suitable also to cover short distances (~2km) in pure electric driving. In fact when K0 is open the traction power can be supplied entirely by motor while the engine is off. Moreover the e-machine can perform more efficiently regenerative braking by opening K0 in order to eliminate engine drag losses. The torque assist performed is relevant thanks to electric machine power.

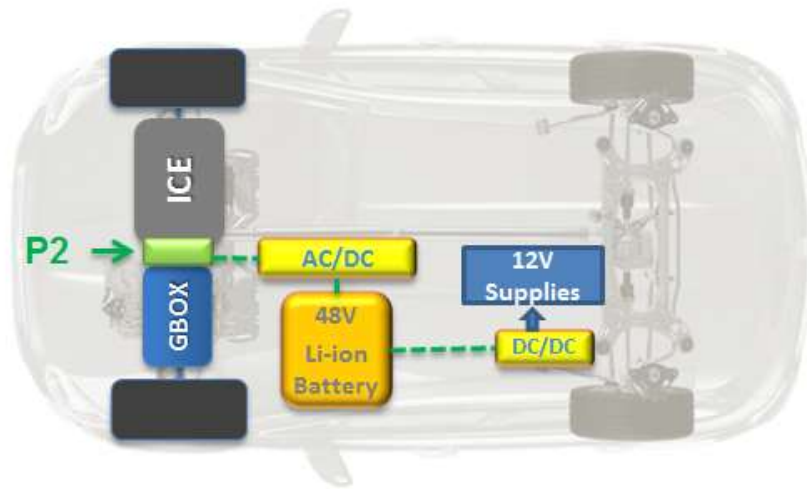


Figure 61. P2 48V layout

### 7.2.1 P2 48V components

The 48V electric machine described is manufactured by Schaeffler. Its technical specifications are reported on Table 17.

Schaeffler 48V motor	
Technology	Permanent Magnets Synchronous Machine
Torque boost power [kW]	15
Maximum speed motor mode [rpm]	7000
Regenerative braking power[kW]	23
Maximum speed generator mode [rpm]	7000
Max Torque cranking [Nm]	180
Axial length [mm]	80
Weight [kg]	34
Cooling [kg]	Liquid cooled

Table 17. Schaeffler 48V motor specifications

The power curves both in motor and generator mode is reported on Figure 56.

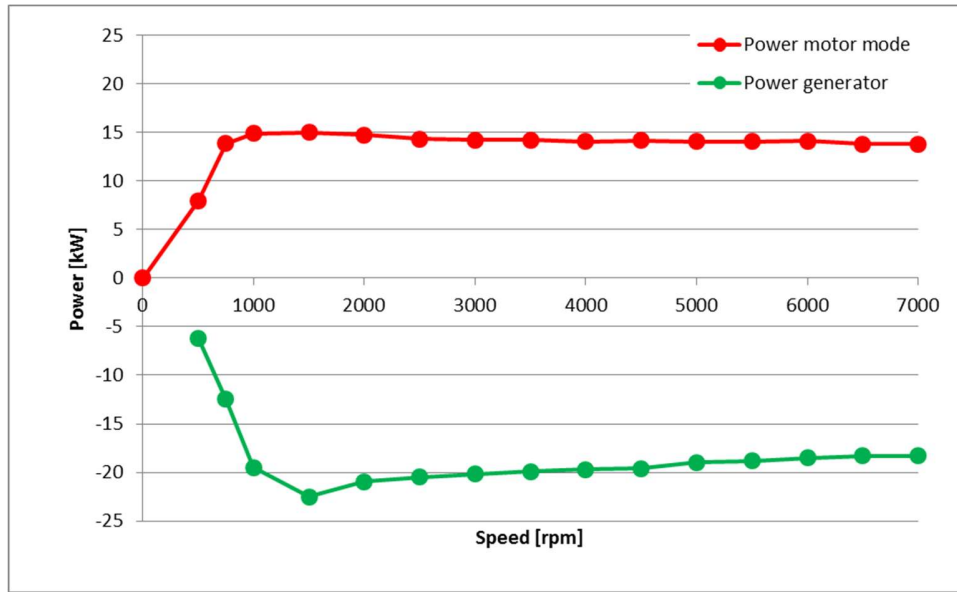


Figure 62. Schaeffler 48V motor power curves



Figure 63. Schaeffler 48V motor

The energy storage described is a Power Pack Unit (PPU), including DC/DC converter and battery. Its technical description is reported on Table 13.

48 V Power Pack Unit (PPU)	
Capacity [Ah]	17
Available energy [Wh] (SOC 70%-30%)	332
Voltage range [V]	41-49
Geometry (L x W x H) [mm]	530 x 360 x 180
Weight [kg]	20
Cooling	Active air

Table 18. 48 V Power Pack Unit

### 7.2.2 Impact of a P2 48V system on vehicle architecture

This system modifies the conventional vehicle architecture essentially because it requires:

- Installation of a electric machine mounted coaxially to crankshaft between engine and gearbox;
- Positioning of a lithium-ion battery;
- Positioning of a DC/DC converter, which can be integrated into battery pack or stand-alone;
- Revision of electric board net.

Therefore the integration of this system involves a series of operations here listed:

- A macroscopic verification about the transversal clearance due to the assembly engine-electric machine-gearbox, which has to be lower than interaxis distance between the two front side rails;
- It is necessary to find the optimal location of the lithium-ion battery complying with following constraints:
  - It must fulfill the safety compliance, for instance respect to crash test;
  - It cannot be positioned in the engine compartment due to the high risk of fire, at temperatures over 70 °C and in case of damage;
  - Its position has not to impact excessively on the vehicle roominess;
  - Its correct refrigeration has to be insured;
- The DC/DC converter position has to be chosen according to the following constraints:
  - It must fulfill the safety compliance, for instance respect to crash test;
  - Its position has not to impact excessively on the vehicle roominess;
  - Its correct refrigeration has to be insured;
  - It has not to be too far from the lead acid battery to avoid relevant losses, due to the Joule effect and to the voltage drop through the wires;
- New wires are installed in order to link electric machine to the lithium-ion battery and DC/DC converter to lead acid battery;
- It could be necessary to review the engine mounting point location and mounts themselves for structural and NVH (Noise, Vibration and Harmonics) requirements.

The list of operations required to integration of P2 48 V system is summarized on Table 19.

An indicative estimation of P2 48V impact on vehicle weight is reported on the . It needs to underline the “Starter” delta is due to the absence of conventional starter because crankshaft mounted e-machine can perform Start&Stop also in cold engine conditions.

<b>Electric machine</b>	<ul style="list-style-type: none"> <li>• Eventual packaging modifications in the engine compartment</li> <li>• Possible variations of engine mounts</li> <li>• Thermal management evaluations</li> </ul>
<b>Lithium-Ion battery</b>	<ul style="list-style-type: none"> <li>• Position decided in order to: <ul style="list-style-type: none"> <li>• fulfill safety requirement,</li> <li>• not impact negatively on vehicle roominess</li> <li>• to insure correct refrigeration</li> </ul> </li> </ul>
<b>DC/DC converter</b>	<ul style="list-style-type: none"> <li>• Position decided in order to: <ul style="list-style-type: none"> <li>○ fulfill safety requirement,</li> <li>○ not impact negatively on vehicle roominess</li> <li>○ insure correct refrigeration</li> <li>○ limit electric losses</li> </ul> </li> </ul>
<b>Electric vacuum pump</b>	<ul style="list-style-type: none"> <li>• Installation to guarantee brake booster functionality during pure electric driving</li> </ul>
<b>Lead acid battery</b>	<ul style="list-style-type: none"> <li>• No modifications</li> </ul>
<b>Electrical onboard network</b>	<ul style="list-style-type: none"> <li>• New cables and their integration</li> </ul>

Table 19. Summary on interventions required for P1f 48V integration

<b>Component</b>	<b>Delta weight [kg]</b>
<b>Electric machine</b>	+33
<b>Li-Ion battery</b>	+17
<b>DC/DC converter</b>	+3
<b>Mounting brackets</b>	+5
<b>Electric and electronics components</b>	+15
<b>Starter</b>	-3
<b>Total</b>	<b>+70</b>

Table 20. Additional weight due to P2 48V system

## 8. Application of P1f 12 V system on vehicle architecture

The most important issues regarding the application of a P1f 12V system on the vehicle architecture are :

- Installation of the belt driven electric machine;
- Positioning of lithium-ion battery.

The required interventions must be aim to satisfy a series of constraints which regards strictly the components but above all which regards the vehicle, for instance in terms of roominess and safety. Especially in the initial steps of new car development, the concept selection between the possible solution is accompanied to packaging sessions to investigate the feasibility of an installation. In this chapter, it is reported a packaging session performed on software Vismockup using FCA data, whose only partial sections are showed.

### 8.1 Installation of the belt driven electric machine

The initial step of this study has been the mounting of electric machine, on engine adopting the housing previously reserved to the alternator, and the revision of front end accessory drive due to the bidirectional drive-tensioning system, considering the envelope of every its possible position.

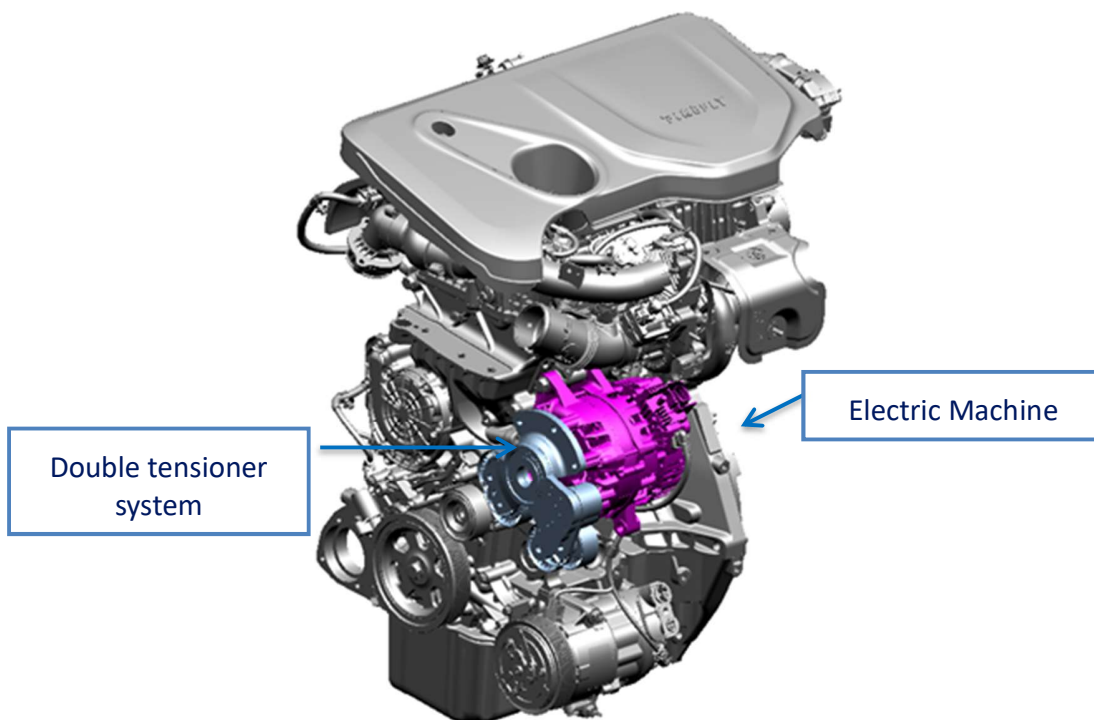


Figure 64. Installation of P1f on engine

Assembled the engine with electric machine, it has been located in the engine compartment to verify eventual interferences. Since it has not found interferences, it has been checked the minimum distance prescribed by FCA internal standard respect to the front side rail and to the front-end, as shown in Figure 65 where measurement indications has been removed because they are confidential.

This macroscopic analysis has shown as the installation of electric machine does not require heavy modifications in engine compartment. Nevertheless, it is evident that with a more detailed study it can easily emerge the necessity of modifications on wiring and piping belonging to the different subsystems.

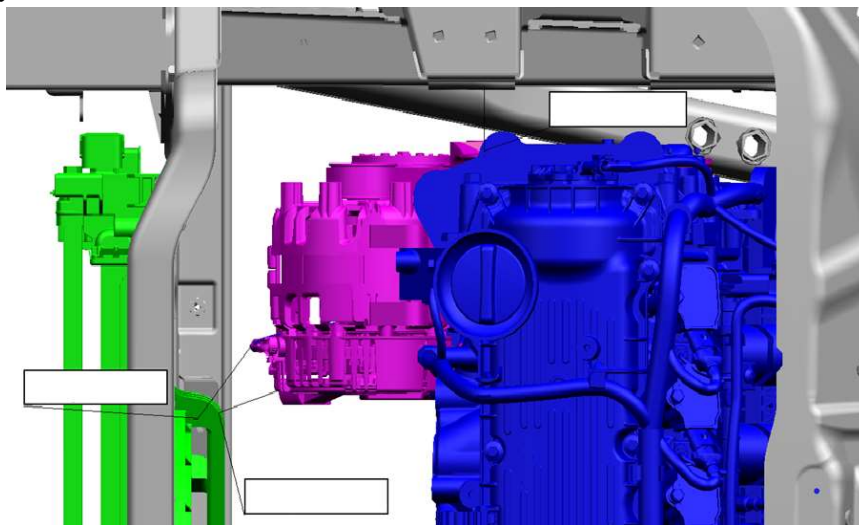


Figure 65. Verification of interference and minimum distances

## 8.2 Positioning of lithium-ion battery

While the positioning of electric machine does not requires excessive efforts because it substitutes essentially the alternator, the lithium-ion battery location has to satisfy a series of constraints, discussed 5.4.2, and the concept selection study can result more complex.

Starting from the fact the battery cannot be positioned in the engine compartments because of risk of fire and it is preferable a short distance from the electric machine, the two scenarios evaluated ( Figure 66) are:

- Scenario 1: battery positioned under on front floor passenger side;
- Scenario 2: battery positioned under the frontal passenger seat;

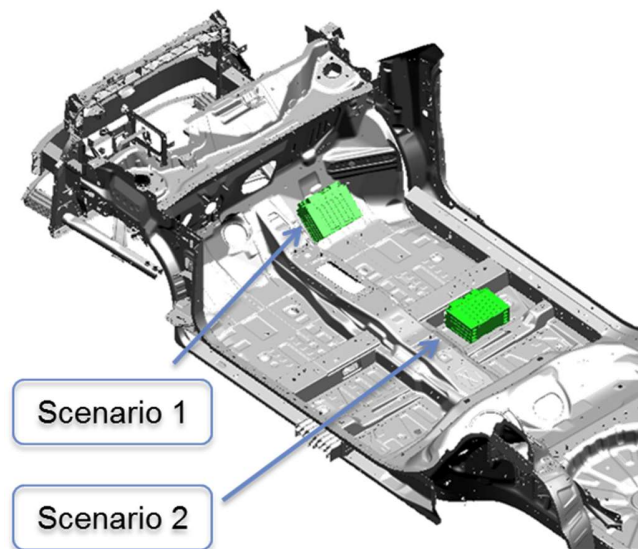


Figure 66. Description of possible scenarios

### 8.2.1 Scenario 1

The battery installation on front floor passenger side is evaluated considering the section in Figure 67. It shows the offset required in the front floor carpet necessary to allocate the battery, starting from actual production layout.

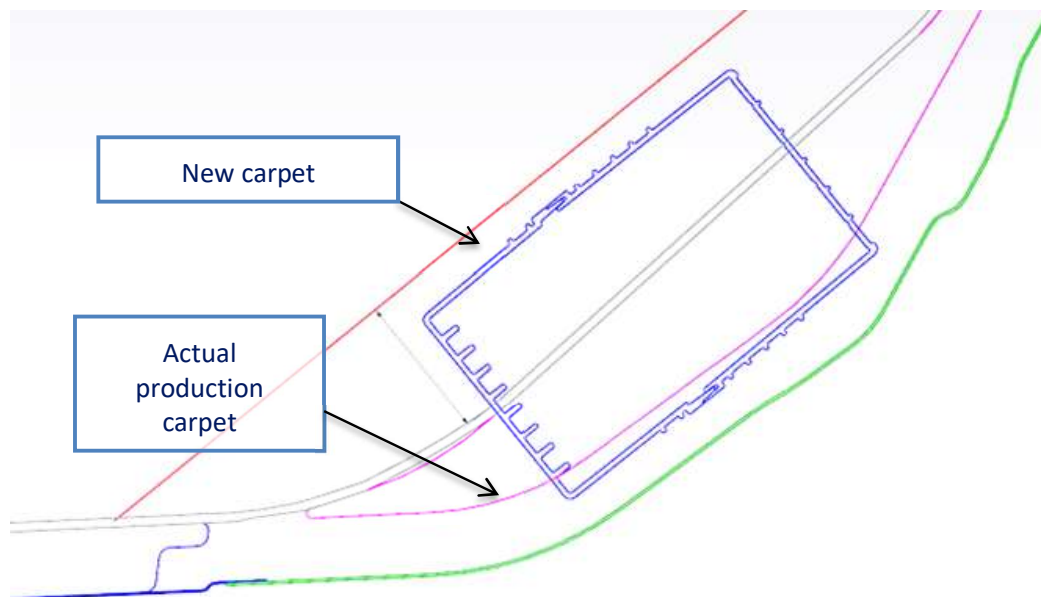
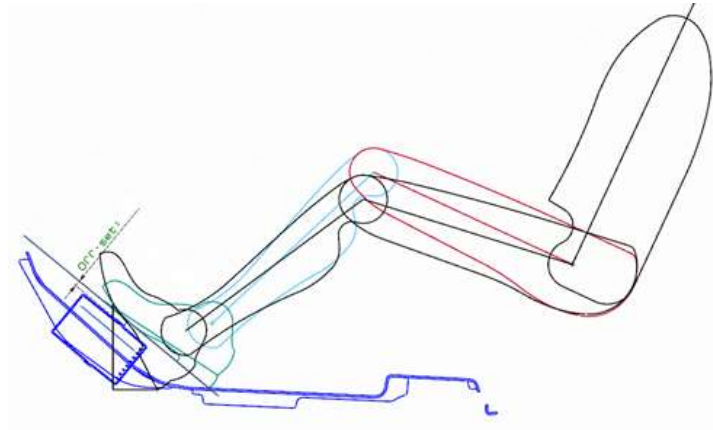


Figure 67. Section of installation on front floor passenger side

The solution is substantially valid regarding to the electric losses, because the battery is quite near to electric machine considering that its installation on engine compartment is not admitted. With respect to safety requirements, it results compliant, in fact the position chosen is not significantly interested by deformation area due to side pole impact test, according to FCA Safety simulations.



On the other hand, from an ergonomics analysis it emerges that the off-set due to the battery dimensions has a negative impact on the vehicle roominess, expressed by a reduction of accommodation percentile ( quota of a statistical population which fits comfortably in a given space). In Figure 68, the blue and red lines underlines this effect compared to initial condition drawn in black.



**Figure 68. Installation Effect on roominess**

Finally the scenario appears feasible because the required intervention does not involve significant modifications to the architecture but, for the ergonomics issue, it could be desirable a research of a smaller dimension battery by other suppliers.

## 8.2.2 Scenario 2

The battery installation under frontal passenger seat is evaluated considering the section in Figure 69. It highlights that this installation respects the minimum distance between battery and seat, represented with the envelope of every its possible position, but it is evident also the interference between battery and air conduct.

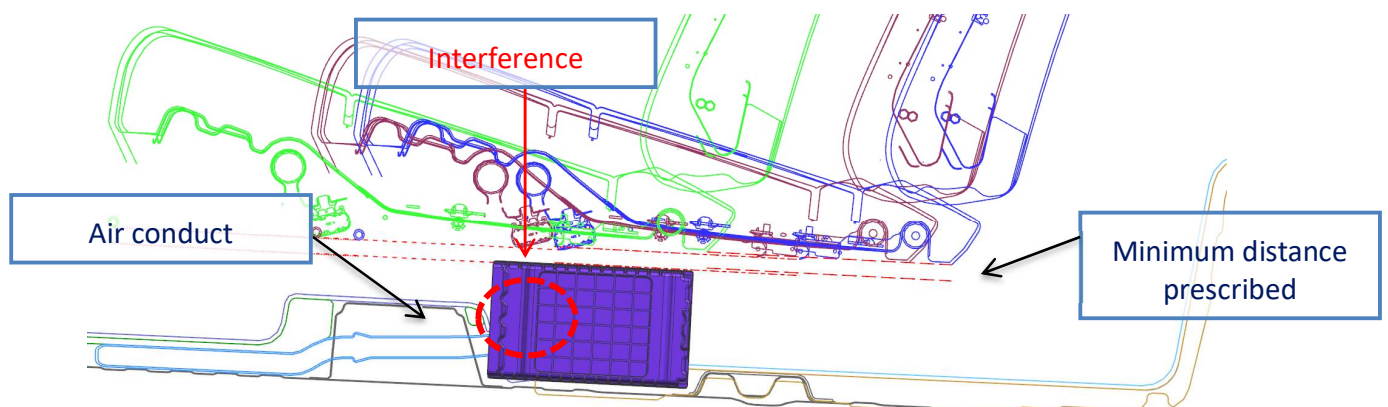


**Figure 69. Section of the installation under frontal seat passenger side**



The solution is substantially valid regarding to the distance from electric machine, because the battery is not excessively distant from electric machine considering that its installation on engine compartment is not accepted.

With respect to safety requirements, it results compliant, in fact the position chosen is not significantly interested by side pole crash test.

With respect of ergonomics, the battery under frontal passenger seat limits the space available for rear passenger's feet, as shown in Figure 70, reducing the accommodation percentile (quota of a statistical population which fits comfortably in a given space).

Then the scenario can be considered feasible because it requires interventions a modification of rear passenger air conduct layout in order to remove the interference. Nevertheless, it is certainly necessary to take into account the entity of percentile reduction.

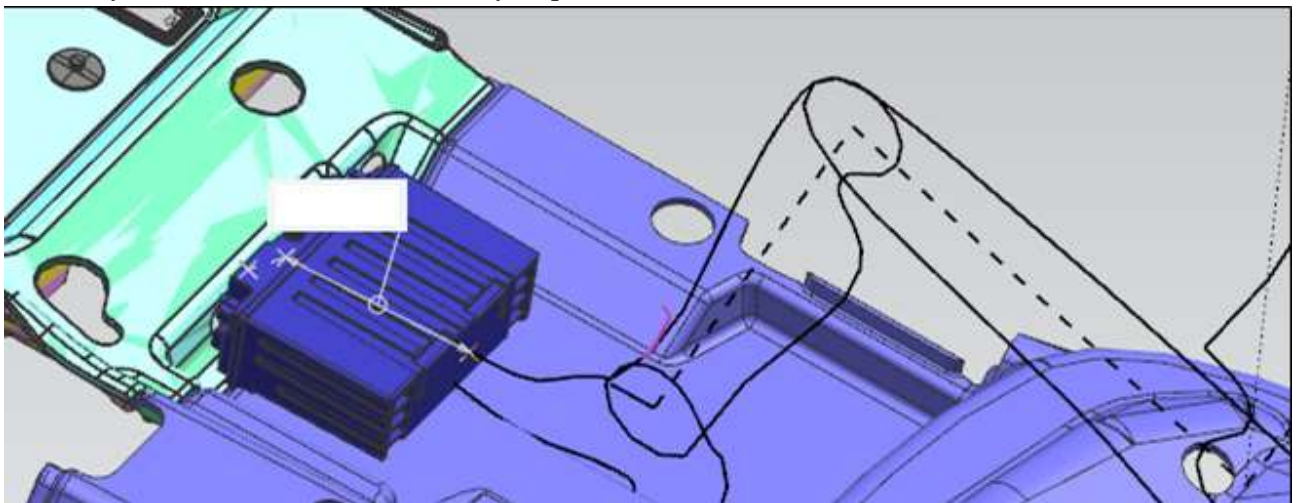


**Figure 70. Installation effect on accommodation percentile**

## 9. Application of P2 48 V system on vehicle architecture

The most important issues regarding the application of a P2 48V system on the vehicle architecture are :

- Installation of the belt driven electric machine;
- Positioning of DC/DC converter;
- Positioning of lithium-ion battery.

The required interventions must be aim to satisfy a series of constraints which regards strictly the components but above all which regards the vehicle, for instance in terms of roominess and safety. Especially in the initial steps of new car development, the concept selection between the possible solution is accompanied to packaging sessions to investigate the feasibility of an installation. In this chapter, it is reported a packaging session performed on software Vismockup using FCA data, whose only partial sections are showed.

### 9.1 Installation of electric machine

The initial step of this study has been the assembly of electric machine between engine and gearbox.

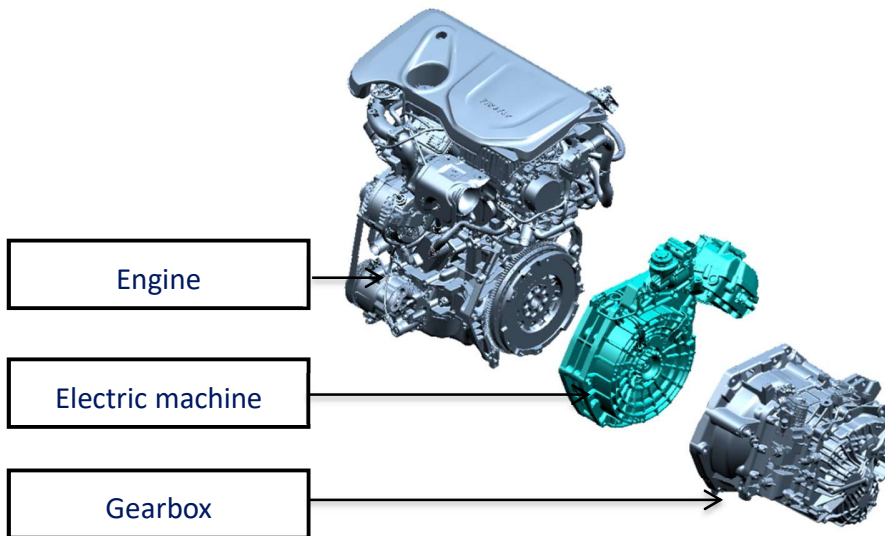


Figure 71. Installation of P2 48V on engine

Completed this assembly, it has been located in the engine compartment to verify eventual interferences and minimum distances.

Before it has been performed more attempts because not all combinations engine-gearbox fit with between the two front side rails track, due to their axial clearance. Finally the additional axial dimension of electric machine has conducted to choose the engine-gearbox as compact as possible. For the selected powertrain it has been checked the minimum distance, prescribed by

internal standards, respect to the two front side rails and to the front-end, as shown in transversal section of Figure 72.

This macroscopic analysis has shown as the installation of electric machine is feasible in the engine compartment of actual production. Nevertheless, it is evident that with a more detailed study it can easily emerge the necessity of modifications on wiring and piping belonging to the different subsystems.

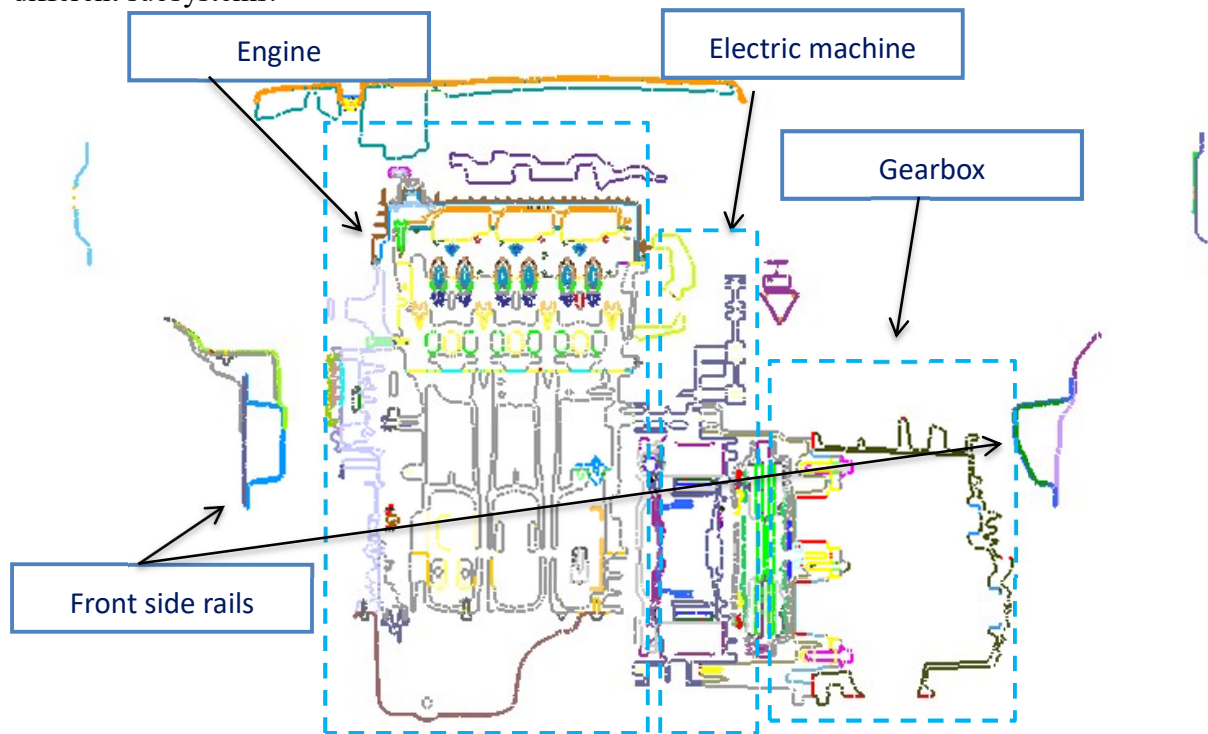


Figure 72. Transversal section of engine compartment

## 9.2 Positioning of lithium-ion battery

The lithium-ion battery location has to satisfy a series of conditions, as discussed on paragraph 6.2.2. Starting from the fact that the battery cannot be positioned in the engine compartments due to risk of fire and because of its larger volume, the only scenario evaluated has been in the trunk compartment.

The battery installation in the trunk is evaluated considering the transversal section in Figure 73 . It shows evidently that battery positioned in the spare wheel housing does not impact negatively on the trunk volume, but a kit Fix&Go is required to substitute spare wheel.

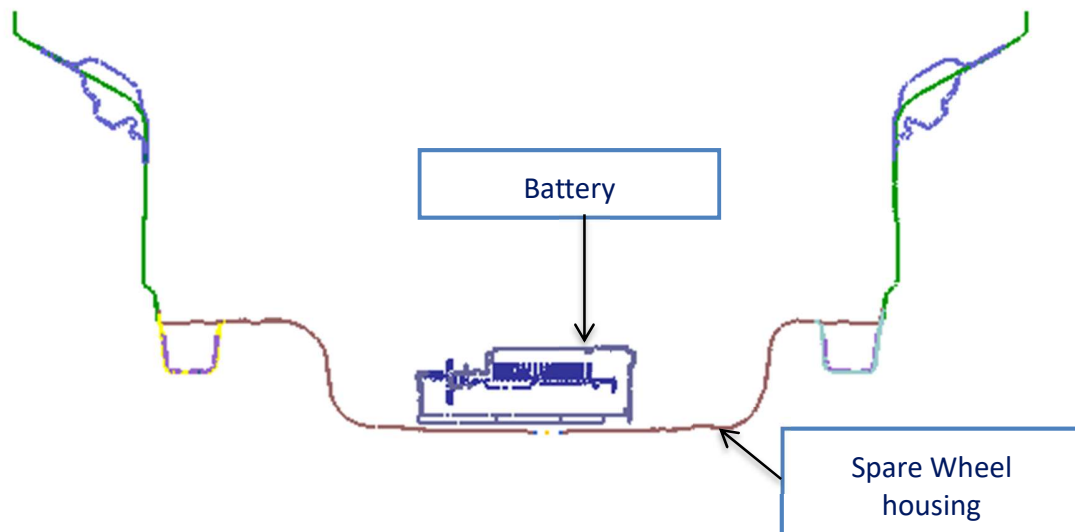


Figure 73. Section of battery installation in the trunk

The distance from the electric machine is not particularly problematic because in 48V systems the current intensity and consequently electric losses are less relevant compared with 12 V systems.

With respect to safety requirements it is results compliant, in fact the position chosen is not significantly interested by rear impact test

Regarding to thermal management, the battery needs to be refrigerated by circulating air, which should be delivered by means of specific conducts.

Finally this scenario appears feasible but the intervention required are:

- the creation of a mounting bracket for the battery;
- the realization of specific conducts to insure the battery refrigeration;

### 9.3 Positioning of DC/DC converter

The DC/DC converter location has to satisfy a series of conditions, as discussed in paragraph 6.2.2. Starting from the assumption that the battery is already positioned in the trunk, the three scenarios evaluated are:

- Scenario 1: DC/DC converter positioned in the trunk over the battery;
- Scenario 2: DC/DC converter positioned under the frontal seat;
- Scenario 3: DC/DC converter positioned on panel assembly;

### 9.3.1 Scenario 1

The DC/DC converter installation in the trunk over the battery is evaluated considering the section in Figure 74. It shows that the positioning in spare wheel housing does not subtract volume from trunk, an important requisite from customer perspective, but as already discussed the spare wheel has to be substituted with kit Fix&Go.

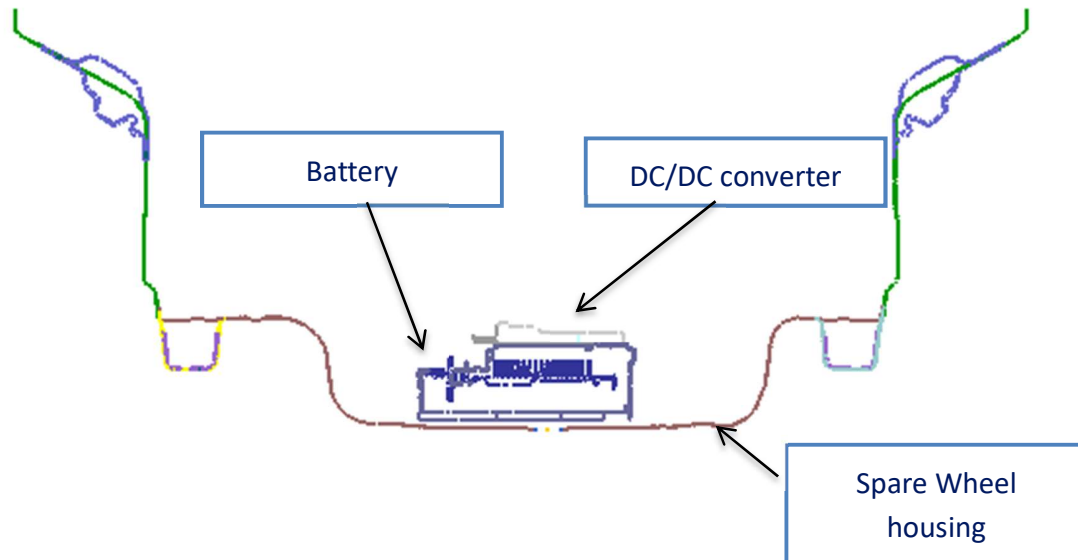


Figure 74. Section of DC/DC converter installation in the trunk

With respect to safety requirement, it can be considered a robust solution because the longitudinal coordinate is practically equal to battery, already declared compliant respect to rear impact.

The distance between DC/DC converter and lead acid battery positioned in the engine compartment represents a negative aspect because it generates significant electric losses due to effect Joule and voltage drop. In fact, being equal the power, 12 V wires are interested by about 4 times higher current intensity compared to 48 V.

Regarding to thermal management, the DC/DC converter selected is passive air cooled therefore it requires fresh circulating air to optimize the heat transfer. The interaction between heat produced and received from battery in a closed housing represents a limit.

Finally this scenario appears feasible but a creation of mounting bracket for DC/DC converter is required.

### 9.3.2 Scenario 2

The DC/DC converter installation under the frontal seat is evaluated considering the sections in Figure 75. It highlights that this installation has a considerable distance from the seat but it results too near to rear passenger air conduct.

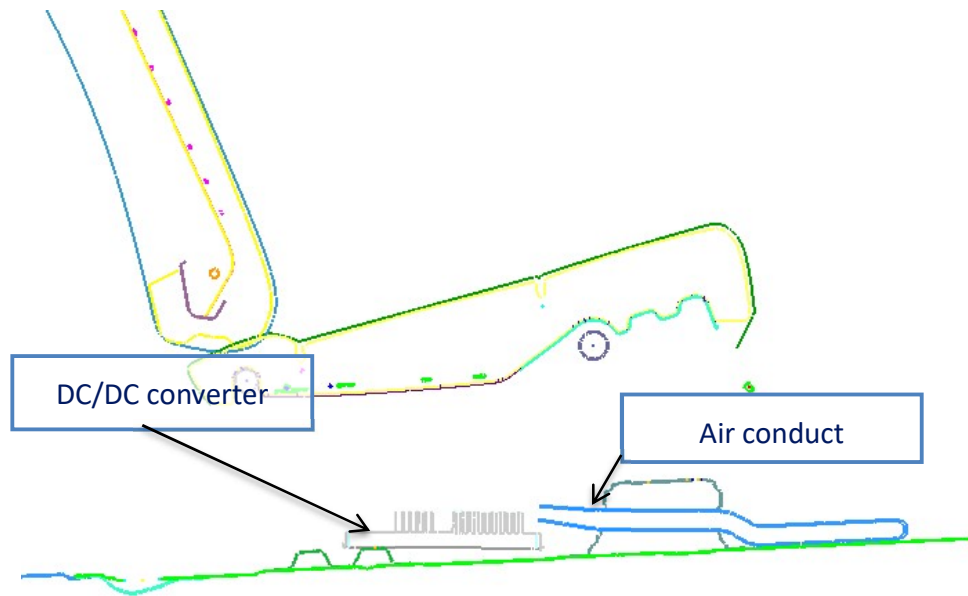


Figure 75. Section of DC/DC converter installation under passenger seat

The solution is substantially valid regarding the electric losses, because the DC/DC converter is less distant from lead acid battery, compared with trunk installation.

With respect to safety requirements, it results compliant, in fact the position chosen is not significantly interested by side pole crash test,

Regarding to ergonomics, the DC/DC converter under front seat could limits the space available for rear passenger's feet,

Then the scenario can be considered feasible but in a first analysis it is required a modification of rear passenger air conduct layout, in order to avoid overheating especially when HVAC supplies hot air in cockpit.

### 9.3.3. Scenario 3

The DC/DC converter installation in panel assembly on engine side is evaluated considering the section in Figure 76. It shows that in this installation is evident an interference with a HVAC pipe.

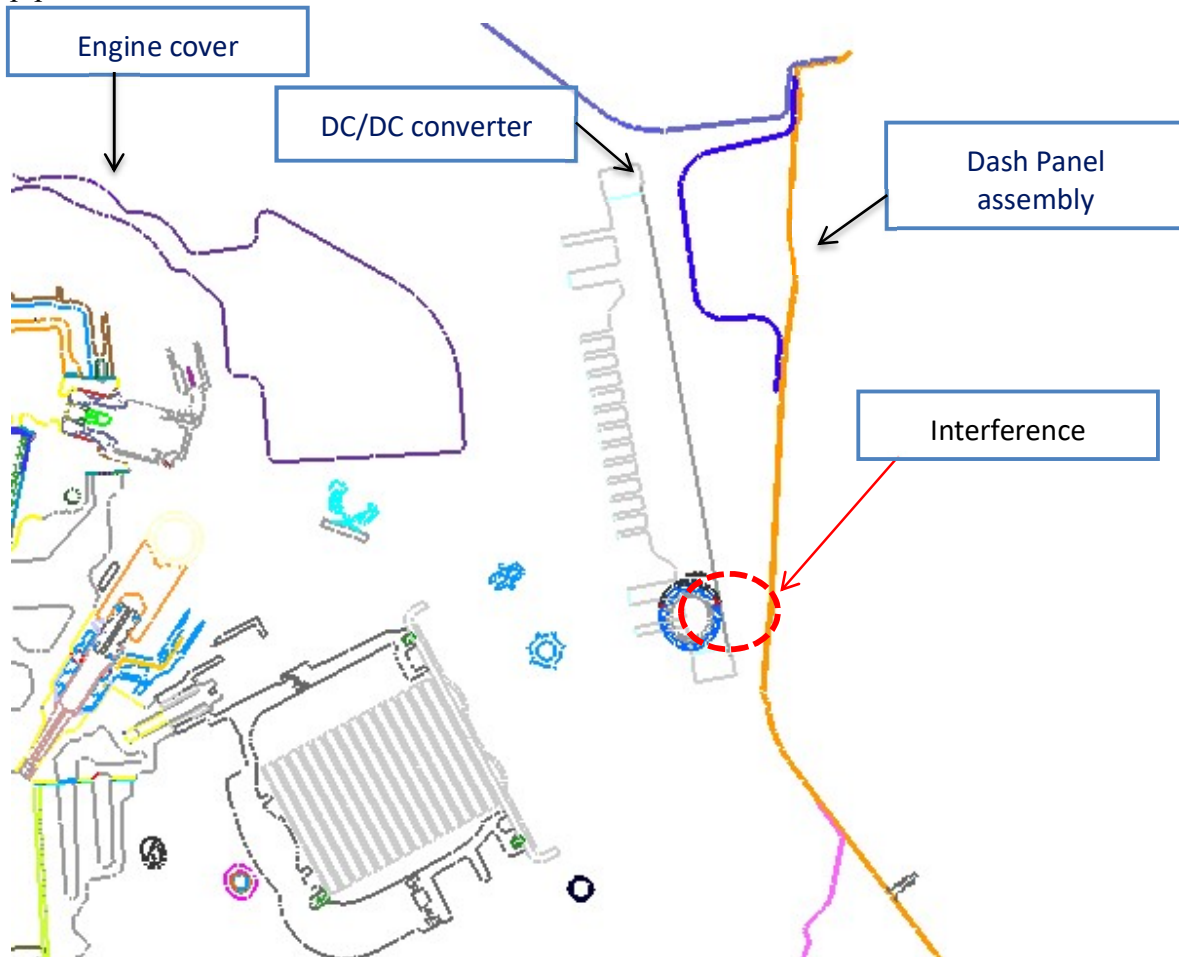


Figure 76. Section of DC/DC converter installation under passenger seat

Regarding to electric losses, this positioning offers an optimal solution because of limited distance from lead acid battery.

From a thermal point of view, the device in the engine compartment has the correct fresh air circulation necessary for an optimal refrigeration.

Finally the scenario appears feasible but before it prescribed a packaging revision regarding HVAC piping to solve the existing interference with DC/DC converter.

## 10. Creation of a model to estimate Performance Index, Fuel Consumption and CO<sub>2</sub> emissions

An important activity in vehicle architecture team is the concept selection between different systems based mainly on comparison of performance and emissions. For this purpose it was developed a tool on Scilab to investigate the implications on Performance Index, Fuel Consumption and CO<sub>2</sub> emissions. In addition it was integrated a function to calculate VDE (Vehicle Demand Energy) which allows to discriminate different vehicle segments, in the interest of architectural point of view. It is evident that this tool has not the aim to be excessively sophisticated but it is conceived to give an overall sensibility on low voltage hybrid architectures. It can support vehicle architecture activities to make the first macroscopic considerations, especially in the early phase of product development.

### 9.1 Vehicle Demand Energy (VDE)

The vehicle demand energy (VDE) to complete a drive cycle is calculated summing  $E_i$  over the cycle time between  $t_{start}$  and  $t_{end}$ , according to equation ( 4 ).

$$E = \sum_{t_{start}}^{t_{end}} E_i \quad (4)$$

Where:

- $t_{start}$  is the time at which the test cycle starts;
- $t_{end}$  is the time at which the test cycle ends;
- $E_i = F_{rl} \times d_i$  is the energy demand during time period (i-1) to (i) considering only positive forces;
- $F_{rl}$  is the road load force during time period (i-1) to (i), [N], expressed by ( 8 ).

$$F_i = F_0 + F_1 \times \left(\frac{v_1 + v_{1-i}}{2}\right) + F_2 \times \frac{(v_1 + v_{1-i})^2}{4} + TM \times a_i \quad (5)$$

Where:

- $F_0, F_1, F_2$  are the coast-down coefficients expressed in [N], [N/km/h] and [N/(km/h)<sup>2</sup>] respectively.
- $v_i$  is the target velocity at time  $t_i$ ;
- $t_i$  is time, [s]
- $TM$  is the test mass;
- $a_i$  is the acceleration during time period (i-1) to (i) calculated by ( 6 ).



$$a_i = \frac{v_i - v_{i-1}}{3,6 \times (t_i - t_{i-1})} \quad (6)$$

## 10.2 PI (Performance Index) calculation

The effect on performance has been evaluated by means of PI (Performance Index) which is defined by ( 7 ).

$$PI = \left( \frac{3600}{V_{\max}} \right) + t_{0-100} + t_{60-100} + t_{80-120} \quad (7)$$

Where:

- $V_{\max}$  is the maximum speed vehicle;
- $t_{0-1}$  is the time needed to accelerate from 0 to 100 km/h using the gearstick. It considers also the time to start from standstill and the time needed to change gear;
- $t_{60-100}$  is the time needed to accelerate from 60 to 100 km/h with the N-1 gear engaged (elasticity time);
- $t_{80-120}$  is the time needed to accelerate from 60 to 100 km/h with the N gear engage (elasticity time);
- N is the total number of gearbox ratios;

The PI calculation starts from the equation of the vehicle longitudinal dynamics ( 8 )

$$P_{\text{trac}} - P_{\text{res}} = m_e V \frac{dV}{dt} \quad (8)$$

Where:

- V is the vehicle speed;
- $\frac{dV}{dt}$  is vehicle acceleration;
- $P_{\text{trac}}$  is the traction power available at the wheels and it is calculated subtracting from total power, deriving from the sum of engine and electric motor power, mechanical losses due to gearbox, driveline and residual braking torque on the wheels, by means of ( 9 ).

$$P_{\text{trac}} = P_{\text{ICE+EM}} \eta_{\text{gbx}} - P_{\text{dvl}} - P_{\text{brk}} \quad (9)$$

Where:

- $P_{\text{ICE+EM}} \eta_{\text{gbx}}$  is the sum of engine and electric motor power, discounted of power loss in the gearbox.  $\eta_{\text{gbx}}$  is the gearbox efficiency;

- $P_{dvl}$  is the power loss due to entire driveline downstream the gearbox and it is modeled using a constant term  $T_0$  and a term  $T_1$  multiplicative of the vehicle speed with equation ( 10 ).

$$P_{dvl} = (T_0 + T_1 V) V \quad (10)$$

- $P_{brk}$  is the power loss due to the residual braking torque, it is calculated using residual braking torque  $T_{brk}$  and tire rolling radius  $R$  using the ( 11 ).

$$P_{brk} = \left( 4 \frac{T_{brk}}{R} \right) V \quad (11)$$

- $P_{res}$  is the resistant power calculated by equation ( 12 ).

$$P_{res} = P_{aer} + P_{roll} + P_{cli} \quad (12)$$

Where:

- $P_{aer}$  is the aerodynamic resistant power calculated using vehicle frontal area  $S$ , drag coefficient  $C_x$  and air density  $\rho$  by means of formula ( 13 ).

$$P_{aer} = \left( \frac{1}{2} \rho S C_x V^2 \right) V \quad (13)$$

- $P_{roll}$  is the rolling resistant power written by ( 14 ).

$$P_{roll} = (B_0 + B_2 V^2) mg V \quad (14)$$

Where:

- $B_0$  , also called RR, is the static component of rolling resistance coefficient, depending on type of tire;
- $B_2$  is the viscous component of the rolling resistance;
- $P_{cli}$  is the climbing resistant power which is neglected in the numeric model since the performance index is computed in flat road condition.
- $m_e$  is the vehicle equivalent mass which allows to consider, besides translational inertia, also rotational inertia resulting from the engine and the wheels. It is defined by ( 15 ).

$$m_e = m + \frac{J_e \tau_g^2 \tau_f^2}{R^2} + \sum \frac{J_w}{R^2} \quad (15)$$

Where:

- $m$  is the vehicle mass;
- $J_e$  is the engine rotational inertia;
- $J_w$  is the wheels rotational inertia;
- $\tau_g$  is the transmission ratio of gear engaged;
- $\tau_f$  is the transmission ratio of final drive gear;
- $R$  is the rolling tire radius;

Otherwise the vehicle longitudinal dynamics can be also described by means of a formula ( 16 ) containing coast down coefficients, which are obtained by experimental test and constitute the road load, assembling practically the several terms of resistance already introduced.

$$P_{ICE+EM}\eta_{gbx} = (F_0 + F_1V + F_2V^2)V + m_e \frac{dV}{dt} V \quad ( 16 )$$

Where:

- $F_0 = B_0 mg + T_0 + 4 \frac{T_{brk}}{R}$ , [N], takes into account mainly rolling resistance;
- $F_1 = T_1$ , [N/(km/h)], takes into account the driveline losses proportional to speed;
- $F_2 = \frac{1}{2} \rho S C_x V^2 + B_2$ , [N/(km/h)<sup>2</sup>], takes into account especially aerodynamic drag.

Coming back to the PI calculation, the maximum speed vehicle  $V_{max}$  is obtained by the intersection point between the traction power with the higher gear ratio engaged and the resistant power.

Instead the acceleration times required is computed by using inverse formula of vehicle longitudinal dynamics equation:

$$t = \int_{V_1}^{V_2} \frac{m_e V}{P_{trac} - P_{res}} dV \quad ( 17 )$$

Where  $V_1$  and  $V_2$  are initial and final vehicle speed for the considered interval.

### 10.3 Fuel consumption and CO<sub>2</sub> emission calculation

The first operation implemented in the model is the creation of the speed profile discretized into intervals of one second, with the gearshift indication prescribed by NEDC.

The power supplied by electric machine  $P_{EM}$  represents a quota, conveniently chosen on the basis of working point, of total power output required to follow the speed profile.

The boost function performed by electric motor depends essentially on the energy availability in the battery. Besides the initial battery SOC (State of Charge), the electric machine allows to recovery energy during deceleration phases over the drive cycle and this functionality is included the code.

During deceleration phases (  $\frac{dV}{dt} < 0$  ), the inertia power (  $m_e \frac{dV}{dt} V$  ) overcomes the road load power (  $F_0 + F_1 V + F_2 V^2$  ) and it allows the vehicle motion without necessity of burning fuel.

In a conventional vehicle when the deceleration desired by driver is higher compared with that resulting from road load power the energy is dissipated in heat by mean of braking system. In a hybrid vehicle the difference of power  $\left| m_e \frac{dV}{dt} V - (F_0 + F_1 V + F_2 V^2) V \right|$  can be used whole or partially, depending on the situation, to store energy in the battery.

The instantaneous mechanical power available at wheels  $P_{rb}$ , during deceleration phases (  $\frac{dV}{dt} < 0$  ), is expressed by ( 18 ).

$$P_{rb} = \left| m_e \frac{dV}{dt} V - (F_0 + F_1 V + F_2 V^2) V \right| \quad ( 18 )$$

In this model it is assumed the difference of power is entirely destined to increase the energy in the battery, as long as the electric machine characteristics in regenerator mode allows this. When the available power in input to electric machine is excessive for that working point, the generator recovers only a part of power and other part is dissipated in braking system.

The instantaneous electric power at battery level in regenerative braking  $P_{rbBATT}$  has to take into account mechanical losses through gearbox and driveline, already included in the coast down coefficients, and electric losses through inverter and electric machine. For this purpose, it is used the equation ( 19 ).

$$P_{rbBATT} = P_{rb} \eta_{gbx} \eta_{EMg} \eta_{INV} \quad ( 19 )$$

Where:

- $\eta_{gbx}$  is the gearbox efficiency;
- $\eta_{EMg}$  is the electric machine efficiency in generator mode;
- $\eta_{INV}$  is inverter efficiency;

The instantaneous electric power at battery level in boost mode  $P_{ebBATT}$  is derived from mechanical power  $P_{EM}$  and in order to take into account the losses through the electric machine, it is adopted the formula ( 20 ).

$$P_{ebBATT} = \frac{P_{EM}}{\eta_{EMm} \eta_{INV}} \quad (20)$$

Where  $\eta_{EMm}$  is the electric machine efficiency in motor mode.

The energy stored in the battery is continuously monitored using the formula ( 21 ).

$$E_{BATT} = \int_{t_i}^t (P_{rbBATT} - P_{ebBATT}) dt \quad (21)$$

Where  $t_i$  is initial step of drive cycle and  $t$  is a generic time. This parameter is particular important because the tool developed presents a function which prevents the boost mode when the battery energy is below a certain threshold.

For each point of the speed profile the power supplied by internal combustion engine  $P_{ICE}$  is calculated with

( 22 ).

$$P_{ICE} = \frac{(F_0 + F_1 V + F_2 V^2)V + m_e \frac{dV}{dt} V}{\eta_{gbx}} - P_{EM} \quad (22)$$

In order to read the specific fuel consumption from the BSFC map, it needs to convert the engine power into bmep with ( 23 ) and vehicle speed into engine rotational speed  $n_{ICE}$  with ( 24 ).

$$n_{ICE} = \frac{V}{3.6} \frac{\tau_g \tau_f}{2\pi R} 60 \quad (23)$$

$$bmep = \frac{P_{ICE} 2}{V_{cyl} n_{ICE}} \quad (24)$$

The instantaneous fuel consumption  $FC_{ins}$  expressed in [g/s] is calculated by using the equation ( 25 ).

$$FC_{ins} = \frac{bsfc P_{ICE}}{3600} \quad (25)$$

Where:

- bsfc is the brake specific fuel consumption extracted from BSFC map, [g/kwh];
- $P_{ICE}$  is the power delivered by combustion engine, [kW];

In addition, the fuel consumption is subject to a series of corrections:

- During deceleration phases, above a certain rpm threshold, the fuel consumption is set equal to zero because it is necessary to take into account fuel cut-off;
- At vehicle standstill, the fuel consumption is set to the minimum value because the engine is on, in the case of conventional vehicle;
- At vehicle standstill and below certain speed during deceleration phases, the fuel consumption is set to zero, in the case of hybrid vehicle in order to represent the advanced Start&Stop;

The cumulated fuel consumption  $FC_{cum}$  expressed in [g] over whole drive cycle is obtained by ( 26 ).

$$FC_{cum} = \int_{t_i}^{t_f} FC_{ins} dt \quad (26)$$

The combined fuel consumption usually expressed in [l/100] km is calculated with ( 27 ).

$$FC_{comb} = FC_{cum} \frac{100}{\rho_f Dist_{NEDC}} \quad (27)$$

Where:

- $\rho_f$  is the fuel density, equal to 720 g/dm<sup>3</sup> for gasoline at 15°C;
- $Dist_{NEDC}$  is the total distance covered by NEDC, equal to 10,93 km;

The CO<sub>2</sub> emissions indicated in g/km are computed using ( 28 ).

$$CO_2 = \frac{FC_{comb} 2380}{100} \quad (28)$$

Where 2380 are the grams of CO<sub>2</sub> produced for every liter of burned gasoline.

The main simplifications used to create the model are:

- Thermal transient during warm-up is not taken into account;
- Real vehicle speed is not simulated. It is assumed the driver is able to follow exactly the speed profile imposed by drive cycle, on the basis of a kinematic approach;
- The driving cycle is simulated as a sequence of steady state conditions.

Nevertheless, it gives the opportunity to evaluate a number of issues regarding hybrid applications but also the sensitivity respect to rolling resistance, aerodynamic drag, inertia, final drive ratios and rolling tire radius.

## 10.4 Validation of the numerical model

The results obtained has shown a great accordance with homologation data, in the case of application already in actual production, and with internal simulation results, in the case of new applications. For this reason, it has been chosen to report results only expressed in terms of percentage delta.

The deviation of about 5-10% between the results of this study and car maker data is attributable mainly to the assumptions necessary to simplify reasonably the physical problem. However it can be considered negligible because the main aim of the work is to give an overview about effect of some hybrid systems in terms of performance and emissions. Furthermore sensitivity of different parameters is tested and the results found are within the ranges indicated by technical literature.

## 11. Analysis of results

The simulations has been performed on vehicles belonging to different segments in order to give a transversal overview useful for an architectural approach. It is not possible report coast-down coefficient because they are strictly confidential. The mass of vehicles used as reference is shown in Table 21. Vehicle.

Vehicle	Mass [kg]
Hatchback 5D	1275
SUV	1395
LCV	1490

Table 21. Vehicles mass

In the various simulations it has been maintained the same powertrain in terms of engine and gearbox, the same final drive ratio and tire rolling radius, with the aim to make a coherent comparative analysis.

The engine and gearbox technical specifics are reported respectively into Table 22 and Table 23.

Engine 1.4 T-Jet 120 CV	
Fuel	Gasoline
N° Cylinders	4 L
Bore x Stroke [mm]	72 x 84
Displacement [cm <sup>3</sup> ]	1368
Compression ratio	9,8:1
Emission standard	Euro 6
Max torque [Nm]	206 @ 2000 rpm
Max power [kW]	88 @ 5000 rpm

Table 22. Engine technical specifics

Gearbox	
Final drive ratio	4,133
Gear	Transmission ratio
1°	4,154
2°	2,118
3°	1,486
4°	1,116
5°	0,897
6°	0,767

Table 23. Gearbox technical specifics

## 11.1 PI simulations

Every simulation performed is based on the following assumptions:

- Engine power values comes from full power curve, also called WOT (Wide Open Throttle);
- Boost performed by electric machine derives from its maximum power characteristics;
- Boost is active during the entire simulation time;
- The gearshift has been set when the available power at wheels reaches the maximum value for a given transmission ratio.

The input data regarding vehicles are reported on Table 21, whereas data regarding powertrain are reported on Table 22 (engine) and on Table 23 (gearbox).

### 11.1.1 PI simulation on vehicles equipped with P1f 12V system

The installation of P1f 12V system on a conventional vehicle causes an additional weight of about 10 kg. Strictly speaking, this involves a small variation of coast down coefficient  $F_0$ , which however does not modify significantly the road load power. Then the Performance Index improvement depends essentially on the increase of traction power operated by electric motor.

As shown by red curves in Figure 77, the electric motor contribution is limited and it covers only low engine speeds. In fact the transmission ratio between engine and electric machine is assumed equal to 2.5 and, for engine speeds higher than 2400 rpm, the motor overcomes its maximum speed (6000 rpm).

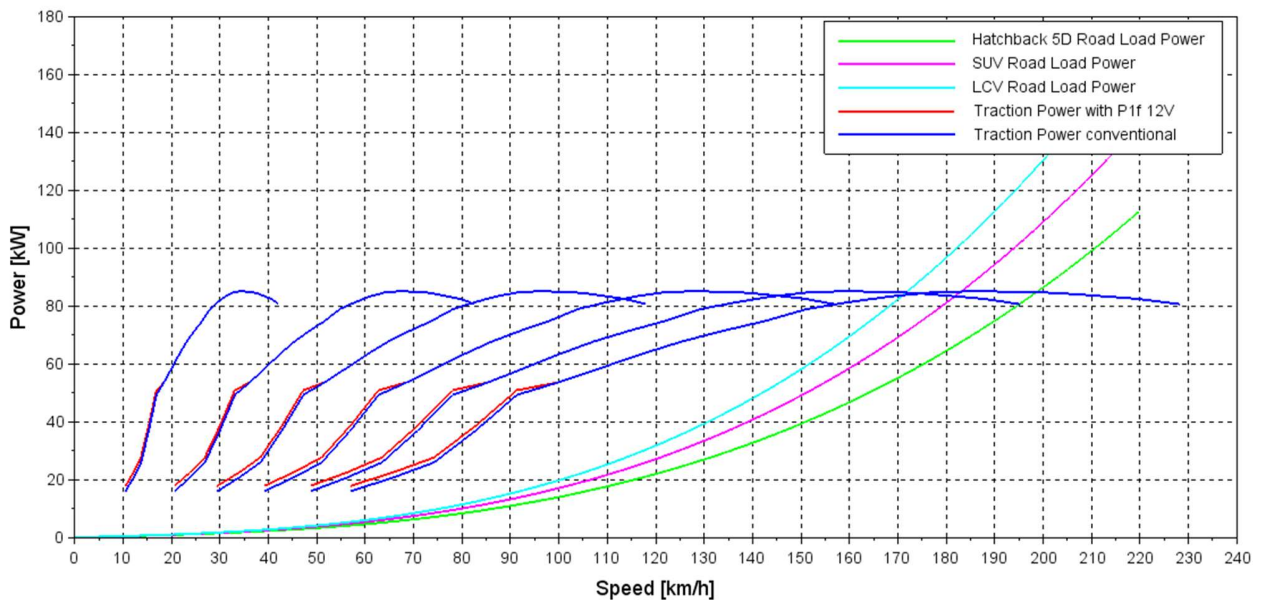


Figure 77. Traction power vs road load power (P1f 12V case)

The PI deltas versus conventional vehicle reported on Table 24 and on Figure 78 underline a slightly different sensitivity to performance improvement, in particular higher for SUV and LCV. In fact the mass increment due to the system weight is less relevant for heavier vehicles and the



supplementary traction power given by electric machine counts more in percentage for vehicles with higher road load power, that is when the difference  $P_{\text{trac}} - P_{\text{res}}$  is smaller.

	PI $\Delta$ P1f 12V [%]
<b>Hatchback 5D</b>	-0,3
<b>SUV</b>	-0,4
<b>LCV</b>	-0,4

Table 24. PI deltas (P1f 12V case)

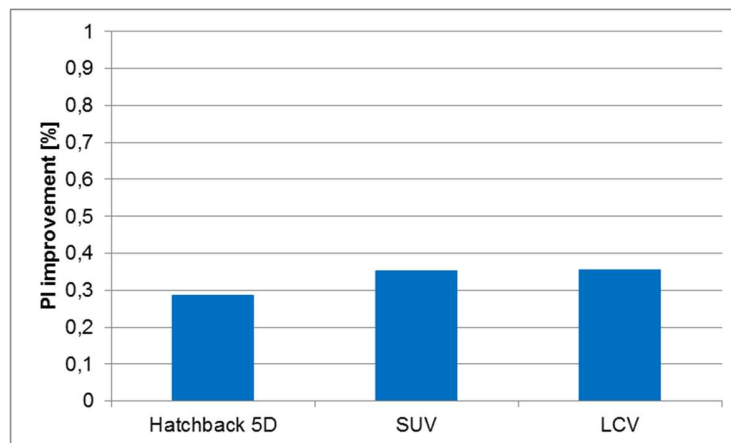


Figure 78. PI improvement (P1f 12V case)

### 11.1.2 PI simulation on vehicles equipped with P1f 48V system

The installation of P1f 48V system on a conventional vehicle causes an additional weight of about 30 kg. Strictly speaking this involves a limited variation of coast down coefficient  $F_0$ , which however does not impact significantly on the road load power. Then the Performance Index improvement depends essentially on the increase of traction power operated by electric motor.

As highlighted by red curves in Figure 79 , the electric motor contribution is quite relevant but it does not cover the entire engine operating range. In fact the transmission ratio between engine and electric machine is assumed equal to 2.5 and, for engine speeds higher than 4000 rpm, the motor overcomes its maximum speed (10000 rpm).

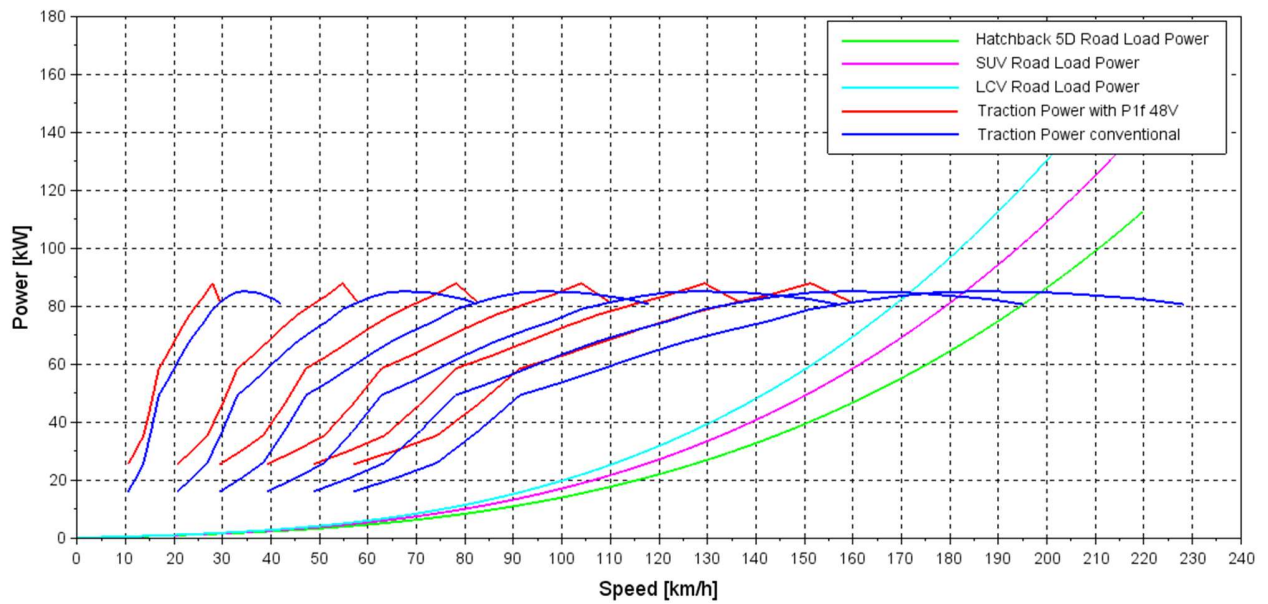


Figure 79. Traction power vs road load power (P1f 48V case)

The PI deltas versus conventional vehicle reported on Table 25. PI deltas (P1f 48V case) and on Figure 80 underline a slightly different sensitivity to performance improvement, in particular higher for SUV and LCV. In fact the mass increment due to the system weight is less relevant for heavier vehicles and the supplementary traction power given by electric machine counts more in percentage for vehicles with higher road load power, that is when the difference  $P_{\text{trac}} - P_{\text{res}}$  is smaller.

	PI $\Delta$ P1f 48V [%]
Hatchback 5D	-6,7
SUV	-7,4
LCV	-8,3

Table 25. PI deltas (P1f 48V case)

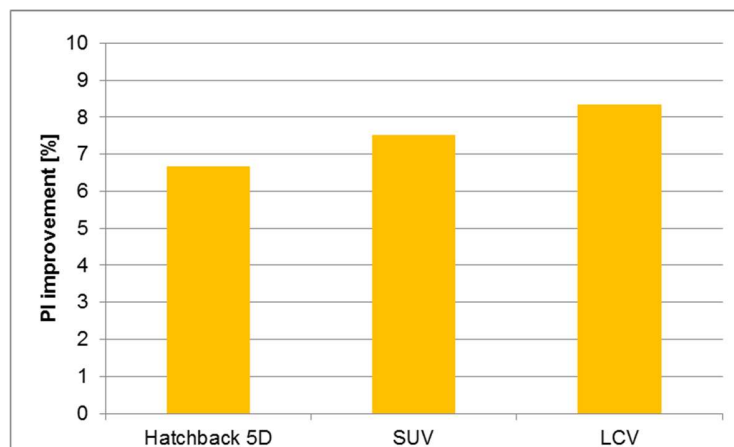


Figure 80. PI improvement (P1f 48V case)

### 11.1.3 PI simulation on vehicles equipped with P2 48 V system

The installation of P2 48 V system on conventional vehicle causes an additional weight of about 70 kg. Strictly speaking, this involves a variation of coast down coefficient  $F_0$ , which however does not modify significantly the road load power. Then the Performance Index improvement depends essentially on the increase of traction power operated by electric motor.

As highlighted by red lines in the Figure 81, the electric motor contribution to traction power available at wheels is significant and it covers the whole engine operating range. In fact the rotational speed of engine and motor is the same because they are mounted coaxially and this allows also to reach a higher maximum speed.

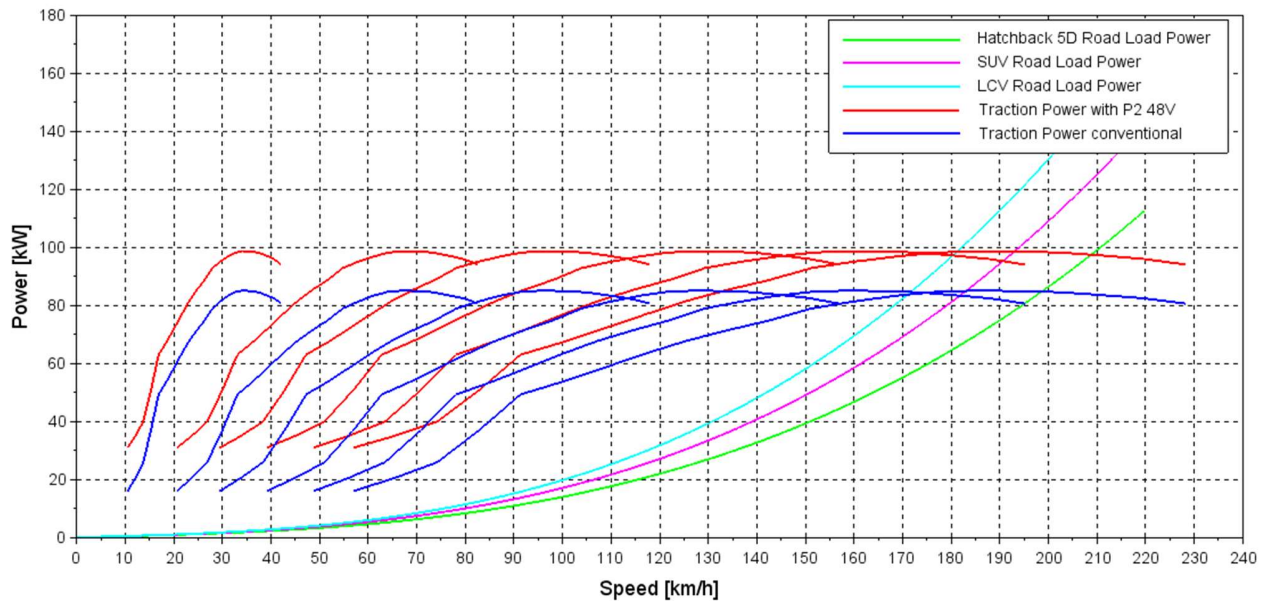


Figure 81. Traction power vs road load power (P2 48V case)

The PI deltas versus conventional vehicle reported on Table 26 and on Figure 82 underline a slightly different sensitivity to performance improvement, in particular higher for SUV and LCV. In fact the mass increment due to the system weight is less relevant for heavier vehicles and the supplementary traction power given by electric machine counts more in percentage for vehicles with higher road load power, that is when the difference  $P_{\text{trac}} - P_{\text{res}}$  is smaller.

The results reported as negative delta corresponds to a performance improvement, because PI is proportional to the sum of times required for the various accelerations.

	PI $\Delta$ P2 48V [%]
<b>Hatchback 5D</b>	-13,6
<b>SUV</b>	-14,8
<b>LCV</b>	-15,7

Table 26. PI deltas (P2 48V case)

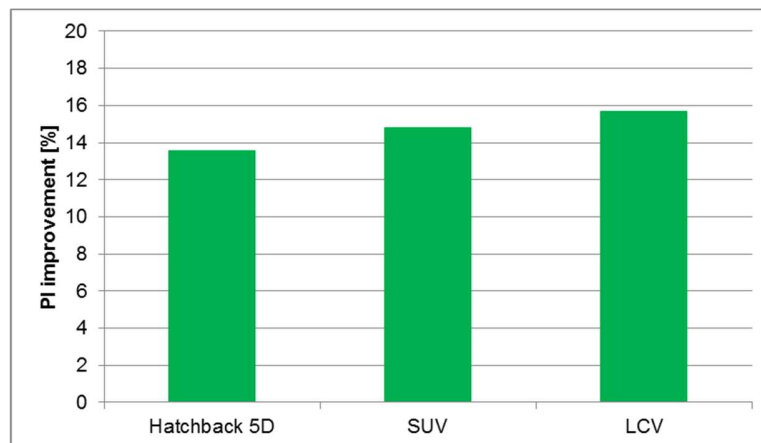


Figure 82. PI improvement (P2 48V case)

#### 11.1.4 Summary on PI improvement

A summary on PI improvement on the various vehicles is reported on Table 27 and graphically represented on Figure 83.

	P1f 12V PI Δ [%]	P1f 48V PI Δ [%]	P2 48V PI Δ [%]
<b>Hatchback 5D</b>	-0,3	-6,7	-13,6
<b>SUV</b>	-0,4	-7,5	-14,8
<b>LCV</b>	-0,4	-8,3	-15,7

Table 27. Summary on PI deltas

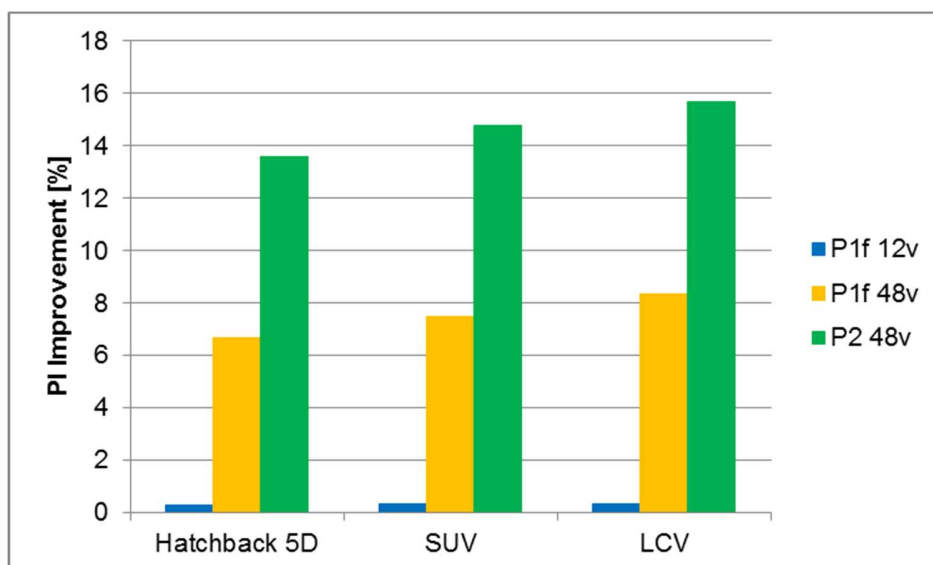


Figure 83. Summary on PI improvement

For each hybrid architecture, the entity of PI improvement is variable depending on the type of vehicle, because of different mass and road load power. Evidently it depends also by the engine and gearbox characteristics but this correlation here is not investigated because the same powertrain is used for all simulations.

For a given vehicle segment, PI deltas achieved by each system is due mainly to:

- Electric machine power characteristics in motor mode ;
- Electric machine operating range, depending on machine and on mechanical linkage to ICE.

A synthesis is reported on Table 28 and the comparison of power characteristics is shown in Figure 84. Finally the P2 48V system offer better performances compared with P1f systems not only because it is more powerful but also because it is capable to perform the boost over the whole operating range of ICE.

	P1f 12V	P1f 48V	P2 48V
<b>Maximum speed EM in motor mode [rpm]</b>	6000	10000	7000
<b>Gear ratio between EM and ICE</b>	2,5-3	2,5-3	1
<b>Electric power in motor mode [kw]</b>	2	10	15
<b>Effective boost range for ICE [rpm]</b>	0-2400	0-4000	0-7000

Table 28. Synthesis of electric machine power characteristics

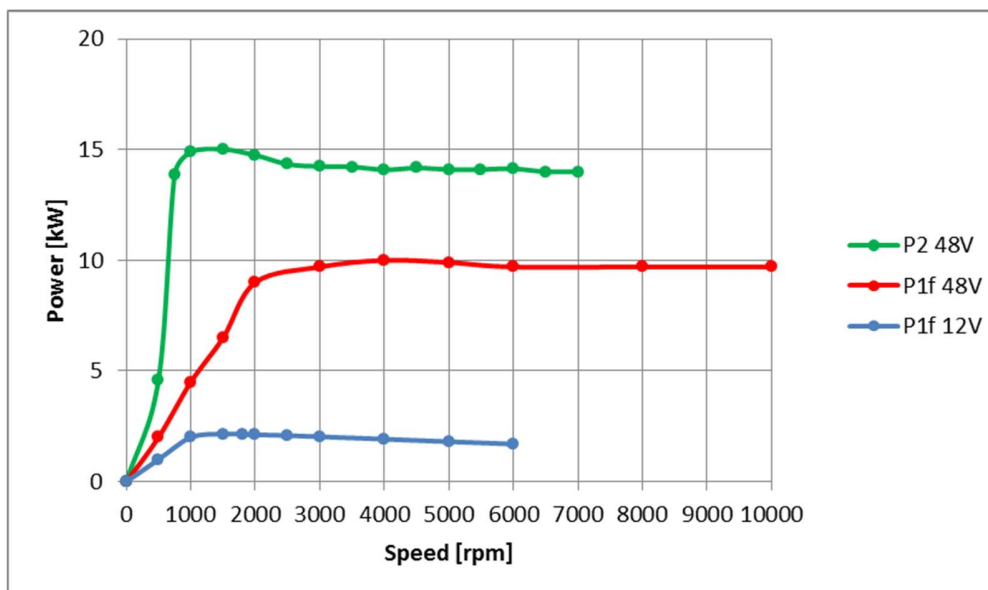


Figure 84. EM mechanical characteristics comparison

## 11.2 Fuel consumption and CO<sub>2</sub> emissions simulations

The fuel consumption, shortened also as FC, and CO<sub>2</sub> emissions are calculated simulating NEDC on vehicles belonging to different segments. The deltas presented relative to CO<sub>2</sub> are the same for fuel consumption because these two parameters are proportional.

Every simulation performed is based on the following assumptions:

- The regenerative braking functionality can be limited by maximum peak power characteristics, if the available power in input to electric machine is excessive for considered working point, the generator recovers only a part of power and other part is dissipated in braking system;
- Electric machine and inverter losses has been considered through a mean value of efficiency;
- Mechanical losses from the wheels to the propulsion system, composed by electric motor and engine, has taken into account by means of gearbox mechanical efficiency and coast-down coefficient  $F_1$ ;
- A function implemented in the model allows to not apply the boost when the available energy in the battery is lower than 30%;
- The additional weight of various systems requires an adaptation of coast-down coefficient  $F_0$ , which is computed by the code;
- Power consumptions by electric board net is considered negligible during the entire drive cycle;
- Energy required to perform S&S function is neglected.

For all simulations the input data regarding vehicles are reported on Table 21, whereas those regarding powertrain are reported on Table 22(engine) and on Table 23(gearbox).

The results here presented are relative to different vehicle which is possible to distinguish quantitatively by VDE (Vehicle Demand Energy), being function of mass, rolling resistance and aerodynamic drag. The architecture point of view is aimed more to know the benefit of an hybrid architecture on a wide range of vehicles than the absolute advantage on a given vehicle.

### 11.2.1 FC and CO<sub>2</sub> emission simulations on vehicles equipped with P1f 12V

In this case study the specific assumptions, added to general ones already described in paragraph 11.2, are:

- It is performed the conventional Start&Stop, when the vehicle is stationary, and the advanced Start&Stop, when the vehicle speed is below 10 km/h during decelerations;
- The boost is activated during every acceleration of the drive cycle as long as electric machine reaches its maximum speed;
- Engine friction power during regenerative braking is neglected.

The parameters assumed for the simulations are reported on Table 29 .

Simulation on vehicles w/P1f 12V	
Additional weight vs conv. vehicle [kg]	10
Gearbox mechanical efficiency	0,95
Mean efficiency EM in motor mode	0,6
Mean efficiency EM In generator mode	0,7
Mean efficiency Inverter	0,95
Available energy in the battery (SOC 70%-30%) [Wh]	60
Transmission ratio EM/ICE	2,5

Table 29. Input data CO<sub>2</sub> simulation (P1f 12V)

The output power required to complete NEDC speed profile is mostly delivered by engine but during accelerations is supplied partially by electric motor, as represented with red curves in Figure 85.

Considering engine map in Figure 86, this fraction of power tends to shift engine working points towards lower loads until the ICE speed of about 2400 rpm, when the e-motor reaches its maximum speed.

Even if the electric machine shifts the engine operating point towards slightly higher bsfc (brake specific fuel consumption) values, the reduction in fuel consumption and CO<sub>2</sub> emissions is due to the minor engine loads.

The resulting effect on cumulated fuel consumption over the drive cycle is reported on Figure 87.

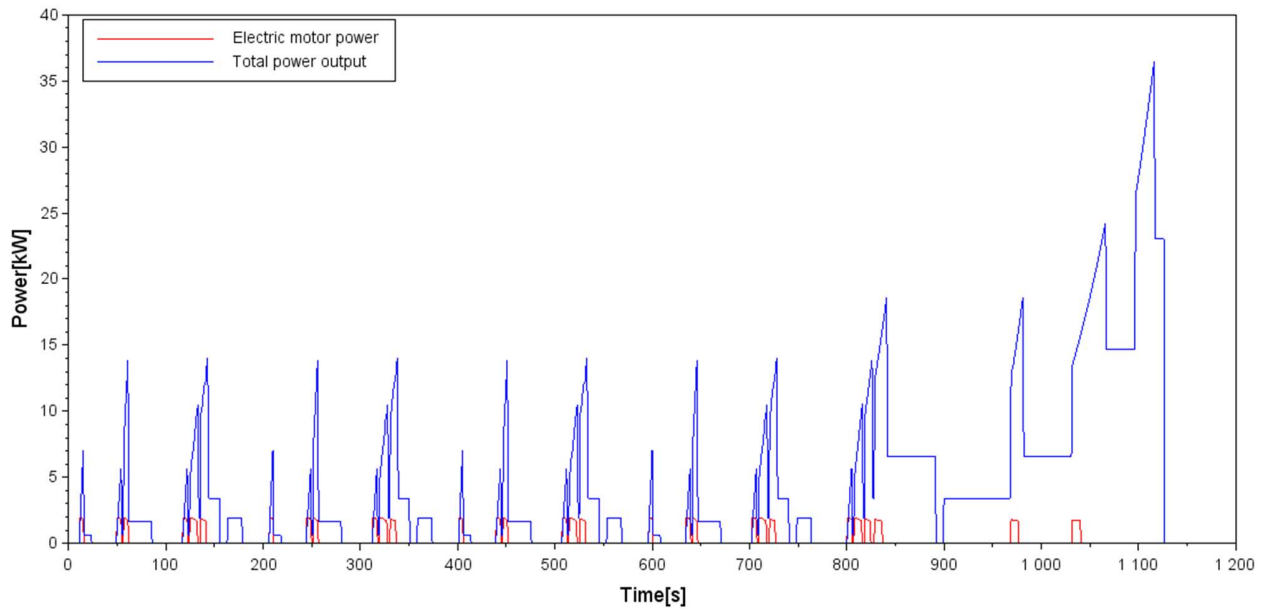


Figure 85. Output power during NEDC (P1f 12V case)

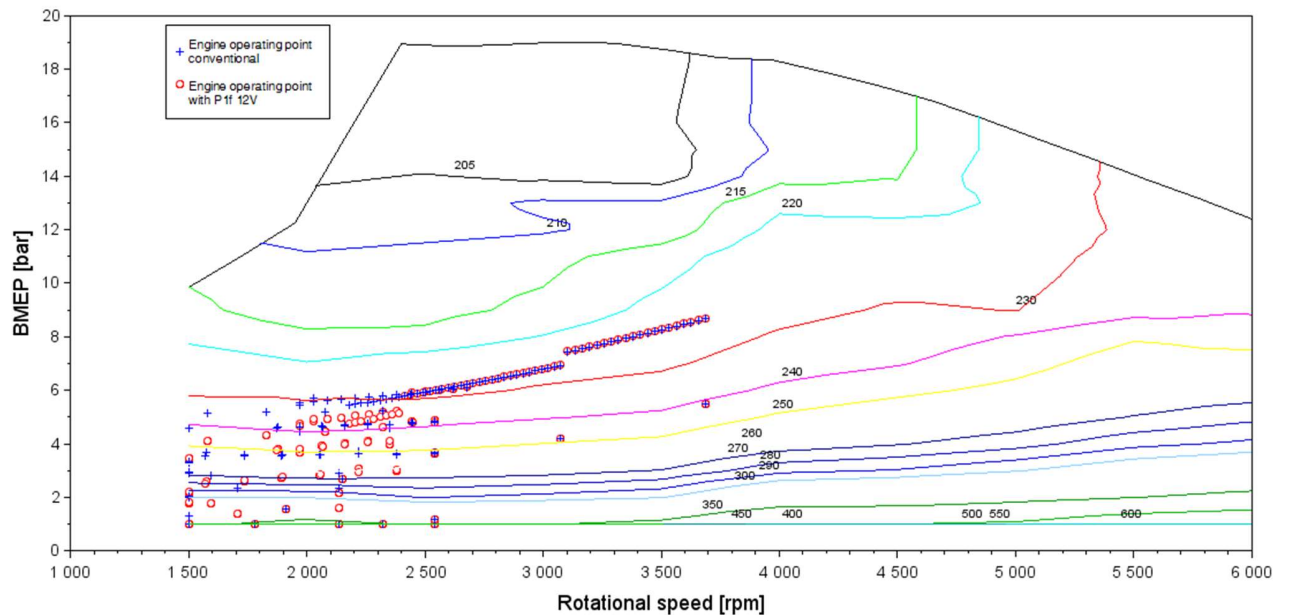


Figure 86. Engine operating points (P1f 12V case)



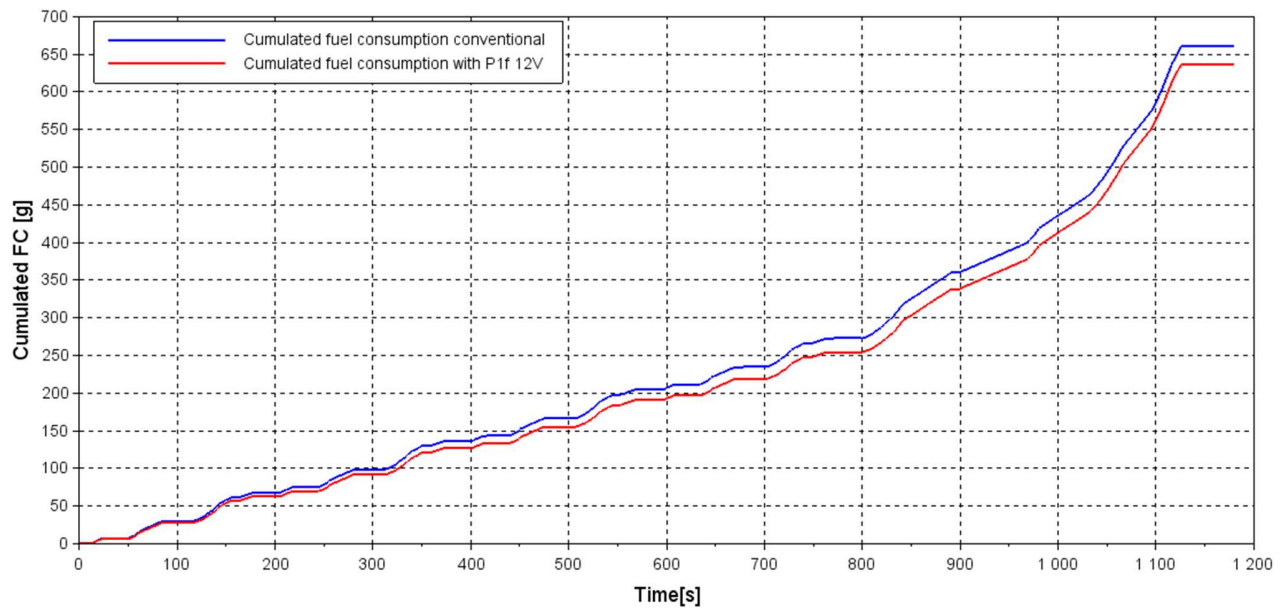


Figure 87. Cumulated fuel consumption (P1f 12V case)

The CO<sub>2</sub> deltas for each vehicle are reported on Table 30 and graphically represented on Figure 88. Analyzing the results it emerges that FC and CO<sub>2</sub> reduction achieved by BSG 12 V system, over baseline vehicle intended equipped with S&S system, drops slightly in percentage with the increase of VDE. In fact, given the boundary conditions assumed, this system allows to save approximately the same absolute quantity of CO<sub>2</sub> but its contribution becomes in percentage less relevant for larger vehicles with higher FC and CO<sub>2</sub> values.

Baseline vehicle	VDE baseline vehicle [MJ]	CO <sub>2</sub> Δ vs vehicle w/S&S [%]
<b>Hatchback 5D</b>	4,64	-3,7
<b>SUV</b>	5,32	-3,5
<b>LCV</b>	5,77	-3,3

Table 30. CO<sub>2</sub> deltas (P1f 12V case)

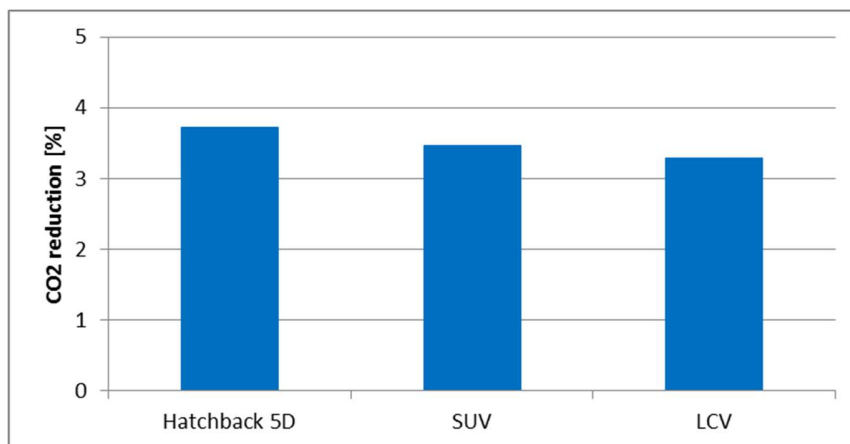


Figure 88. CO<sub>2</sub> reduction (P1f 12V case)

### 11.2.2 FC and CO<sub>2</sub> emission simulations on vehicles equipped with P1f 48 V

In this case study the specific assumptions, added to general ones already described in paragraph 11.2 , are the followings:

- It is performed the conventional Start&Stop, when the vehicle is stationary, and the advanced Start&Stop, when the vehicle speed is below 10 km/h during decelerations;
- The boost is activated during every acceleration of the drive cycle as long as electric machine reaches its maximum speed, compatibly with availability of energy in the battery;
- Engine friction power during regenerative braking is neglected;

The parameters assumed for the simulations are reported on Table 31.

Simulation on vehicles w/P1f 48V	
Additional weight vs conv. vehicle [kg]	30
Gearbox mechanical efficiency	0,95
Mean efficiency EM in motor mode	0,75
Mean efficiency EM In generator mode	0,8
Mean efficiency Inverter	0,95
Available energy in the battery [Wh]	143
Transmission ratio EM/ICE	2,5

Table 31. Input data CO<sub>2</sub> simulation (P1f 48V)

The output power required to complete NEDC speed profile is mainly delivered by engine but during accelerations is supplied partially by electric motor, as represented with red curves in Figure 89. Considering engine map in Figure 90, this fraction of power tends to shift engine working points towards lower loads until the ICE speed of around 3000 rpm.

Even if the electric machine shifts the engine operating point towards slightly higher bsfc (brake specific fuel consumption) values, the reduction in fuel consumption and CO<sub>2</sub> emissions is due to the minor engine loads.

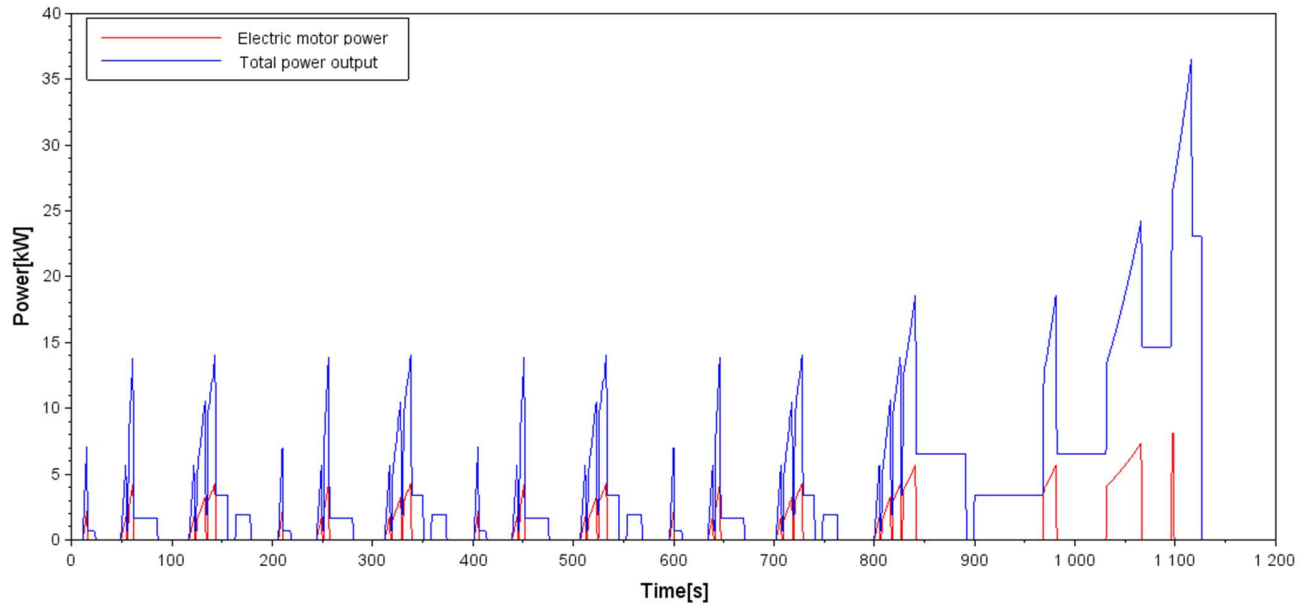


Figure 89. Output power during NEDC (P1f 48V case)

The resulting effect on cumulated fuel consumption over the drive cycle is reported on Figure 90.

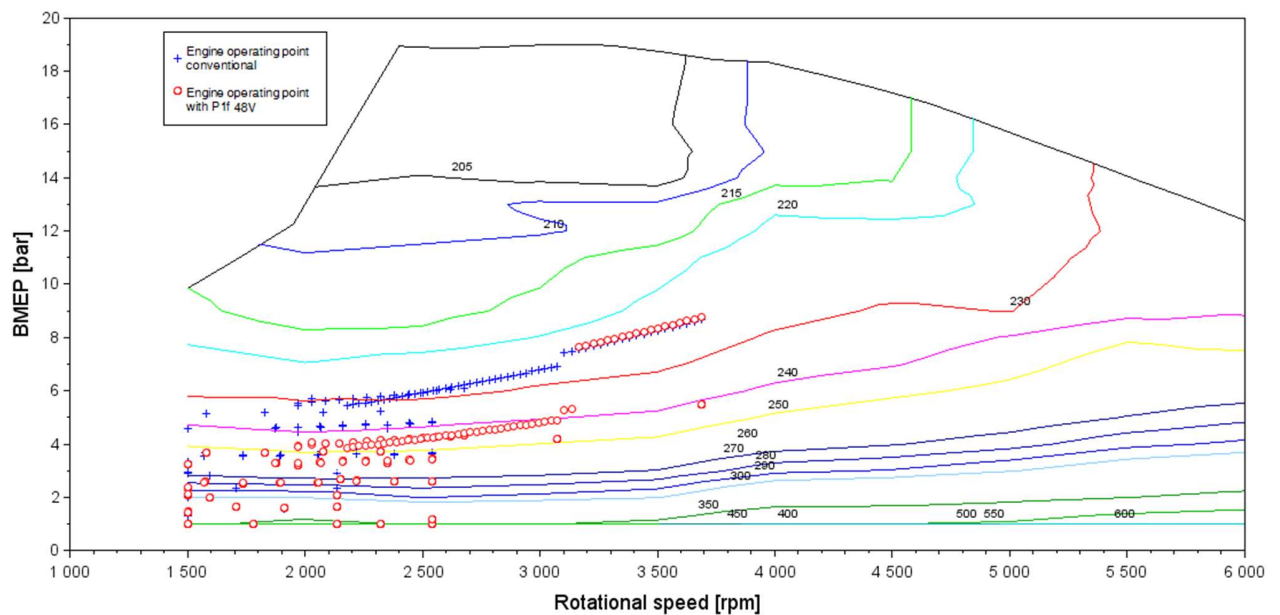


Figure 90. Engine operating points (P1f 48V case)

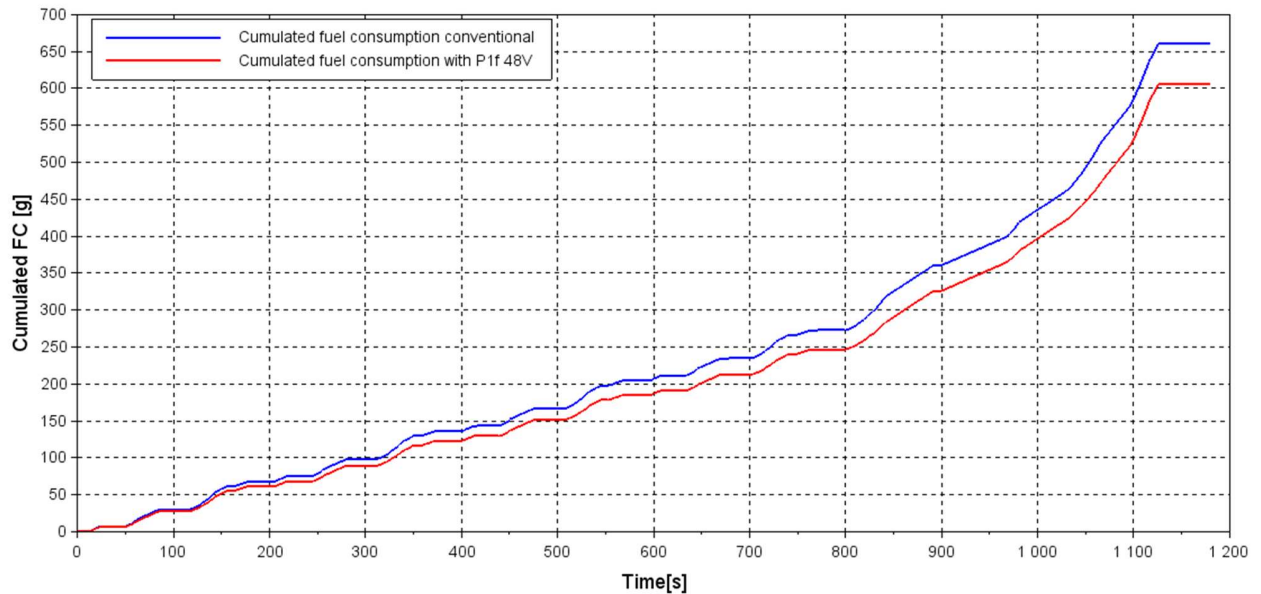


Figure 91. Cumulated fuel consumption (P1f 48V case)

The CO<sub>2</sub> deltas for each vehicle are reported on Table 32 and graphically represented on Figure 92. Analyzing the results it emerges that FC and CO<sub>2</sub> reduction achieved by BSG 48 V system, over baseline vehicle intended equipped with S&S system, drops slightly in percentage with the increase of VDE. In fact, given the boundary conditions assumed, this system allows to save approximately the same absolute quantity of CO<sub>2</sub> but its contribution becomes in percentage less relevant for larger vehicles with higher FC and CO<sub>2</sub> values.

Baseline vehicle	VDE baseline vehicle [MJ]	CO <sub>2</sub> Δ vs vehicle w/S&S [%]
<b>Hatchback 5D</b>	4,64	-8,5
<b>SUV</b>	5,32	-8,2
<b>LCV</b>	5,77	-7,7

Table 32. CO<sub>2</sub> deltas (P1f 48V case)

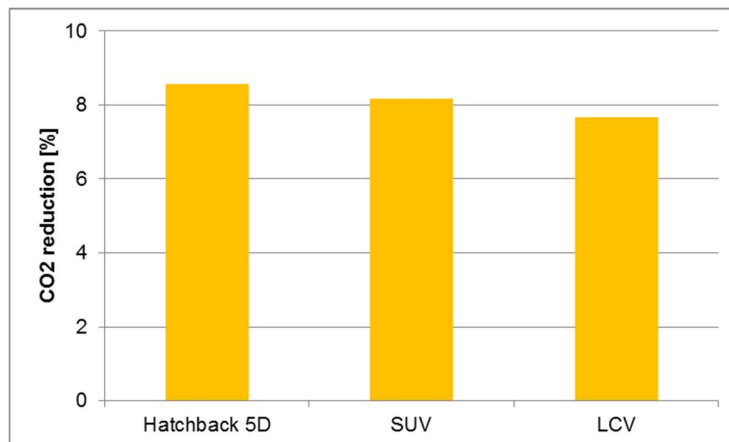


Figure 92. CO<sub>2</sub> reduction (P1f 48V case)

### 11.2.3 FC and CO<sub>2</sub> emission simulations on vehicles equipped with P2 48 V

In this case study the specific assumptions, added to general ones already described in paragraph 11.2, are:

- The pure electric driving is adopted to cover about 2 km of NEDC especially at low speeds, whereas the rest of drive cycle distance is covered exclusively by the combustion engine;
- The e-boost is not performed because the traction power is delivered alternatively by the combustion engine or by the electric motor;

The parameters assumed for the simulations are reported on Table 33.

Simulation on vehicles w/P2 48V	
<b>Additional weight vs conv. vehicle [kg]</b>	70
<b>Gearbox mechanical efficiency</b>	0,95
<b>Mean efficiency EM in motor mode</b>	0,9
<b>Mean efficiency EM In generator mode</b>	0,9
<b>Mean efficiency Inverter</b>	0,95
<b>Available energy in the battery [Wh]</b>	332
<b>Transmission ratio EM/ICE</b>	1

Table 33. Input data CO<sub>2</sub> simulation (P2 48V)

The traction power required over NEDC is alternatively delivered by engine, during accelerations and higher speeds, and by electric motor at lower speeds, as shown with red curves in Figure 93.

Considering engine map in Figure 94, the power supplied by electric motor tends to remove engine working points at low loads, whereas others are unchanged because it does not occur the boost function.

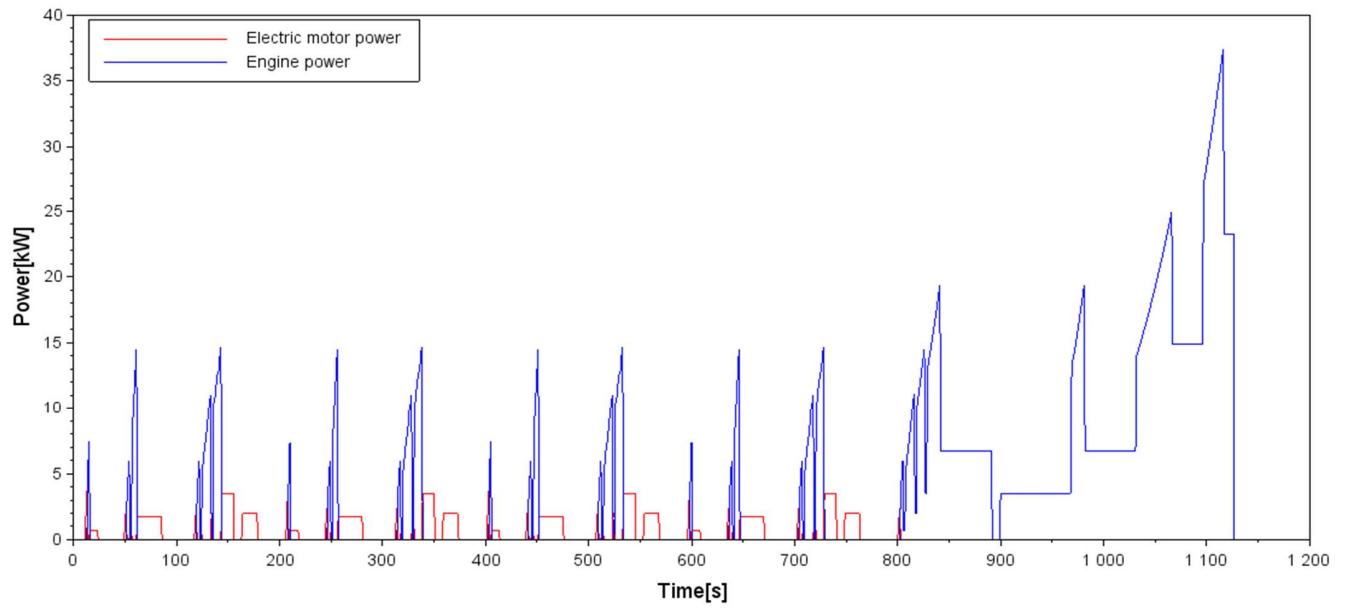


Figure 93. Output power during NEDC (P2 48V case)

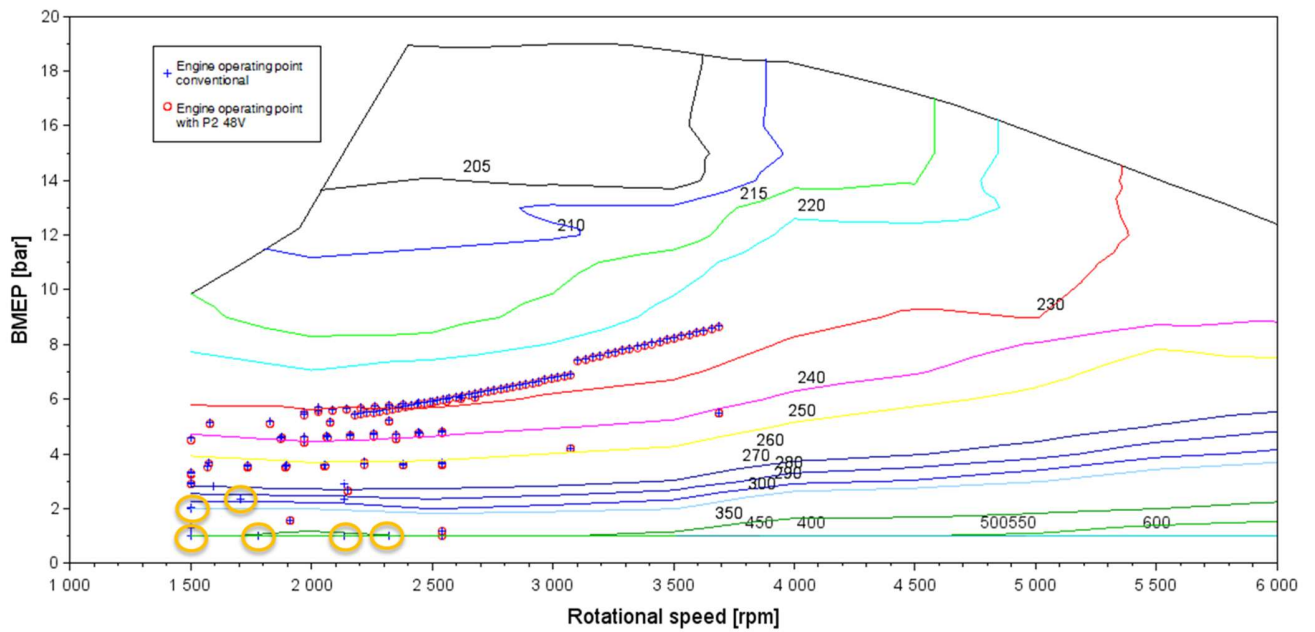


Figure 94. Engine operating points (P2 48V case)

Then, the benefit highlighted in Figure 95 Figure 95. Cumulated fuel consumption (P2 48V case) derives from the eliminated fuel consumption in the discussed working points thanks to the pure electric driving.

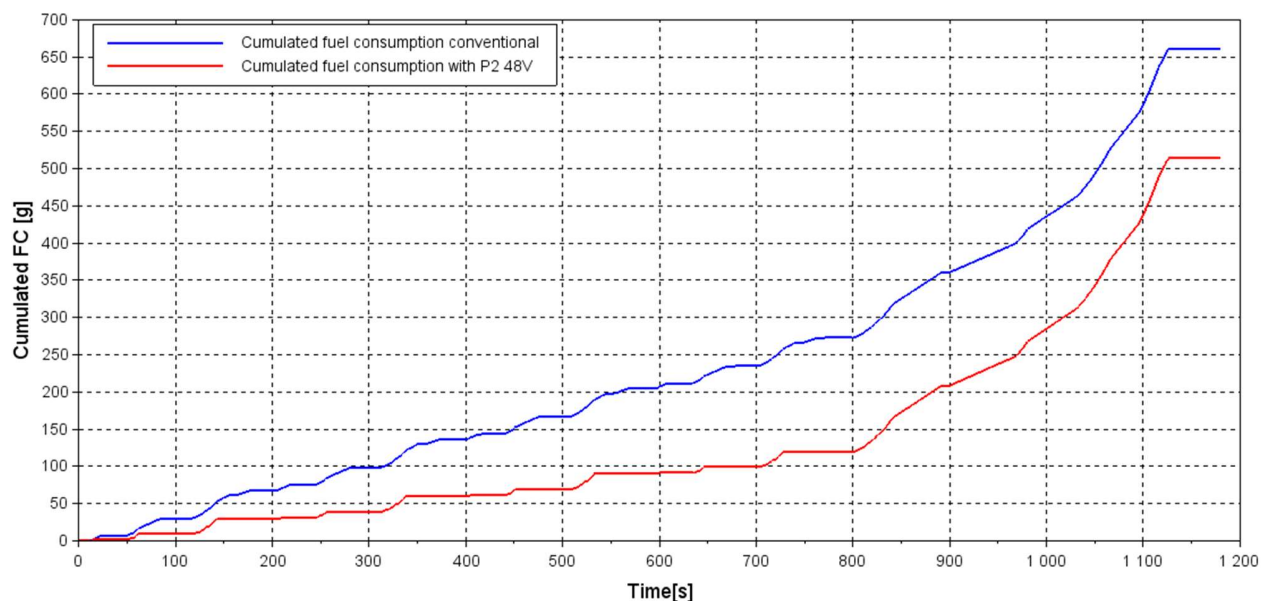


Figure 95. Cumulated fuel consumption (P2 48V case)

The CO<sub>2</sub> deltas for each vehicle are reported on Table 34 and graphically represented on Figure 96. Analyzing the results it emerges that CO<sub>2</sub> reduction, over baseline vehicle intended equipped with S&S system, drops slightly in percentage with the increase of VDE. In fact, given the boundary conditions assumed, this system allows to save approximately the same absolute quantity of CO<sub>2</sub> but its contribution becomes in percentage less relevant for larger vehicles with higher FC and CO<sub>2</sub> values.

Baseline vehicle	VDE baseline vehicle [MJ]	CO <sub>2</sub> Δ vs vehicle w/S&S [%]
<b>Hatchback 5D</b>	4,64	-23,2
<b>SUV</b>	5,32	-21,7
<b>LCV</b>	5,77	-20,9

Table 34. CO<sub>2</sub> deltas (P2 48V case)

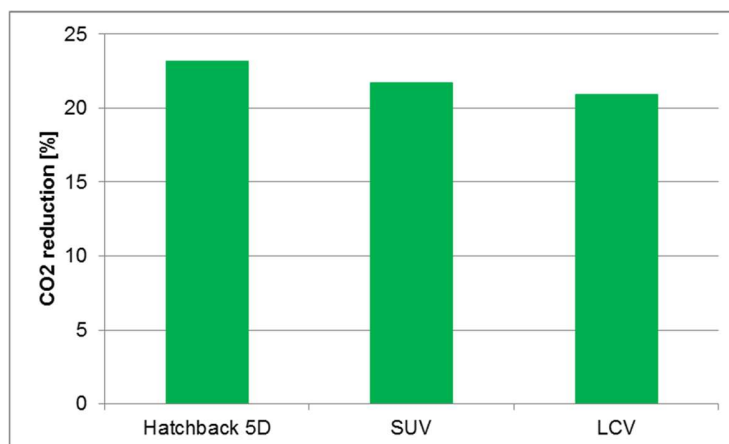


Figure 96. CO<sub>2</sub> reduction (P2 48V case)

P2 48V system achieves a CO<sub>2</sub> benefit evidently superior compared with BSG systems because the pure electric driving allows to shut off the engine at low loads and at low rotational speeds, generally associated to high values of specific fuel consumptions. Furthermore a distance of 2 km without CO<sub>2</sub> emission referred to the total drive cycle distance of 11 km represents approximately the 20% and it is clearly relevant in percentage.

#### 11.2.4 Summary on FC and CO<sub>2</sub> emission reduction

A summary on CO<sub>2</sub> reduction on the various vehicles is reported on Table 35.

Vehicle baseline	VDE basel. vehicle [MJ]	P1f 12V CO <sub>2</sub> Δ vs vehicle w/S&S [%]	P1f 48V CO <sub>2</sub> Δ vs vehicle w/S&S [%]	P2 48V CO <sub>2</sub> Δ vs vehicle w/S&S [%]
<b>Hatchback 5D</b>	4,64	-3,7	-8,5	-23,2
<b>SUV</b>	5,32	-3,5	-8,2	-21,7
<b>LCV</b>	5,88	-3,3	-7,7	-20,9

Table 35. Summary on CO<sub>2</sub> deltas

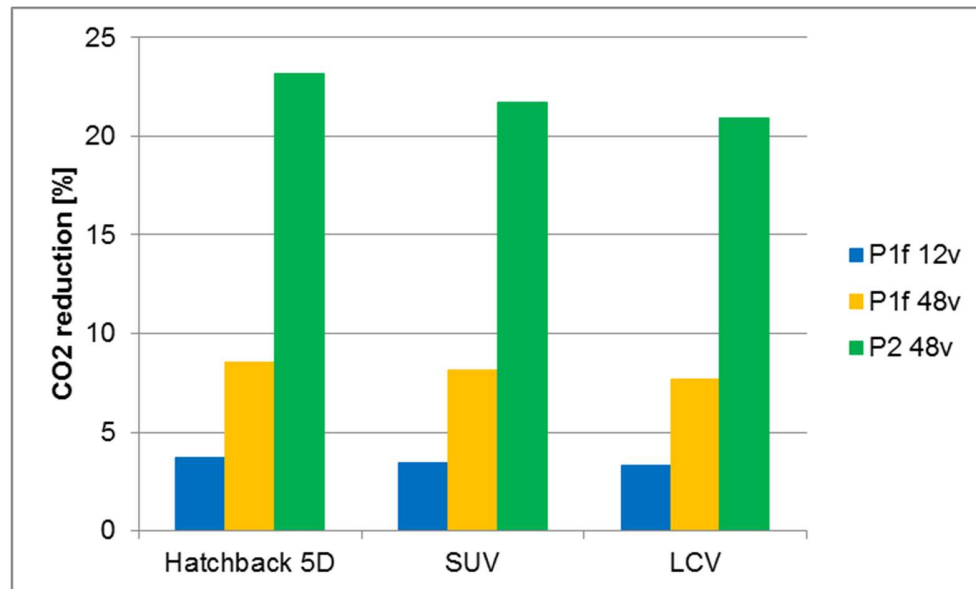


Figure 97. Summary on CO<sub>2</sub> reduction

From Figure 97, it is evident that the CO<sub>2</sub> percentage reduction achieved by each hybrid architecture is dependent on vehicle type, distinguished by VDE which is essentially a synthesis parameter.

Whereas for a given vehicle segment, CO<sub>2</sub> deltas deriving from each system is due mainly to:



- Electric machine power characteristics in boost mode and regenerative braking;
- Electric machine operating range, depending on machine and on mechanical linkage to ICE;
- Battery available energy, considering a 70%-30% SOC range;
- Pure electric driving capability;

	P1f 12V	P1f 48V	P2 48V
<b>Electric power in motor mode [kw]</b>	2	10	15
<b>Effective boost range for ICE [rpm]</b>	0-2400	0-4000	0-7000
<b>Pure electric driving capability</b>	No	No	Yes
<b>Battery available energy [Wh] (70%-30% SOC)</b>	~50	~150	~150-300

**Table 30**

Definitely the CO<sub>2</sub> benefit of P2 48V is much higher than BSG systems thanks to higher power, larger boost range and above all the pure electric driving functionality.

## 12. Cost analysis

A fundamental parameter which enables the OEM (Original Equipment Manufacturer) to discern which technology is economically convenient is the cost-benefit ratio, expressed by equation ( 29 ) in €/gCO<sub>2</sub>. The cost is the variable cost of system hardware not considering the investments, whereas the benefit is intended as grams of CO<sub>2</sub> saved.

$$\text{Cost vs Benefit ratio} = \frac{\text{Variable cost of system}}{\text{CO}_2 \text{ saved}} \quad ( 29 )$$

Since from 2020, if manufacturer's average CO<sub>2</sub> values exceeds it is applied a penalty of 95 € for every g/km excess the target multiplied by the number of vehicles sold, the cost-benefit ratio of any technology has evidently to be inferior to 95€/g .

Assuming for vehicle types analyzed the CO<sub>2</sub> absolute values reported on Table 36, it has been calculated the cost-benefit ratios shown Figure 98.

The CO<sub>2</sub> benefit in percentage taken from simulation results has been used to determine the grams of CO<sub>2</sub> save while the variable cost is known from internal know-how.

Vehicle	CO <sub>2</sub> [g/km]
<b>Hatchback 5D</b>	130
<b>SUV</b>	150
<b>LCV</b>	180

Table 36. CO<sub>2</sub> values assumed

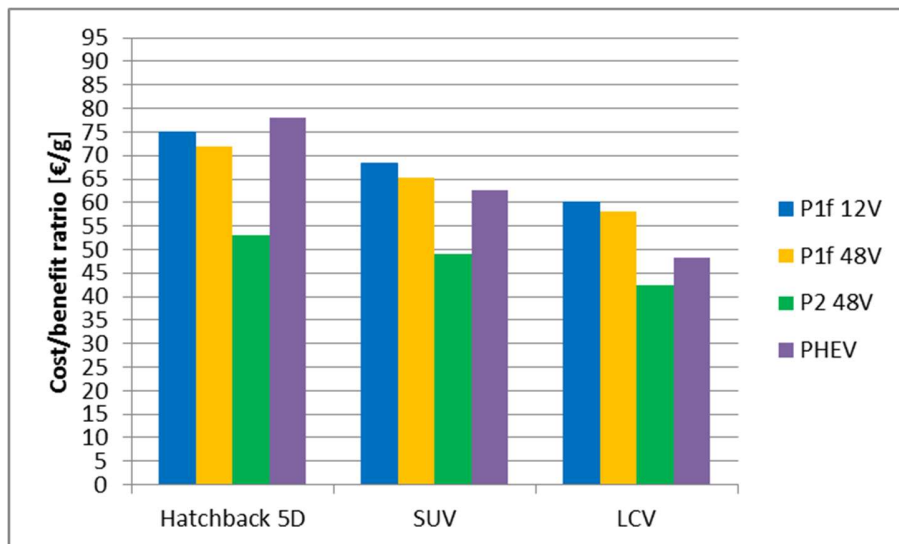


Figure 98. Cost benefit ratio for different vehicles and technologies

From Figure 98, it is noticeable that a given technology on different vehicles achieves different cost-benefit ratios. In fact a technology which insures a certain percentage benefit referred to different the CO<sub>2</sub> absolute values leads to diverse grams of CO<sub>2</sub> saved .

P1f 12V system and P1f 48V systems show a cost-benefit about between 60 and 75 €/g, whereas P2 48V between about 40 and 50 €/g.

In order to compare the results also with Full Hybrid applications, it was added PHEV data which highlights a ratio about between 50 and 70 €/g. This hybrid architecture represents a convenient solution especially when the starting CO<sub>2</sub> value is elevated, that is for SUV and LCV.

This shows the hybridization degree has to be adapted depending on vehicle segment. While low cost hybrid applications are aimed to limit CO<sub>2</sub> values for the lower segments, Full Hybrid applications serve to decrease in a consistent way fleet CO<sub>2</sub> values.

From the customer point of view, it has been analyzed the impact in percentage of various systems cost on the vehicle price. Here it is assumed that the additional price due to hybrid powertrain results about two times compared with variable cost of system.

The initial vehicle prices assumed are reported on Table 37 and the results are illustrated on Figure 99.

Vehicle	Average Price [€]
<b>Hatchback 5D</b>	19000
<b>SUV</b>	25000
<b>LCV</b>	20000

Table 37. Assumed vehicle prices

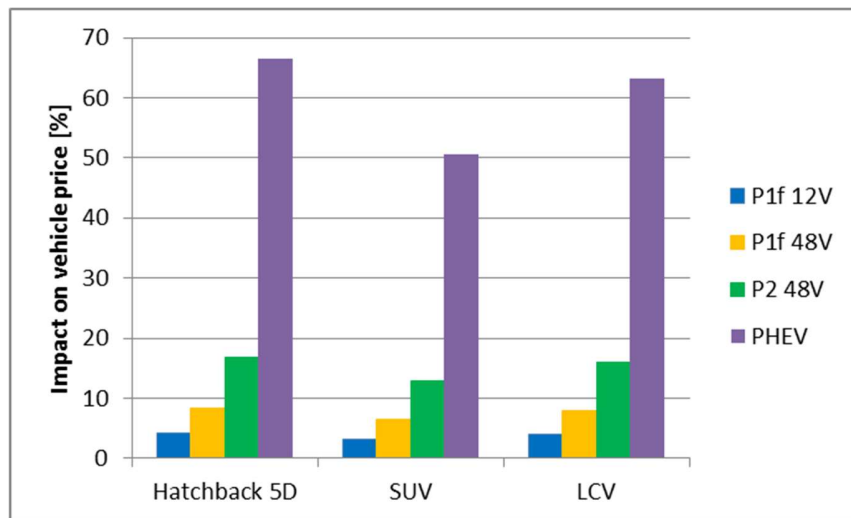


Figure 99. Impact on vehicle price for different vehicles and technologies

From the graph in Figure 99, it emerges that impact in the case of P1f 12V systems is inferior to 5%, for P1f 48V is between 6 and 9% and finally for P2 48V is between 13 and 17%. PHEVs can require an additional price of about 50-60% compared to the baseline vehicle. This means that this hybrid category is suitable especially to more expensive vehicles, like SUVs as evident in figure. Considering graphs in Figure 98 and Figure 99, it emerges that Micro and Mild Hybrids basically with higher cost-benefit influence less the final vehicle price.

PHEVs have high cost-benefit ratios and influence sensibly vehicle price but, meanwhile, are able to lower CO<sub>2</sub> emissions below 50 g/km.

### 13. Comparative analysis

The study on low cost hybrid architectures has been performed analyzing their installation on existing vehicles and their effect on performance, emissions and cost.

In general it was found that the systems with minor complexity as Micro Hybrids involve a simpler application on existing vehicle but give a modest contribution to performance and emission, because of their limited power. On the other side, the advantages of Mild Hybrids application are certainly more relevant as long as to accept more integration issues and major investments. In fact the components required are evidently larger and more expensive.

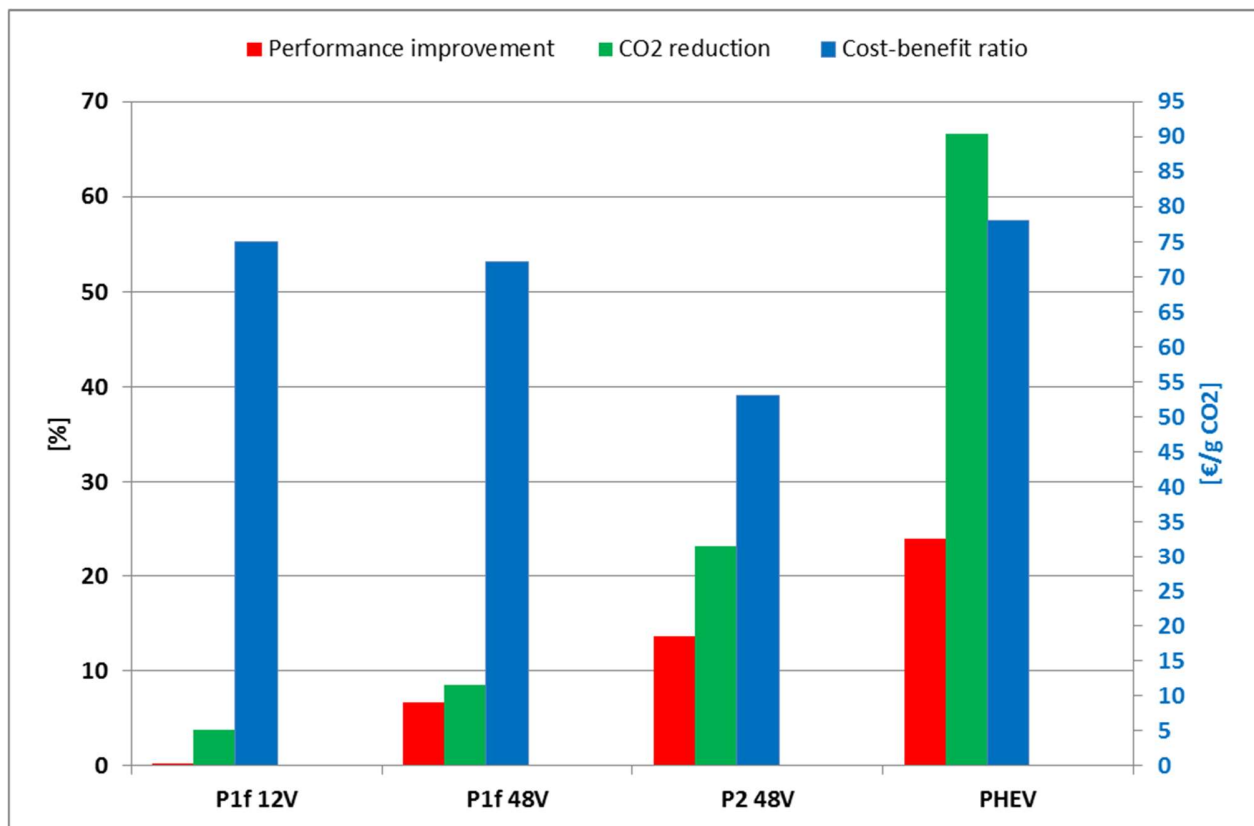


Figure 100. Comparative analysis of systems

From graph in Figure 100 it possible to make a series of considerations:

- P1f 12V system does not offer significant advantages in terms of performance (<0,5%), CO<sub>2</sub> emissions (<5%) and it presents a relatively high cost benefit ratio. It essentially performs a more comfortable S&S thank to the belt driven machine and its hybrid functions has limited effectiveness due to the power constraints. It is almost “transparent” to the customer and for this reason it can required a user interface to justify its additional price. Its marketability is mainly linked to the possibility of homologation of hybrid, which implicates minor car tax and the access to restricted area.

- P1f 48V system influences more both the performance, with deltas between 6 and 8%, and emissions approximately with reduction of about 8%. The cost benefit ratio is comparable to P1f 12V systems.

Despite the higher power values managed, it is penalized by the belt mechanical linkage to ICE on the front end accessory drive. In fact this prevents from performing hybrid functions such as pure electric driving which on the drive cycles are decisive with respect to the fuel economy.

- P2 48V represents a type of hybrid which sensibly modifies sensibly emissions (more than 20%) and performance, compared to baseline vehicle. This is due essentially to the hardware power and to the specific topology which allows to performs also pure electric driving. The cost benefit ratio is clearly more favorable compared to the previous systems but it involves additional price on vehicle which could represent in future an alternative to Diesel propulsion.
- PHEVs, introduced to supply a comparative terms with full hybrid systems, achieve CO<sub>2</sub> reduction decisively higher compared to low cost hybrids but similar cost benefit ratio and they insures an excellent performance improvement. Its impact on vehicle price makes this architecture more suitable for segments such as SUV, where baseline vehicle price is higher.

## 14. Conclusions

The purpose of this work has been the examination of low voltage hybrid systems in terms of performance, fuel consumption and cost, from an architectural point of view.

In the initial chapters it seemed appropriate supply a technical background in order to describe installation constraints and to create the reference theoretical basis.

The installation verifications has been performed by means of software Vismockup on proprietary CAD files and they have supplied an overview on the main technical issues which occurs during concept selection phase. In fact Vehicle Architecture is constantly committed to find the best compromises which allows to reduce the industrialization cost of new cars sharing a given solution between vehicles belonging to the same platform.

The calculation code necessary to determine the effect on performances and CO<sub>2</sub> emissions has been developed formulating a series of assumptions, which would guarantee the interpretation of physical phenomena involved with a reasonable approximation. In fact it is conceived to support Architecture team to make macroscopic and rapid evaluations, before a detailed activity completed by the specialized departments

The tool has been used to perform simulations of different hybrid systems on three types of vehicles (Hatchback 5 doors, Sport Utility Vehicle and Light Commercial Vehicle).

The results has underlined that, for a given hybrid system, CO<sub>2</sub> reduction decreases slightly passing from a smaller to a larger vehicle. On the other hand, the sensitivity to performance improvement has shown the opposite tendency.

With respect to cost benefit, for a given hybrid type, the lower values compete to larger vehicles. In fact a certain CO<sub>2</sub> reduction in percentage applied on higher absolute initial CO<sub>2</sub> value maximizes the benefit.

The hybrid systems which appear more advantageous is affected by major complexity. With increasing degree of hybridization, the number and the size of components grows and this requires evidently a larger integration effort.

Definitely the concept selection between the hybrid systems based on criteria illustrated is not resolvable univocally, in fact it has to declined opportunely depending on the vehicle types and on the company strategy.

Currently, the Micro and Mild Hybrids represent compromise solutions capable of limiting the emissions for smaller vehicles with a reasonable cost. Whereas a major degree of hybridizations which involves higher costs both for OEM and customers can lower heavily the fleet average CO<sub>2</sub> values.

In conclusion, the main challenge for each car maker remains to offer the right mix of vehicles opportunely diversified able to insure compliance with future more stringent targets.

# Bibliography

A. Emadi, “Advanced Electric Drive Vehicles”, *CRC Press*

A. Stuffer, D. Heinrich, C. Hauck, T. Schmidt, H. Stief “Introduction of 48 V Belt Drive System”, *Schaeffler Symposium*, 2014

C. Mi, M. Abul Masrur, “Hybrid Electric Vehicles. Principles and Applications with Practical Perspectives”, *Wiley*

F. Badin “Hybrid vehicles from components to system” *Editions Technip*

D. Meszler, J. German, P. Mock, A. Bandivadekar, “CO2 reduction technologies for the European car and van fleet, a 2025-2030 assessment” *ICCT (The International Council on Clean Transportation)*

Economic Commission for Europe, “Proposal for amendments to global technical regulation No. 15 on Worldwide harmonized Light vehicles Test Procedure (WLTP)”, *Official Journal of the European Union*

European Commission “Regulation no. 333/2014”, *Official Journal of the European Union*

European Commission “Regulation no. 443/2009”, *Official Journal of the European Union*

European Vehicle Market Statistics Pocketbook 2016/17, *ICCT (The International Council on Clean Transportation)*

FCA internal documents

[https://www.dieselnet.com/standards/cycles/ece\\_eudc.php](https://www.dieselnet.com/standards/cycles/ece_eudc.php)

<https://www.dieselnet.com/standards/cycles/wltp.php>

<https://www.theaa.com/driving-advice/fuels-environment/euro-emissions-standards>

<https://x-engineer.org/automotive-engineering/vehicle/hybrid/mild-hybrid-electric-vehicle-mhev-control-function/>

In-market Application of Start-Stop Systems in European Market, *FEV group final report 2011*

Mark E. Case and Dean Tomazic, “Drive cycles”, *Encyclopedia of Automotive Engineering*

M. Cossale, “Multi-phase Starter-Generator for 48 V Mild-Hybrid Powertrains”  
*Ph.D. Dissertation*, 2017

P. Mock, J. Kühlwein, U. Tietge, V. Franco, A. Bandivadekar, J. German “The WLTP: How a new test procedure for cars will affect fuel consumption values in the EU” , *ICCT (The International Council on Clean Transportation)*

S. Baldizzone “Performance and Fuel Economy Analysis of a Mild Hybrid Vehicle Equipped with Belt StarterGenerator”,*Master’s thesis Dissertation*, 2012.



## List of Figures

Figure 1. Architectural perimeter.....	4
Figure 2. CO <sub>2</sub> trend in the last years .....	7
Figure 3. CO <sub>2</sub> target and weight relationship in 2015 and 2020.....	9
Figure 4. NEDC speed profile.....	10
Figure 5. WLTC speed profile .....	11
Figure 6. Speed profile NEDC vs WLTC .....	13
Figure 7. Interpolation family .....	14
Figure 8. Effect of mass on CO <sub>2</sub> target and emission .....	16
Figure 9. +5% Fleet Mass 2020 scenario .....	17
Figure 10. Target and emission trend +5% Fleet Mass 2020 scenario .....	18
Figure 11. -5% Fleet Mass 2020 scenario.....	18
Figure 12. Target and emission trend -5% Fleet Mass 2020 scenario .....	19
Figure 13. Influence of regenerative braking on braking power.....	22
Figure 14. Coasting effect on distance covered .....	23
Figure 15. Series hybrid layout .....	24
Figure 16. Parallel hybrid layout.....	24
Figure 17. Split power hybrid layout .....	25
Figure 18. Classification of parallel hybrids.....	27
Figure 19. P1f layout.....	27
Figure 21. P1r layout.....	28
Figure 23. P1r application on Daimler S400.....	28
Figure 24. P2 non-coaxial layout .....	29
Figure 26. P2 coaxial layout .....	29
Figure 28. P3 e-machine by Borg Warner .....	30
Figure 29. P4 e-machine by Borg Warner .....	30
Figure 30. Motoring torque curve .....	31
Figure 31. Generating power curve.....	32
Figure 32. Circuit of an inverter.....	33
Figure 33. Pulse Width Modulation.....	33
Figure 34. Circuit of a DC/DC converter.....	34
Figure 35. Diode scheme .....	34
Figure 36. MOSFET scheme .....	35
Figure 37. Ragone Plot.....	35
Figure 38. Conventional on-board electrical network .....	36
Figure 39. <i>Efficiency Line</i> specifics .....	37
Figure 40. <i>ReStart reinforced starter</i> .....	38
Figure 41. <i>Tandem Solenoid Starter</i> .....	38
Figure 42. Valeo <i>StARS</i> .....	39
Figure 43. Exploded view of <i>i-StARS</i> .....	39

Figure 44. P1f 12V layout.....	40
Figure 45. Power curve BSG 12V Valeo <i>i-StARS</i> in motor mode.....	41
Figure 46. Power curve BSG 12V Valeo <i>i-StARS</i> in generator mode .....	41
Figure 47. Samsung 12V Lithium-Ion Battery .....	42
Figure 48. Front End Accessory Drive .....	45
Figure 49. Motor mode .....	45
Figure 50. Generator mode .....	46
Figure 51. Decoupling tensioner .....	46
Figure 52. SVHS by Suzuki .....	47
Figure 53. Installation of Lithium-Ion Battery.....	47
Figure 54. e-HDi by PSA .....	48
Figure 55. P1f 48V layout.....	50
Figure 56. Bosch 48V BRM power curves .....	51
Figure 57. Bosch 48V BRM .....	51
Figure 58. Bosch 48V Lithium-Ion.....	52
Figure 59. Electrical layout of 48V systems .....	52
Figure 60. Bosch DC/DC converter.....	53
Figure 61. P2 48V layout .....	55
Figure 62. Schaeffler 48V motor power curves.....	56
Figure 63. Schaeffler 48V motor .....	56
Figure 64. Installation of P1f on engine.....	59
Figure 65. Verification of interference and minimum distances .....	60
Figure 66. Description of possible scenarios .....	61
Figure 67. Section of installation on front floor passenger side .....	61
Figure 68. Installation Effect on roominess .....	62
Figure 69. Section of the installation under frontal seat passenger side .....	62
Figure 70. Installation effect on accomodation percentile.....	63
Figure 71. Installation of P2 48V on engine .....	64
Figure 72. Transversal section of engine compartment .....	65
Figure 73. Section of battery installation in the trunk.....	66
Figure 74. Section of DC/DC converter installation in the trunk .....	67
Figure 75. Section of DC/DC converter installation under passenger seat.....	68
Figure 76. Section of DC/DC converter installation under passenger seat.....	69
Figure 77. Traction power vs road load power (P1f 12V case) .....	78
Figure 78. PI improvement (P1f 12V case) .....	79
Figure 79. Traction power vs road load power (P1f 48V case) .....	80
Figure 80. PI improvement (P1f 48V case) .....	80
Figure 81. Traction power vs road load power (P2 48V case) .....	81
Figure 82. PI improvement (P2 48V case).....	82
Figure 83. Summary on PI improvement.....	82
Figure 84. EM mechanical characteristics comparison .....	83

Figure 85. Output power during NEDC (P1f 12V case).....	86
Figure 86. Engine operating points (P1f 12V case).....	86
Figure 87. Cumulated fuel consumption (P1f 12V case).....	87
Figure 88. CO <sub>2</sub> reduction (P1f 12V case).....	87
Figure 89. Output power during NEDC (P1f 48V case).....	89
Figure 90. Engine operating points (P1f 48V case).....	89
Figure 91. Cumulated fuel consumption (P1f 48V case).....	90
Figure 92. CO <sub>2</sub> reduction (P1f 48V case).....	90
Figure 93. Output power during NEDC (P2 48V case).....	92
Figure 94. Engine operating points (P2 48V case).....	92
Figure 95. Cumulated fuel consumption (P2 48V case).....	93
Figure 96. CO <sub>2</sub> reduction (P2 48V case).....	93
Figure 97. Summary on CO <sub>2</sub> reduction.....	94
Figure 98. Cost benefit ratio for different vehicles and technologies.....	96
Figure 99. Impact on vehicle price for different vehicles and technologies.....	97
Figure 100. Comparative analysis of systems.....	98

## List of tables

Table 1. EU emission standards.....	6
Table 2. Input parameters formula ( 1 ). .....	8
Table 3. NEDC statistics .....	10
Table 4. WLTC statistics .....	12
Table 5. NEDC vs WLTC statistics .....	13
Table 6. Initial situation data.....	17
Table 7. Summary on mass change scenarios.....	19
Table 8. BSG 12V Valeo <i>i-StARS</i> specifications.....	41
Table 9. Samsung 12V Lithium-Ion Battery data.....	42
Table 10. Summary on interventions required for P1f 12V integration .....	44
Table 11. Additional weight due to P1f 12V system .....	44
Table 12. Bosch 48V BRM specifications.....	50
Table 13. Bosch 48V Lithium-Ion Battery data.....	52
Table 14. Bosch DC/DC converter .....	53
Table 15. Summary on interventions required for P1f 48V integration .....	54
Table 16. Additional weight due to P1f 48V system .....	54
Table 17. Schaeffler 48V motor specifications.....	55
Table 18. 48 V Power Pack Unit.....	56
Table 19. Summary on interventions required for P1f 48V integration .....	58
Table 20. Additional weight due to P2 48V system .....	58
Table 21. Vehicles mass.....	77
Table 22. Engine technical specifics.....	77
Table 23. Gearbox technical specifics .....	77
Table 24. PI deltas (P1f 12V case).....	79
Table 25. PI deltas (P1f 48V case).....	80
Table 26. PI deltas (P2 48V case).....	81
Table 27. Summary on PI deltas .....	82
Table 28. Synthesis of electric machine power characteristics.....	83
Table 29. Input data CO <sub>2</sub> simulation (P1f 12V).....	85
Table 30. CO <sub>2</sub> deltas (P1f 12V case) .....	87
Table 31. Input data CO <sub>2</sub> simulation (P1f 48V).....	88
Table 32. CO <sub>2</sub> deltas (P1f 48V case) .....	90
Table 33. Input data CO <sub>2</sub> simulation (P2 48V) .....	91
Table 34. CO <sub>2</sub> deltas (P2 48V case).....	93
Table 35. Summary on CO <sub>2</sub> deltas.....	94
Table 36. CO <sub>2</sub> values assumed.....	96
Table 37. Assumed vehicle prices.....	97